Fall 11-13-2017

Bacterial Siderophore Production in Lechuguilla and Spider Caves, Carlsbad National Park (CCNP) Carlsbad, New Mexico

Tammi R. Duncan
University of New Mexico - Main Campus

Tammi Rae Duncan
Candidate

Biology
Department

This dissertation is approved, and it is acceptable in quality and form for publication:

Approved by the Dissertation Committee:

Dr. Margaret Werner-Washburne, Chairperson

Dr. Diana E. Northup

Dr. Cristina Takacs-Vesbach

Dr. Clifford N. Dahm

Dr. Penelope J. Boston

Bacterial Siderophore Production in Lechuguilla and Spider Caves, Carlsbad National Park (CCNP) Carlsbad, New Mexico

by

TAMMI RAE DUNCAN

B.S., Microbiology, Arizona State University, 2006
M.S., Microbiology, University of Iowa, 2011

DISSERTATION

Submitted in Partial Fulfillment of the

Requirements for the Degree of

Doctor of Philosophy
Biology

The University of New Mexico

Albuquerque, New Mexico

December 2017

DEDICATION

To all of my mothers, fathers, family, and furries who have inspired me to follow my dreams and to Chris, my love, who encouraged and nurtured me along the way.

ACKNOWLEDGEMENTS

I most genuinely thank my co-advisors for both your patience, encouragement and for your valuable expertise pertaining to this study. A special thanks to Dr. Diana Northup, my co-advisor, for allowing me to take the lead on my research and always having a positive outlook when I was challenged. A special thanks to Dr. Margaret Werner-Washburne, my co-advisor and dissertation chair, for trusting me as a leader in the University of New Mexico (UNM) Pathways program and in the UNM Initiative to Maximize Student Development (IMSD) program. Both your guidance and assistance in my professional development is genuinely heartfelt.

I also want to thank my committee members. I thank Dr. Cliff Dahm, who showed me how to be detailed oriented and provided insights into the structure of siderophores and the ecology of the caves. I thank Dr. Cristina Takacs-Vesbach, who has encouraged me to embrace my research assumptions and to develop and focus on basic research questions. I also thank Dr. Penelope Boston, my outside examiner, who has provided new insights on the slow-growing cave microorganisms and the importance of fundamental information of extremophiles.

Gratitude is also extended to Carlsbad Caverns National Park for their support of our field studies and the issuance of our collection permits. Most of the people that helped out with field work and lab work are acknowledged in each chapter, and I thank them all for their energy and assistance. Special thanks goes to Patricia Seiser, cave enthusiast and friend, for help in the field when samples were collected.

My dissertation work was supported by the UNM IMSD program, the American Society for Microbiology (ASM) Robert D. Watkins Graduate Fellowship, and the Navajo Nation Graduate Fund.

Bacterial Siderophore Production in Lechuguilla and Spider Caves, Carlsbad Caverns National Park (CCNP), Carlsbad, New Mexico

By Tammi Rae Duncan

B.S. in Microbiology, Arizona State University, 2006
M.S. in Microbiology, University of Iowa, 2011
Ph.D. in Biology, University of New Mexico, 2017

Abstract

Lechuguilla and Spider caves, Carlsbad Caverns National Park, contain a rich microbial diversity. Despite oligotrophic conditions, the microorganisms in these caves have developed strategies to acquire essential nutrients. I hypothesized that cave bacteria use siderophores, a ferric iron chelating compound, to acquire iron for essential life processes. To understand the backdrop against which the cave bacteria would produce siderophores, I examined the bacterial physiological characteristics, determined whether cave bacteria have an ability to produce siderophores, and investigated a possible correlation between iron and manganese concentrations in cave deposits and siderophore production by bacteria cultured from the same site. I carried out microbial physiological assays, siderophore assays, small subunit ribosomal RNA (SSU rRNA) sequence-based analyses, and geochemical analyses. Microbial physiological studies showed a dominant presence of Gram-positive bacteria isolated from parent cultures that were inoculated from cave deposits. In addition, physiological assays revealed a higher presence of non-catalase and non-oxidase usage and three growth curve patterns among cave bacterial isolates that were subcultured from a decade-long parent culture incubation. Siderophore assays revealed that most bacterial isolates from caves have the capability to produce siderophores with a preference for hydroxamate siderophores. For the small subunit ribosomal RNA (SSU rRNA) study, DNA was extracted from all bacterial isolates that produce siderophores, and 16S rRNA genes were amplified by PCR, cloned, and sequenced. I found that our siderophore producing isolates classified into Proteobacteria, Actinobacteria, Bacteroidetes, and Firmicutes phyla (from most abundant to least). Geochemical analyses of different cave deposits indicated higher concentrations of iron and manganese in ferromanganese deposits (FMDs) when compared to other secondary mineral deposits and moonmilk. A relationship was revealed of higher iron and

manganese concentrations in these deposits linked to a decrease in fast siderophore production by bacterial isolates collected from the same sites. My studies provide evidence that cave bacteria have the capability to produce siderophores, which may be an essential suite of compounds for survival in oligotrophic cave environments.

Table of Contents

Introduction

Significance and Intellectual Merit

Siderophores are used by microorganisms and plants to obtain insoluble ferric iron, the most prevalent source of surface iron. Although siderophores are primarily used to scavenge ferric iron, they can also bind to other metals in the environment. The binding characteristics of siderophores can be exploited for significant uses in medicine and in the environment.

Biomedically, sideromycins (siderophores linked to an antibiotic) are produced naturally or can be made synthetically. Sideromycins have been shown to be absorbed into a bacterial cell 100-fold better than an antibiotic alone (Braun 1999). Siderophores have been used to treat individuals with elevated iron in their blood and body (used to remove iron). However, siderophores might also be used to treat individuals with low blood iron since siderophore-Fe complexes are naturally more stable in aqueous environments and some siderophores release Fe in acidic environments.

Ecologically, siderophores could be employed in bioremediation, including in the cleanup of radioactive waste sites, as they chelate other heavy metals besides Fe. Furthermore, identifying bacterial siderophores in caves provides the opportunity to differentiate bacterial siderophores from plant siderophores, which may have very different, and potentially beneficial, secondary characteristics. Taken together, identifying potentially novel siderophores in caves is important biomedically and ecologically. In addition, novel bacteria could be discovered, which may lead to basic science findings and further expansion of the Tree of Life with novel subsurface microorganisms.

Background

Iron is the fourth most abundant element on Earth's crust and an essential element for all living organisms with the exception of a few bacterial strains (Straub et al. 2001). Organisms use iron in essential proteins involved in electron transfer, H_2O_2 and O_2 metabolism, the tricarboxylic acid cycle, DNA biosynthesis, N_2 fixation, and

photosynthesis (Neilands 1981, Leong and An 1997). In addition, iron can be used as a final electron acceptor in chemolithotrophic energy-yielding reactions (Madigan et al. 2000, Straub et al. 2001).

In order to be used, insoluble ferric iron has to be collected from the environment and solubilized by organisms. Bacteria have developed both capabilities to use chemolithotrophic energy-yielding reactions and to solubilize ferric iron by using siderophores (Madigan et al. 2000). These capabilities are significant in the subsurface where the conditions are aphotic and oligotrophic and where iron is a limited element. Determining how bacteria acquire iron in the subsurface remains an unanswered question of subterranean ecology and sheds important light on how bacteria can live and grow in caves.

Over 500 distinct siderophores are made by bacteria, fungi, and graminaceous plants (Drechsel and Winkelmann 1997) in response to low intracellular iron levels, as a way to scavenge and process insoluble ferric iron from the environment (Hider and Kong 2010, Ahmed and Holmström 2014). Siderophores are 200 to 2000 Da in size and are highly selective for ferric iron (Chu et al. 2010, Ahmed and Holmström 2014). Siderophores are used by plants to gather needed metals from the environment or to use plant-growth promoting fungal or bacterial siderophores in mutualistic relationships within their rhizospheres (Glick 2003, Ahmed and Holmström 2014).

Siderophores are grouped into four categories based on their electron donating functional group that binds ferric iron. The four categories of siderophores are identified as hydroxamate, catecholate (also known as phenolate), carboxylate, and mixed-type groups (Dave et al. 2006, Hider and Kong 2010). The most studied hydroxamate siderophore is desferrioxamine B made by fungi and bacteria (Miethke and Marahiel 2007). The most common catecholate siderophore is enterobactin, which is produced by enteric bacteria (Hider and Kong 2010, Ali and Vidhale 2013).

The biosynthesis of siderophores by microorganisms, depending on the chemical nature of the siderophore, can occur either in a nonribosomal peptide synthases (NRPS)-dependent or –independent pathway (Miethke and Marahiel 2007). NRPS are large, specific multi-enzyme complexes, also called peptide synthases. They contain unique building blocks (amino, carboxy, and hydroxy acids) that lead to high structural

variability of macrocyclic peptidic products, without the need for a RNA template (Crosa and Walsh 2002, Grünewald and Marahiel 2006). The NRPS-dependent assembly line is dependent on monomer selection and activation, chain elongation, and then chain termination. The repetition of these steps depends on the size of molecules being made and how many peptides are added (Crosa and Walsh 2002). Common products made in this manner are major antibiotics and siderophores. Siderophores that are usually made by the NRPS-dependent pathway are the catecholate-type (aryl-capped siderophores) (Crosa and Walsh 2002).

In contrast to NRPS-dependent, the NRPS-independent pathway relies on a variety of enzyme activities that include monooxygenases, decarboxylases, aminotransferases, ac(et)yltransferases, amino acid ligases, and aldolases (Challis 2005). The NRPS-independent pathway usually occurs in fewer steps than the NRPS-dependent pathway. The siderophores that are commonly made by the NRPS-independent pathway are hydroxamate types, which are usually built in two steps. These steps take advantage of substrate derivatives of various carboxy acids such as acetate (aerobactin), succinate (desferrioxamine E), β-hydroxylbutyrate (pyoverdins and ornibactin C4), or decenoate (rhizobactin 1021) (Miethke and Marahiel 2007).

Siderophores have been found in a variety of terrestrial and marine environments (Sandy and Butler 2009). On the surface, siderophores are found in terrestrial soil, plant rhizospheres, and fresh water. In marine environments siderophores have been found in surface waters of the ocean. Interestingly, siderophores have also been identified in several oligotrophic environments, such as the open-ocean, air, oligotrophic lakes, and cold deserts (Mawji et al. 2008, Sorichetti et al. 2014, Yadav et al. 2015, Boiteau et al. 2016, Vinatier et al. 2016). Siderophores have been identified in oligotrophic caves; however, identifying the ecological roles siderophores have in caves remains to be determined.

The caves in the Guadalupe Mountains are excellent examples of oligotrophic carbonate cave systems. Northup et al. (2003) measured an overall 0.06 wt% of total organic carbon across several samples of ferromanganese deposits in Spider and Lechuguilla caves. Formed from sulfuric acid dissolution of carbonate rock, Spider and Lechuguilla caves are moist with relatively constant 100% humidity and a moderately

warm temperature of approximately 17-18°C or 20°C, respectively (Northup, unpublished). Both caves are completely dark a short distance from the entrance of the caves, and are thus unable to support photosynthesis (Culver and Pipan 2009).

Despite the oligotrophic conditions, microbial biodiversity is rich in oligotrophic cave environments, with a high degree of biodiversity from the Bacteria and Archaea domains (Tomczyk-Żak and Zielenkiewicz 2016). Barton and Jurado (2007) suggest that due to the presence of low amounts of nutrients, which are chemically complex sources of carbon and energy, all high-energy reactions necessary for growth are unlikely to be performed by a single microorganism. Therefore, instead of competition for nutrients, cave bacteria are more likely to be in mutualistic relationships where the high energy cost of siderophore biosynthesis may be shared.

Lechuguilla and Spider caves have several types of cave deposits that include wet carbonate structures, moonmilk, and ferromanganese deposits (FMDs) that may offer the optimal conditions for use of siderophores by cave microorganisms (Northup and Lavoie 2001, Barton and Northup 2007). One of these cave deposits is the FMDs that range in a variety of colors from light pink to jet black (Northup et al. 2003, Spilde et al. 2005). FMDs are the outer most colored layer, which overlies a layer of soft altered bedrock called punk rock, which resides above the unaltered carbonate bedrock (Spilde et al. 2005).

Siderophore production by cave bacterial isolates in Lechuguilla and Spider caves, CCNP

My dissertation focuses on detecting siderophores and identifying siderophore-producing bacteria in Lechuguilla and Spider caves, CCNP, by asking the following questions:

-What culturable bacterial species are present in Lechuguilla and Spider caves, CCNP and what are their growth phenotypes?

-Do these cultured cave bacterial species have the capability to produce siderophores, what type of siderophores are being produced, and which cultured cave bacteria are producing siderophores under low iron conditions?

-What are the nutrient concentrations of cave deposits and is there a correlation between siderophore production and nutrient concentrations?

The results of the investigation of these questions are reported in Chapters 2-4. Chapter 2 takes a closer look at the physiological characteristics of cave bacteria and offers clues to the type of assays that can be used to determine cave-adapted bacteria. This chapter also presents growth curve phenotypes of pure cave bacteria that have not been presented in previous cave bacteria studies. Chapter 3 presents evidence for the capability of cave bacterial isolates to use siderophores. This chapter also addresses the preference of siderophore type and the 16S rRNA phylogenetic studies present details of the identity of bacteria using siderophores. Chapter 4 details the nutrient concentrations of different cave deposits and presents a possible correlation between iron and manganese concentrations and the ability of cave bacterial isolates subcultured from the same deposits to produce siderophores. This study also offers insights and suggestions for future studies to help researchers understand the environments in which siderophores can be produced.

References

Ahmed E, Holmström, SJM. 2014. Siderophores in environmental research: roles and applications. Microbial Biotech 7:196-208.

Ali SS, Vidhale NN. 2013. Bacterial siderophore and their application: a review. Internat J Curr Microbiol App Scien 2:303-312.

HA Barton, Jurado V. 2007. What's up down there? Microbial diversity in caves. Microbe American Society for Microbiology 2:132.

Barton HA, Northup DE. 2007. Geomicrobiology in cave environments: past, current and future perspectives. J Cave Karst Studies 69:163-178.

Boiteau RM, Mende DR, Hawco NJ, McIlvin MR, Fitzsimmons JN, Saito MA, Sedwick PN, DeLong EF, Repeta DJ. 2016. Siderophore-based microbial adaptations to iron scarcity across the eastern Pacific ocean. Proceed Nat Acad Science 113: 14237-14242.

Braun V. 1999. Active transport of siderophore-mimicking antibacterials across the outer membrane. Drug Resis Updat 2:363-369.

Challis GL. 2005. A widely distributed bacterial pathway for siderophore biosynthesis independent of nonribosomal peptide synthetases. ChemBioChem 6:601-611.

Chu BC, Garcia-Herrero A, Johanson TH, Krewulak KD, Lau CK, Peacock RS, Slavinskaya Z, Vogel HJ. 2010. Siderophore uptake in bacteria and the battle for iron with the host; a bird's eye view. Biometals 23:601-611.

Crosa JH, Walsh CT. 2002. Genetics and assembly line enzymology of siderophore biosynthesis in bacteria. Micro and Mol Bio Rev 66:223-249.

Culver DC, Pipan T. 2009. The Biology of Caves and Other Subterranean Habitats. New York, NY: Oxford University Press.

Dave B, Anshuman K, Hajela P. 2006. Siderophores of halophilic archaea and their chemical characterization. Ind J Experi Biol 44:340-344.

Drechsel H, Winkelmann G. 1997. Iron chelation and siderophores. In: Harwood academic publishers, editors. Erspectives in Transition Metal in Microbial Metabolism. Netherlands: Overseas Publishers Association. P 1-50.

Glick BR. 2003. Phytoremediation: synergistic use of plants and bacteria to clean up the environment. Biotechnol Adv 21:383-393.

Grünewald J, Marahiel MA. 2006. Chemoenzymatic and template-directed synthesis of bioactive macrocyclic peptides. Microbio Mol Biol Reviews 70:121-146.

Hider RC, Kong X. 2010. Chemistry and biology of siderophores. Nat Prod Rep 27:637-657.

Leong SA, An Z. 1997. Biosynthetic and Regulatory Aspects of Siderophores. In: Harwood academic publishers, editors. erspective in Transition Metal in Microbial Metabolism. Netherlands: Overseas Publishers Association. P. 51-80.

Madigan MT, Martinko JM, Parker J. 2000. Brock Biology of Microorganisms. 9th ed. New Jersey:Prentice Hall.

Mawji E, Gledhill M, Milton JA, Tarran GA, Ussher S, Thompson A, Wolff GA, Worsfold PJ, Achterberg EP. 2008. Hydroxamate siderophores: Occurrence and importance in the Atlantic Ocean. Environ Science Tech 42:8675-8680.

Miethke M, Marahiel MA. 2007. Siderophore-based iron acquisition and pathogen control. Microbiol Mol Biol Reviews 71:413-451.

Neilands JB. 1981. Iron absorption and transport in microorganisms. Ann Rev Nutr 1:27-46.

Northup DE, Barns SM, Yu LE, Spilde MN, Schelble RT, Dano KE, Crossey LJ, Connolly CA, Boston PJ, Natvig DO, Dahm CN. 2003. Diverse microbial communities inhabiting ferromanganese deposits in Lechuguilla and Spider Caves. Environ Microbiol 5:1071-1086.

Northup DE, Lavoie KH. 2001. Geomicrobiology of caves: A review. Geomicrobiol J 18:199-222.

Sandy M, Butler A. 2009. Microbial iron acquisition: Marine and terrestrial siderophores. Chem Reviews 109:4580-4595.

Sorichetti RJ, Creed IF, Trick CG. 2014. The influence of iron, siderophores and refractory DOM on cyanobacterial biomass in oligotrophic lakes. Freshwater Biol 59:1423-1436.

Spilde MN, Northup DE, Boston PJ, Schelble RT, Dano KE, Crossey LJ, Dahm CN. 2005. Geomicrobiology of cave ferromanganese deposits: A field and laboratory investigation. Geomicrobiol J 22:99-116.

Straub KL, Benz M, Schink B. 2001. Iron metabolism in anoxic environments at near neutral pH. FEMS Microbiol Ecol 34:181-186.

Tomczyk-Żak K, Zielenkiewicz U. 2016. Microbial diversity in caves. Geomicrobiol J 33:20-38.

Vinatier V, Wirgot N, Joly M, Sancelme M, Abrantes M, Deguillaume L, Delort AM. 2016. Siderophores in cloud waters and potential impact on atmospheric chemistry:

Production by microorganisms isolated at the Puy de Dôme Station. Environ Sci Tech 50:9315-9323.

Yadav AN, Sachan SG, Verma P, Saxena AK. 2015. Prospecting cold deserts of north western Himalayas for microbial diversity and plant growth promoting attributes. J Biosci Bioeng 119:683-693.

Physiological Aspects of Cultivable Cave Bacteria from Lechuguilla and Spider Caves in Carlsbad Caverns National Park (CCNP)

Tammi R. Duncan*, Margaret Werner-Washburne, and Diana E. Northup
Department of Biology, University of New Mexico, Albuquerque, New Mexico, 87131

*Corresponding author: Tammi R. Duncan, tammid31@unm.edu

Abstract

Next generation sequencing of the 16S rRNA genes and metagenomic surveys of cave microorganisms have identified a wide range of bacterial diversity in a variety of caves worldwide. However, understanding the roles that these bacteria play in caves and their adaptations to the cave environment requires classical microbiology techniques. To accomplish these goals, we investigated potential oligotrophic characteristics of cave bacteria collected from Lechuguilla and Spider caves in Carlsbad Caverns National Park (CCNP). We hypothesized that Long-term (LT) bacterial isolates collected from parent cultures growing for at least six years total (cave and lab incubation) would have more cave-adapted physiological characteristics than Short-term (ST) bacterial isolates collected from parent cultures growing for less than 26 days total (cave and lab incubation). Using physiological assays (Gram stain, catalase and oxidase enzymes, and growth curves) we analyzed previous parent cultures inoculated with several cave deposits and secondary minerals from Spider and Lechuguilla caves. We isolated 80 LT bacterial isolates and 90 ST bacterial isolates. We found that the majority of all bacterial isolates collected were Gram-positive. The majority of LT bacterial isolates had a catalase/oxidase-negative phenotype. In contrast, the majority of ST bacterial isolates were catalase/oxidase-positive. The ST isolates mostly had a traditional, shorter duration growth curve, while LT isolates had three patterns of growth curves and were longer in duration. Eighteen pure bacterial isolates were identified with 16S rRNA gene sequencing and were classified into the Proteobacteria (Alpha-, Beta-, and Gamma-), Actinobacteria, Firmicutes, and Bacteroidetes phyla. Our results suggest that the

combination of Gram stain, catalase and oxidase enzyme assays, and growth curves may be used to identify oligotrophic cave-adapted bacteria that may possess novel secondary metabolites. These studies shed light on the characteristics of cave-adapted bacteria in the subsurface.
Keywords: oxidase, growth curve, bacteria, subsurface, caves

Introduction

The advent of next generation sequencing has shown that caves have higher microbial diversity than expected in such low nutrient environments (e.g. Engel et al. 2004, Barton et al. 2007, Ortiz et al. 2013). Today, very few microbial ecological studies include classical microbial techniques combined with molecular studies. The investigation of using such classical microbial techniques is of interest to provide essential information for understanding how bacteria survive and best utilize the cave resources available in low nutrient and low energy heterotrophic or chemolithotrophic life styles. The commonplace extreme oligotrophic conditions of caves are likely to drive selective pressures for bacteria to extend growth and survival. These growth and survival characteristics may promote the use of novel relevant bioactive secondary metabolites that otherwise may not be expressed by non-oligotrophic bacteria. Using the physiological and growth curve phenotypes of cave-adapted bacteria would separate the population for further studies of oligotrophic bacteria. Therefore, caves represent a very interesting environment for the study of how oligotrophic cave-adapted bacteria survive.

Large-scale surveys of catalase, oxidase, and Gram status physiological assays of greater than twenty-five cave bacteria are lacking. Smaller studies that included physiological assays with low numbers 8, 15, and 24 of cultivated cave bacteria have been conducted in Grave Grubbo Cave, Crotone, Italy (Cacchio et al. 2012) Pajsarjeva jama Cave, Slovenia (Velikonja et al. 2014), and Krem Syndia Cave, Meghalaya, India (Baskar et al. 2016), respectively. These studies showed a majority of bacterial isolates to be Gram positive, with mixed oxidase and catalase status. However, none of the bacterial isolates cultivated in these studies have included greater than one year parent culture incubation.

Previous studies are important, but inconsistencies of not collecting the catalase, oxidase, and Gram status for all bacterial isolates imposes some limits on their potential use as oligotrophic bacteria phenotypes. Investigations of microorganisms from oligotrophic caves have included limited physiological assays. Furthermore these published studies do not provide a comprehensive survey of microbial physiological attributes in the studied environment. To characterize a newly isolated bacterium requires reporting the catalase, oxidase, Gram status, and optimal temperatures of growth for bacteria, but characterization does not generally include growth curve phenotypes (O'Sullivan et al. 2005, Kim and Jung 2007, Tóth et al. 2017). Nonetheless, these physiological characteristics, including growth curves, are an important part of a description of a microbial community, especially in oligotrophic environments, where cultivation is rarely combined with molecular studies. By combining cultivation with molecular studies we are able to improve the foundation of our understanding of cave microbial physiology in the era of high-throughput sequencing.

To provide these crucial data, this study completed physiological assays of cave bacterial isolates that were subcultured from Long-term (LT) parent cultures (growing for at least six years total) and Short-term (ST) parent cultures (growing for less than 26 days total). These physiological assays included catalase, oxidase, Gram status, and growth curves. We hypothesized that the LT isolates would have more cave-adapted physiological features that would include catalase/oxidase negative, Gram-positive, and a longer growth curve time period compared to the ST isolates. To our knowledge, this study is the first to identify physiological characteristics of potential oligotrophic microorganisms on LT and ST bacterial isolates collected from the same caves.

Materials and Methods

Site and sample descriptions

We sampled from Spider and Lechuguilla caves, CCNP that formed in the moderately dissected tilted plateau composed of the Giant reef and back reef strata, above the Guadalupe Escarpment, in the Guadalupe Mountains (Hayes 1964, Palmer and Palmer 2009). Within the same unit of the Giant reef and back reef strata, Spider Cave formed and has 8.13 km of passageway with 41.5 m of vertical overhead extent (Gulden

2014). Lechuguilla Cave formed also within the unit of the Giant reef and back reef strata, and formed 222.6 km of passageway and 489 m of vertical overhead extent (Gulden 2014).

Three groups of cave deposits were collected. Punk rock is a porous layer of the cave wall bedrock. Ferromanganese deposits (FMDs) range from light pink to jet black and have a light and fluffy texture. These deposits usually contain a higher amount of Fe- and Mn-oxides (Northup et al. 2003, Spilde et al. 2005). Rimstone, popcorn, flowstone, column, white dots, spar knob, upper lip, and knobby spar are all carbonate structures.

Sample collection for Parent cultures

To collect cave deposits for inoculation of LT parent cultures, a sterile loop was used to collect sample from the cave walls or cave structures (Supplementary Table S1). The sterile loop with cave deposits was stabbed into four sterile test tubes of basal medium, enriched, or not enriched, with reduced manganese (Mn) or iron (Fe). The basal medium was composed of the following (per liter): 0.5g NaCl, 0.5g $CaCO_3$, 0.5g $MgSO_4 \cdot 7H_2O$, 0.75g K_2HPO_4 , 0.25g NaH_2PO_4, 0.1g KNO_3. For semisolid agar consistency, 4g/l Bacto agar was added. For Mn enrichments, 0.02g/l of $MnCl_2$ was added and for Fe enrichments, one sterile, reduced iron carpet tack was added to the bottom of the test tube before the media were poured. The LT inoculated test tubes were incubated in the cave and transported in a cooler to a lab incubator for the incubation times listed in Supplementary Table S3.

To collect cave deposits for inoculation of ST parent cultures, a sterile BD polyester fiber tipped application swab (Falcon) moistened with sterile 1X Ringer's solution were used to collect cave deposits followed by streaking onto five types of sterile agar media (Supplementary Table S2). The 1X Ringer's solution was made as follows per liter: 7.2g NaCl, 0.37g KCl, 0.17g $CaCl_2$, reagent grade H_2O, and pH adjusted to 7.3-7.4. The media types are: ½ Reasoner's 2A medium (R2A, Difco™, Sparks, MD), ½ R2A with rock flour (Lower Guadalupe Mountains limestone that was pulverized in a rock crusher and autoclaved), BG11 (Difco 1984), Actinomycetes Isolation Agar (AIA, Difco™, Sparks, MD), and AIA with nyastatin (0.072mg/ml). The ST inoculated agar

plates were incubated in the cave and transported in a cooler to a lab incubator for the incubation times listed in Supplementary Table S3.

Collecting bacterial isolates from Parent cultures

A sterile loop was used to collect a loop-full of cells from parent cultures and spread as a lawn on sterile subculture isolation agar media plates. Bacterial isolates from LT parent cultures were subcultured on three types of plates, R2A with $FeCl_3$ (0.005g/l), R2A with $MnCO_3$ (0.05g/l), and AIA with $FeCl_3$ (0.005g/l) and $MnCO_3$ (0.05g/l). Bacterial isolates from ST parent cultures were subcultured on ½ R2A agar plates (Supplementary Table S3). The inoculated subcultured isolation agar plates were incubated at 20°C and individual colonies were picked over time, less than 25 d for LT subcultures and less than seven days for ST subcultures. The bacterial isolates were restreaked onto new/sterile original subculture isolation agar plates. Each bacterial isolate was grown in subculture isolation broth media for preparation of 20% glycerol freezer stocks, and stored at -80°C.

Physiological characterizations

Gram stain, catalase, and oxidase assays were determined according to procedures listed in Lammert (2007). Briefly, bacterial isolates were streaked onto original subculture isolation media agar plates from freezer stocks and incubated at 20°C. A sterile loop was used to transfer a minimum amount of cells from incubated cultures to a microscope slide and assays completed. Three replicates of the catalase and oxidase analysis were completed. The Gram stain result was used to determine if bacterial isolates were composed of one cell shape for purity. Subsequently, the pure bacterial isolate was sequenced; a clean sequence chromatograph confirmed the purity of bacterial isolate.

Growth curve analysis

Bacterial isolates were streaked from freezer stocks and grown on individual subculture isolation media agar plates for three days at 20°C. Subsequently, a sterile loop was used to heavily streak a lawn of cells on sterile ISP4 with $FeSO_4$-$7H_2O$ agar plates (4

g/l soluble starch, 0.3 g/l casein, 2 g/l KNO_3, 0.5 g/l $MgSO_4 \cdot 7H_2O$, 0.02 g/l $CaCO_3$, 0.01 g/l $FeSO_4 \cdot 7H_2O$ and 25 g/l agar) and incubated at 20°C for seven days. For growth curves, an overnight culture of bacterial isolates were prepared by transferring a sterile loop of cells from ISP4 with $FeSO_4$-$7H_2O$ agar plates to three ml of ISP4-no added $FeSO_4$-$7H_2O$ (4 g/l soluble starch, 2 g/l KNO_3, 0.5 g/l $MgSO_4 \cdot 7H_2O$, 0.02 g/l $CaCO_3$, 1 g/l yeast extract) liquid medium and grown approximately 12-15 hours, rolling at 40 rpm, in a dark 20°C incubator. From overnight liquid cultures, approximately 100,000 cells/ml were used to start three ml of sterile ISP4-no added $FeSO_4$-$7H_2O$ liquid broth. An uninoculated control was included. The OD_{600} were collected over time using a Biomate 3 Spectrometer (Thermo Spectronic, Houston, TX). Three replicates were completed for each growth curve.

DNA isolation and sequencing

Due to the mixed nature of most of the isolates, eighteen pure bacterial isolates from freezer stocks were inoculated aseptically onto individual subculture isolation media agar and incubated at 20°C for three days. DNA extraction of cultured cells was carried out following the manufacturer's procedures of the MoBio UltraClean Microbial DNA Isolation kit (MoBio, Carlsbad, CA). The 16S rRNA gene (1384 bp) was amplified with 8F (5'-AGAGTTTGATCCTGGCGCAG-3') and 1492R (5'-GGTTACCTTGTTACGACTT-3') bacteria primers (Lane 1991). Briefly, reactions were carried out in a 25 µl volume with 10X PCR buffer with 15 mM Mg^{2+}, 0.3 µM of each primer, 0.25 mM of each dNTPs, 5 µg of 50 mg/ml BSA (Ambion Austin, TX, USA) and 1U Ampli-Taq LD (Applied Biosystems, Foster City, CA, USA). The PCR reaction was performed with an MJ thermocycler with the program, 94°C for 5 min, 30 cycles at 94°C for 30 s, 55.5°C for 30 s, 72°C for 1.5 m and final extension at 72°C for 7 m. The PCR amplicons were purified using ExoSAP-IT ® (Affymetrix, Santa Clara, CA) and used as a template for in-house BigDye 1.1 sequencing with 46F (5'-GCYTAAYACATGCAAGTCG -3') and 1409R (5'-GTGACGGGCRGTGTGTRCAA -3'). In-house sequencing and assembly was performed with ABI 3130 and 377 Automated DNA Sequencers.

Operational taxonomic unit (OTU)-based analysis and phylogenetic analysis

Sequencing was performed with ABI Prism 3130 Automated DNA Sequencer at UNM-Molecular Biology Facility, Albuquerque, NM. Using Sequencer 5.1 (Gene Codes Corp., Ann Arbor, MI) ambiguous portions were trimmed, edited, and aligned. The trimmed sequences had greater than 90% sequence quality. Operational taxonomic units (OTUs) were determined using a custom MATLAB script that measured similarity between each OTU. The contigs that were ≥98.9% similar were considered an individual OTU. Using a selection process of the following criteria was used: at least two bacteria from all different genera; cultured bacteria; and uncultured representative taxonomic assignments downloaded from BLAST (Altschul et al. 1990). A chimera check of all sequences was completed using QIIME v.1.9.1 program**.** A sequence alignment was performed using default parameters of EMBL-EBI webPRANK (http://www.ebi.ac.uk/goldman-srv/webprank/) and subsequently a similarity matrix was determined using a custom R script. A maximum likelihood tree was determined by using IQ-TREE web server: fast and accurate phylogenetic trees under maximum likelihood (http://iqtree.cibiv.univie.ac.at/) with 1000 replicates (Minh et al. 2013). The tree files were visualized and annotated with the interactive Tree of Life (iTOL) v.3.5.3 program (http://itol.embl.de/) and vector-drawing program Inkscape v.0.92.1.

Results

Cultivation of LT and ST bacterial isolates from parent cultures

A total of 170 bacterial isolates were collected. To select for the most oligotrophic type of bacterial isolates, 80 bacterial isolates were subcultured from four LT parent cultures that were inoculated in situ and incubated according to incubation times listed in Supplementary Table S3. These LT isolates were collected from fewer parent cultures, at least 13 isolates/parent culture (Supplementary Table S1). To select for a wide spectrum of cave bacterial isolates, 90 bacterial isolates were subcultured from 40 ST parent cultures that were inoculated in situ and incubated according to the incubation times listed in Supplementary Table S3. These ST isolates were collected from more parent plates, 2-3 isolates/parent plate (Supplementary Table S2).

Physiological characteristics of LT and ST bacterial isolates

Fifty-one percent of the LT bacterial isolates tested catalase/oxidase negative, while 19% tested catalase/oxidase positive. Eighteen percent tested catalase positive/oxidase negative, while 12% tested catalase negative/oxidase positive. The majority (43%) of LT bacterial isolates were gram positive compared to gram negative (21%) and both (36%) (Supplementary Figure S1).

Thirty-nine percent of the bacterial isolates were catalase/oxidase positive, 16% were both catalase/oxidase negative, 23% were catalase positive/oxidase negative, and for catalase negative/oxidase positive there was 22%. Overall, the ST bacterial isolates constituted 39% versus 19% in the LT bacterial isolates for catalase/oxidase positive (Figure 1). Thus, the LT and ST bacterial isolates are reversed in their catalase/oxidase status. The majority (45%) of ST bacterial isolates were gram positive compared to gram negative (14%) and both (41%) (Supplementary Figure S1).

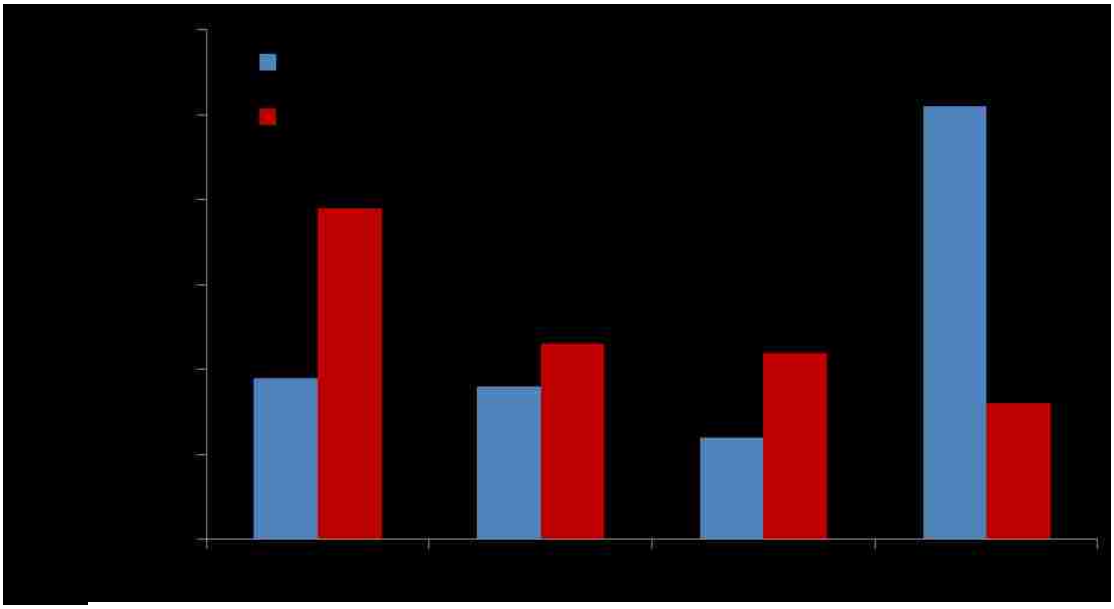

Growth curve analysis of LT and ST bacterial isolates

Eighteen growth curves were measured to early stationary phase for the pure bacterial isolates and classified into three general phenotypes: Traditional, Biphasic, and Irregular (Table 1, Figure 2). The majority of bacterial isolates with the Traditional phenotypes measured to early stationary within eight days (Table 1, Figure 2A). Half of the Biphasic growth curves measured to a second early stationary phase in less than eight days, while the other half entered the second early stationary growth phase within 15 days (Table 1, Figure 2B). The bacterial isolates that classified into the Irregular phenotype started with a traditional or biphasic growth pattern and at approximate three days transferred into an irregular growth pattern with large deviations (Figure 1C, Table 1).

With the exception of bacterial isolate 1-28, the majority of the bacterial isolates that had a less than 0.4 maximum optical densities (OD_{600}) had a Traditional growth phenotype and completed their growth cycle to early stationary phase in less than eight days. With the exception of bacterial isolate 2-42, the majority of bacterial isolates that had an OD_{600} greater than 0.4 had a Biphasic or Irregular phenotype and completed their growth curve to early stationary phase in greater than eight days (Table 1). Overall, LT growth phenotypes had Traditional, Biphasic, and Irregular growth phenotypes whereas ST had Traditional and Biphasic growth phenotype.

Table 1. Growth Curve Phenotypes of Eighteen Pure Bacterial Isolates

Group	Bacterial Isolate	Growth Curve Phenotype	Growth Curve period (days)	OD_{600} (STD)
LT	1-12	Traditional	3	0.250 (.027)
	1-13	Traditional	3	0.283 (.001)
	1-18	Irregular	14	0.990 (.110)
	1-20	Traditional	3	0.265 (.005)
	1-22	Traditional	3	0.332 (.008)
	1-23	Traditional	4	0.358 (.003)
	1-28	Biphasic	5	0.359 (.001)
	1-30	Biphasic	15	1.390 (.036)
	1-33	Biphasic	15	1.587 (.034)
	1-43	Traditional	3	0.309 (.005)
	1-44	Irregular	15	1.394 (.527)
	1-47	Irregular	5	0.679 (.272)
ST	2-13	Traditional	2.5	0.236 (.006)
	2-22	Traditional	1.5	0.238 (.010)
	2-33	Traditional	2.5	0.346 (.023)
	2-42	Traditional	6	1.825 (.028)
	2-65	Traditional	2	0.163 (.005)
	2-83	Biphasic	7.5	1.197 (.008)

LT-Long-term, ST-Short-term, STD-Standard deviation

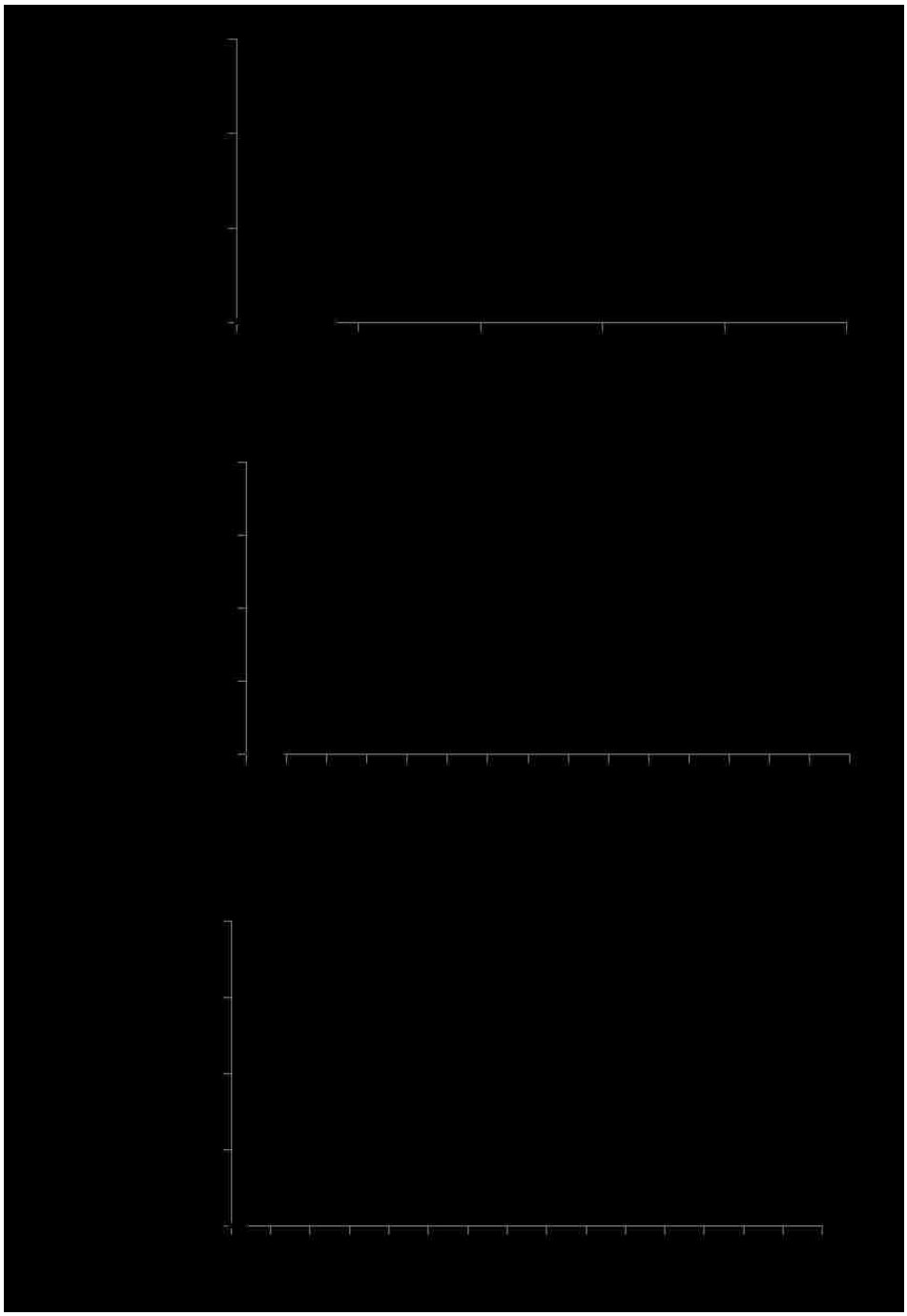

Phylogenetic tree of pure bacterial 16S rDNA sequences from LT and ST bacterial isolates

Due to the mixed nature of most isolates, only eighteen pure bacterial isolates were sequenced. The phylogenetic analysis of 16S rDNA gene sequences of the eighteen pure bacterial isolates classified into four phyla: the Proteobacteria (Alpha-, Beta-, and Gamma- classes), Bacteroidetes, Firmicutes, and Actinobacteria (Table 2, Figure 3). Fifty-six percent of the pure sequences were closest relatives to members in the Proteobacteria (data not shown). In the Alphaproteobacteria class, the isolates were closely related to the *Sphingopyxis*, *Rhizobium*, and *Brevundimonas* genera. In the Betaproteobacteria class, the isolates were closely related to the *Achromobacter* genus. In the Gammaproteobacteria class, the isolates were closely related to the *Acinetobacter* and *Pseudomonas* genera. There was one isolate that was closely related to an uncultured bacterium clone CN2 80, recovered from polycyclic aromatic hydrocarbons (PAH)-contaminated soil from Lugones, Asturias, Spain (Guazzaroni et al. 2013)(Table 2).

Table 2. Phylogenetic 16S rDNA Closest Identified Relatives of Eighteen Pure Bacterial Isolates.

Group	Isolate	Length (bp)	Phylogenetic group	Closest identified relative	Identity (%)
LT	1-12	1290	Gammaproteobacteria	UC bacterium clone CN2 80	99
	1-13	1275	Bacteroidetes	*Olivibacter soli* Gsoil 034	99
	1-18	1282	Betaproteobacteria	*Achromobacter spanius* SMV	99
	1-20	1275	Bacteroidetes	*Fluviicola* sp. THG-D9	99
	1-22	1275	Bacteroidetes	*Fluviicola* sp. THG-D9	99
	1-23	1202	Alphaproteobacteria	*Brevundimonas basaltis* 02-9	99
	1-28	1248	Betaproteobacteria	*Achromobacter spanius* SMV	99
	1-30	1233	Alphaproteobacteria	*Sphingopyxis* sp. DA6	99
	1-33	1223	Alphaproteobacteria	*Brevundimonas basaltis* sp. J22	99
	1-43	1289	Bacteroidetes	*Chitinophaga* sp. CHS10	98
	1-44	1251	Alphaproteobacteria	*Rhizobium* sp. RK12	98
	1-47	1265	Actinobacteria	*Intrasporangiaceae* sp. Aza8	99
ST	2-13	1253	Gammaproteobacteria	*Pseudomonas* sp. LZNT2	99
	2-22	1259	Gammaproteobacteria	*Pseudomonas* sp. N4	99
	2-33	1266	Actinobacteria	*Microbacterium oxydans* N142b2	99
	2-42	1257	Actinobacteria	*Arthrobacter oxydans* BJC15 B31	99
	2-65	1258	Gammaproteobacteria	*Acinetobacter johnsonii* MM21	99
	2-83	1299	Firmicutues	*Bacillus* sp. L53	99

UC-uncultured, All isolates had a query percent of 98-100%. LT- Long-term, ST-Short-term. Identity percent is BLAST.

Forty-four percent of the pure sequences grouped with closest relatives in non-Proteobacteria (data not shown). In Bacteroidetes, bacterial isolates were closely related to the *Chitinophaga*, *Olivibacter*, and *Fluviicola* genera. In the Actinobacteria, *Microbacterium* and *Arthrobacter* genera were identified. In addition, one isolate grouped with an undescribed species within the Intrasporangiaceae family. In the Firmicutes phylum, one isolate was closely related to a member in the *Bacillus* genus (Table 2).

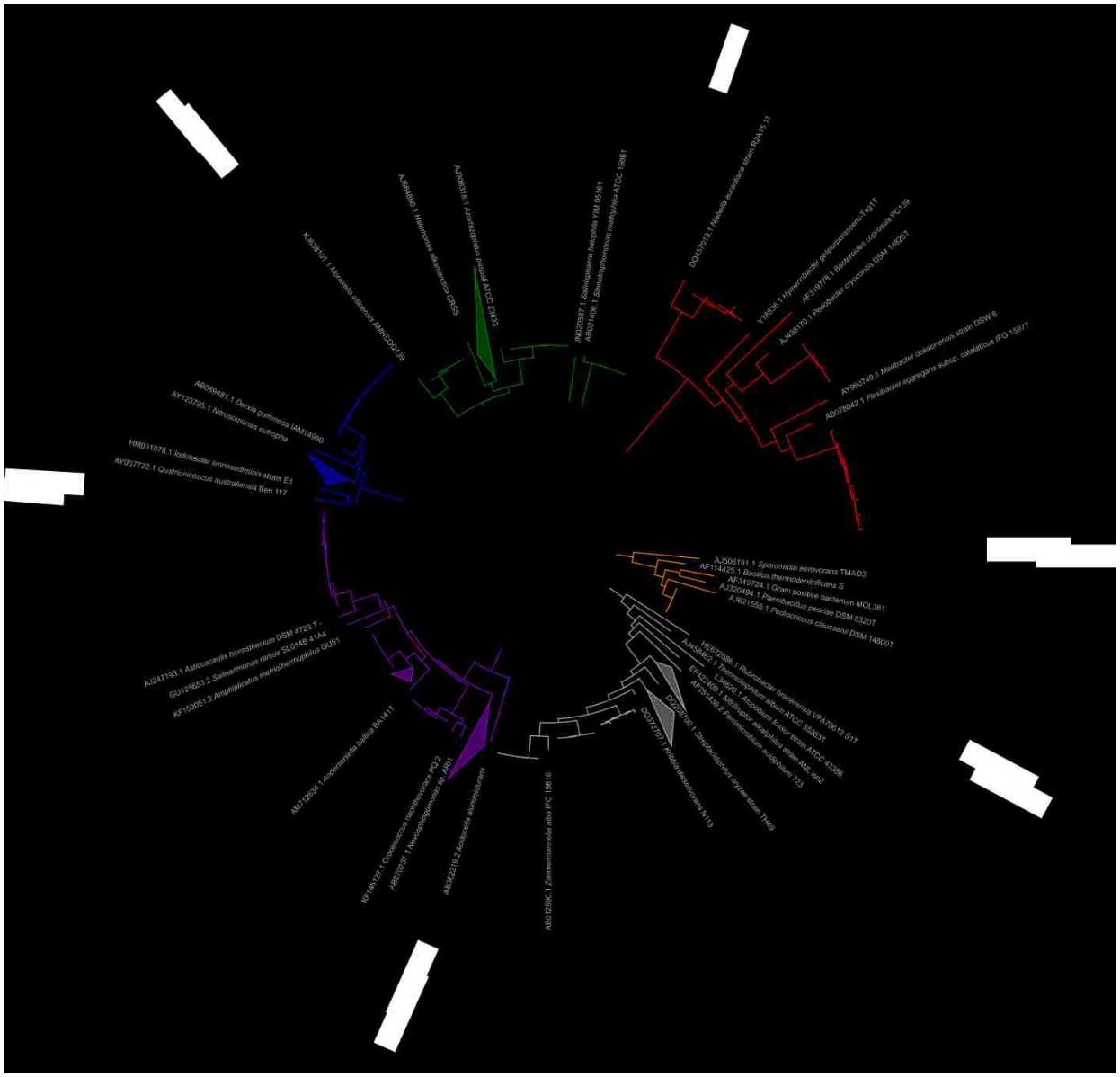

Figure 3. Phylogenetic 16S rDNA tree of pure bacterial isolates. Ultrabootstrap values are >70% on 1000 replicates. The scale bare corresponds to 0.1 nucleotides substitutions per site. LT strains start with 1- and ST strains start with 2- for sequence names. Color code of branches: Grey-Actinobacteria, Orange-Firmicutes, Purple-Alphaproteobacteria, Blue-Betaproteobacteria, Green-Gammaproteobacteria, and Red-Bacteroidetes. Grey name is reference strains and triangles are collapsed reference strain clades.

Discussion

Microbial diversity from uncultured or cultured bacteria has been described in several caves around the world (Tomczyk-Żak and Zielenkiewicz 2016). However, the physiological characteristics of cultivable cave bacteria of more than twenty-five isolates have yet to be described. Gram positive phenotypes seem to be common for cave bacteria (Cacchio et al. 2012, Velikonja et al. 2014, Baskar et al. 2016), but combined with catalase and oxidase phenotypes may be used to distinguish oligotrophic bacteria in cave environments. By targeting the oligotrophic bacteria subsequent examinations of these bacteria for potential novel secondary metabolites can be completed. Characterization of these physiological traits will also shed light on how bacteria adapt to cave environments.

We found that at least eighty percent of 170 mixed bacterial isolates was gram positive or had at least one bacterial member of the mixed isolate that was gram positive. The preference for the thicker peptidoglycan (PG) may be related to the bacterium's ability to remodel PG for a potential source of carbon, nitrogen (N), and energy during nutrient deprivation periods. Gram positive bacteria contain up to 90% PG of cell weight in contrast to Gram negative bacteria that contain up to 10% of cell weight (Liedy 2004). PG can be remodeled by *E. coli* in response to N-starvation (Gyaneshwar et al. 2005). Gyaneshwar et al. (2005) showed that in rich media, *E. coli* makes all of its PG-crosslinks using diaminopimelic acid (DAP) to D-Alanine (D-Ala), with only a few DAP-DAP crosslinks. However, during N-starvation the amount of DAP-DAP crosslinks increases. This change allows *E. coli* to recover D-Ala from PG to use as a nitrogen source. Cave bacteria potentially may remodel their PG for carbon, nitrogen, or energy. However, more research is needed to determine whether cave bacteria employ PG remodeling.

We found that the majority of LT bacterial isolates were catalase/oxidase negative. This catalase/oxidase negative nature may be related to the LT bacterial isolates' preference for fermentative metabolism. Northup et al. (2003) showed the presence of bacterial members of Lactobacilleaceae and Streptococcaceae in Lechuguilla Cave. The presence of Lactobacillaeceae members have also been shown in Spider Cave studies (J. Kimble 2017, unpublished). *Lactobacillus* spp., a common soil organism of the Lactobacilleaceae, do not have cytochromes and rely on fermentation metabolism (Neilands 1994). Thus, the lack of cytochromes would bypass the need for iron, therefore allowing one less need for an already limited nutrient.

Along with fermentation as a possible mechanism to bypass the need for catalase, cave bacteria might use flavoproteins for removal of radicals contributing to oxidative stress. Flavoproteins have been described in the Archaea and Bacteria domains and may be used by anaerobic chemotrophic microorganisms for energy conservation (Wasserfallen et al. 1998, Herrmann et al. 2008). Further research would be needed to explore whether cave microorganisms prefer fermentation metabolism or use flavoproteins.

We found that pure cave bacterial isolates have similar growth curve phenotypes to the surface model organisms, *E. coli* and *B. subtilis*. Several of the cave bacteria had a Traditional (Lag-Log-Stationary Phase) growth curve, which was very similar to the soil bacterium *B. subtilis*. Although we expected the cave bacteria to have a similar growth curve, we also hypothesized that the more cave-adapted bacteria would take longer to complete the growth curve and have a lower overall cell density. *B. subtilis* completed its Traditional growth curve in approximately one day with overall maximum OD_{600} of approximately 1.0. Our cave bacteria had completed their Traditional growth cycle at a minimum of two days and had an overall maximum OD_{600} of approximately 0.4.

The OD_{600} 0.4, a culture with less cells or with less cell mass, may be related to oligotrophic cave bacteria that preferred less crowding in a culture for peak diversity in a low nutrient environment. Velikonja et al. (2014) completed serial dilutions 10^{-1} to 10^{-3} of a one ml suspension of cave silver morphotypes and plated 100 µl on seven different media. By counting colony forming units, Velikonja et al. (2014) showed that a greater diversity of bacteria grew in higher dilutions (10^{-3}) when compared to lower dilutions

(10^{-1}). It may be that our bacterial isolates also have a preference for less crowding, thus causing the lower cell density. Another variation of the growth curves was that cave bacteria completed their growth curves at a minimum of two days, which is at least a day longer than *B. subtilis*. This longer growth time combined with a lower overall OD_{600} is potentially a common feature of oligotrophic cave-adapted bacteria.

We found a subset of cave bacteria had a Biphasic (Lag-Log-Lag-Log-Stationary Phase) growth curve, which usually took five to fifteen days to measure a growth cycle to a second early stationary phase. This Biphasic growth cycle may be related to the diauxic growth cycle that occurs when a preferred carbon source is used up then a secondary source of carbon is used (Monod 1949). Monod (1949) showed that *E.coli* completes a diauxic growth curve when glucose is used up and then a second carbon source is used. We hypothesize that diauxic growth maybe a key feature of cave dwelling bacteria. Thus, completing an adjustment in carbon source, or a lag phase, may extend the growth of oligotrophic cave bacteria. This extension could be possibly up to two years in a lab batch culture, which has been shown by bacteria previously isolated from Lechuguilla Cave (personal communication, P. Boston 2017).

We found a subset of Irregular growth curves only found in the LT group (Figure 2C). These cave bacteria started in a Traditional growth phenotype and approximately three days into their growth curves the curves became erratic. These erratic OD_{600} readings were caused by the bacterial isolates becoming clumpy or sticking to the test tube after three days (data not shown). Future studies will add low amounts of tween or glycerol to the cultures to prevent cells from clumping, which we hypothesize to lead to the growth curves reverting to Traditional or Biphasic growth curves.

We identified bacterial sequences from Lechuguilla and Spider caves that classified into Proteobacteria (Alpha-, Beta-, and Gamma- classes), Actinobacteria, Firmicutes, and Bacteroidetes. Previous phylogenetic studies of Lechuguilla Cave showed that Proteobacteria (Alpha-, Beta-, and Gamma- classes), Actinobacteria, Firmicutes, and Bacteroidetes were consistently found (Northup et al. 2003, Barton et al. 2007). These phyla were also identified in limestone Herrenberg Cave in Germany and Magura Cave in Bulgaria (Rusznyák et al. 2012, Tomova et al. 2013). Not including the Bacteroidetes phylum, the remaining phyla were identified in other karstic caves (Ikner et

al. 2007, Dominguez-Monino et al. 2014, Velikonja et al. 2014, Baskar et al. 2016) making Proteobacteria, Actinobacteria, and Firmicutes common cultivated bacteria in world-wide cave environments. Furthermore these phyla are also consistent with other oligotrophic environments, including Antarctica soil, Atacama Desert soil, and in heavy metal enriched terrestrial environments (Chong et al. 2012, Zhang et al. 2012, Bull and Asenjo 2013).

The bacteria identified offer clues to how the microbial communities are surviving in an oligotrophic cave environment. We found closest relatives that suggest bacterial capabilities that are involved with exchanges within the rhizosphere, i.e. scavenging for essential nutrients, degrading a wide-range of organic acids, nitrogen-fixation, commensal relationships with other bacteria or a plant nodules, and resistance to heavy metals in contaminated sites. These characteristics may be related to pathways for nutrient exchange processes of bacteria in oligotrophic environments.

We identified closest relatives of four bacterial isolates, *Brevundimonas basaltis*, *Pseudomonas* sp. LZNT2, *Pseudomonas* sp. N4, and *Acinetobacter johnsonii* MM2-1, that were related to genera previously identified in Lechuguilla Cave (Barton et al. 2007). In addition, *Achromobacter* sp. was identified as a cave bacterial genome in the BLAST database (Altschul et al. 1990). *Brevundimonas* sp. has the ability to break down a wide-range of organic materials for non-fermentative respiration releasing organic by-products (Segers et al. 1994). *Pseudomonas* sp. and *Acinetobacter* sp. are potential chemolithotrophic energy-deriving microorganisms that have been shown to reduce Arsenic $(Ar)^{V}$ and Chromium $(Cr)^{VI}$ metals, respectively (Francisco et al. 2002, Fernandez et al. 2016).

Similar to other karst cave studies, we identified *Bacillus* sp., *Rhizobium* sp., *Sphingopyxis* sp., *Microbacterium* sp., *Arthrobacter* sp., and an Intrasporangiaceae sp. family member (Groth 2001, Spilde et al. 2005, Velikonja et al. 2014, Fang et al. 2017). Remarkably, several of the bacteria have been described in commensal-types of relationships. *Microbacterium* sp., *Rhizobium* sp., and *Bacillus* sp. have been described in a commensal relationship as a plant endophyte (Afzal et al. 2017). *Rhizobium* sp. has commonly been described as an N-fixation microorganism, which would benefit a microorganism where there is limited-nitrogen (Ludwig 1984). In an interspecies

communication for manganese (Mn)-oxidation, the Mn^{II}-oxidizing gene of *Arthrobacter* sp. is triggered in the presence of *Sphingopyxis* sp. (Liang et al. 2017). Furthermore, cave bacteria identified as closest relatives to *Bacillus* sp., *Sphingopyxis* sp, and *Arthrobacter* sp., have been shown to be siderophore-producers (T.R. Duncan 2017, unpublished). Siderophores have been shown to promote growth of uncultivable bacteria and are shared or cross-fed among cave bacteria in a cooperative relationship (D'Onofrio et al. 2010, O.S. Hershey 2014, unpublished). *Knoellia* sp., in the Intrasporangiaeceae family, has been identified as a rare Actinobacteria from Sigangli Cave in Yumman, China (Fang et al. 2017).

We identified surface-residing bacteria that have not been previously identified in caves. These isolates, from the LT group, were identified as *Chitinophaga* sp., *Olivibacter* sp., and *Fluviicola* sp., members of the Bacteroidetes phylum. Bacteroidetes members are known as degraders of complex organic matter and have been described to share a mutualistic relationship with an animal host (Bäckhed et al. 2005, Thomas et al. 2011). Cheng et al. (2016) described chemoheterotrophic *Chitinophaga jiangningensis* JN53 as a mineral-weathering bacterium, which increases mineral dissolution rates by producing organic acid byproducts. In turn, organic acid byproducts can be made into hydroxamate-siderophores, which could be used to gather needed iron (Miethke and Marahiel 2007). *Olivibacter sitiensis* is a heterotroph and described as a diphenol degrader of the catechol pathway (Ntougias et al. 2014). By having this ability it could be a possible indication of breaking down phenol-containing compounds as an energy source. Phenol-containing compounds may be present in the cave because the caves of the Carlsbad Caverns formed in the Delaware Basin where there is presence of crude oil (Hill 2000). *Fluviicola taffensis* was isolated from water of the River Taff, Cardiff, UK and has been described in high arsenic ground water (Zhang et al. 2017). While these bacteria have potential characteristics that may help them survive in an oligotrophic cave environment, how these bacteria survive in the cave environment remains to be determined.

Conclusions

Our findings shed light on the physiological characteristics of oligotrophic bacteria isolated from caves. LT isolates revealed that having a catalase/oxidase negative and gram-positive nature may enhance survival in the deep subsurface. These isolates may have a preference for possible fermentative respiration, which could enhance the microorganism's ability to survive in arid or semi-arid caves, where conditions are generally more nutrient-limited. Whether these characteristics are typical for oligotrophic bacteria in other oligotrophic environments remains to be determined.

The study of cave microbial physiological characteristics is significant for identifying and targeting oligotrophic cave isolates for discovering potential novel pharmaceutical secondary metabolites. An ongoing search for new antibiotics and secondary metabolites from unexplored ecosystems with oligotrophic bacteria is promising. Additionally, characterization of the physiological traits of cave bacteria will shed light on how they have adapted to oligotrophic cave environments.

Acknowledgements

We thank Penelope Boston and Larry Barton for helpful discussions. We are grateful to Jenny Hathaway, Ara Winter, Jason Kimble, and Dave Hansen for technical assistance. We would also like to thank the staff at the Cave Resources Office at Carlsbad Caverns National Park for granting our collection permit and Patricia Seiser for assistance with sample collection. We thank the UNM Molecular Biology Core Facilities for equipment and DNA sequencing, supported by the National Institute of General Medical Sciences and the National Institute of Health under award number P30 GM110907. The research reported in this publication is solely the responsibility of the authors and does not represent the official views of the National Institutes of Health. This research would not have been possible without the funding provided by the Initiative to Maximize Student Development (IMSD) at UNM Biology and the American Society for Microbiology (ASM) Robert D. Watkins Graduate Research Fellowship.

Supplemental Table S1. Long-term parent cultures and sample type and total subcultured bacteria isolates (n=80).

Parent Cultures	Parent Media	Cave	Parent Sample type	No. of isolates collected from subculture media			Total
				R2A[a]	R2A[b]	AIA[a,b]	
011505-14	Mn-enriched	Spider	Yellow FMD	21	14	5	41
Fe+C[1] 011101-72	Oxidized-Fe enriched	Lechuguilla[c]	Brown and orange FMD	5	8	0	13
Mn+P_o 011101-63	Mn-enriched	Lechuguilla[c]	Punk Rock	6	6	2	14
Mn- C_o 011101-48	No enrichment	Lechuguilla	Brown and orange FMD	4	6	3	13
Total				36	34	10	80

[a]-$FeCl_3$ added, [b]-$MnCO_3$ added, [c]-EA sample site, Ferromanganese deposit (FMD), P-Punk rock white with brown flecks color, Fe+-with cofactors, Mn^+ -with cofactors, Mn^- -with no cofactors, P_o- Punk rock $2x10^{-1}$, C_1-FMD $2x10^{-2}$, and C_o- FMD 2x10

Supplementary Table S2. Short-term Parent cultures, sample location and type, and total subcultured bacterial isolates (n=90).

Location	Parent Cultures	Parent Media	Parent Sample Type
EA Junction	L120303-2[a]	½ R2A+ rock flour	Grey FMD
	L120303-3[a]	BGII	Grey FMD
	L120303-5[a]	AIA	Grey FMD
	L120303-6[a]	½ R2A	Brown FMD
	L120303-10[a]	AIA	Brown FMD
	L120303-12[a]	½ R2A+ rock flour	Punk rock
	L120303-14[a]	AIA+ nystatin	Punk rock
	L120303-17[a]	½ R2A+ rock flour	Yellow FMD
	L120303-18[a]	BGII	Yellow FMD
	L120303-20[a]	AIA	Yellow FMD
Lake Chandelar	L120303-21	½ R2A	Wet Plain Carbonate
	L120303-22	½ R2A+ rock flour	Wet Carbonate Rimstone
	L120303-28	BGII	Carbonate Flowstone
	L120303-30	AIA	Carbonate Flowstone
	L120303-32	½ R2A+ rock flour	Moist Carbonate Flowstone
	L120303-35	AIA	Moist Carbonate Flowstone
	L120303-36	½ R2A	Popcorn[b]
	L120303-37	½ R2A+ rock flour	Popcorn [b]
	L120303-38	BGII	Popcorn [b]
	L120303-40	AIA	Popcorn [b]
Tower Place	L120304-41	½ R2A	Carbonate Flowstone
	L120304-43	BGII	Carbonate Flowstone
	L120304-47	½ R2A+ rock flour	Carbonate Column
	L120304-48	BGII	Carbonate Column
	L120304-49	AIA+ nystatin	Carbonate Column
	L120304-52	½ R2A+ rock flour	Red FMD
	L120304-53	BGII	Red FMD
	L120304-55	AIA	Red FMD
	L120304-57	½ R2A+ rock flour	Carbonate Column
	L120304-58	BGII	Carbonate Column
Briny Pool	L120305-81	½ R2A+ rock flour	White Carbonate Dots
	L120305-82	BGII	White Carbonate Dots
	L120305-84	AIA	White Carbonate Dots
	L120305-85	½ R2A	Carbonate Spar Knob
	L120305-87	BGII	Carbonate Spar Knob
	L120305-88	AIA+ nystatin	Carbonate Spar Knob
	L120305-89	AIA	Carbonate Spar Knob
	L120305-91	½ R2A+ rock flour	Carbonate Upper Lip
	L120305-94	AIA	Carbonate Upper Lip
	L120305-95	½ R2A	Carbonate Knobby Spar

a. Three bacterial isolates were taken from each parent culture. All locations are in Lechuguilla Cave. b- Carbonate popcorn structure with dusting of soil.

Supplementary Table S3. Overall incubation times for Long-term (LT) and Short term (ST) parent cultures.

Parent Culture		Parent Cave incubation	Parent Lab incubation	Total Parent incubation	Subculture Isolation media[a] Lab incubation
LT	011505-14	6y	5y	≤11y	≤ 25d
	Fe^{+} C^{1}011101-72	1-3d	10y	≤10y 3d	≤ 25d
	Mn^{+} P^{o} 011101-63	1-3d	10y	≤10y 3d	≤ 25d
	Mn- C^{o} 011101-48	1-3d	10y	≤10y 3d	≤ 25d
ST	All parent cultures	1-3d	23d	≤26d	≤7d

a. Isolation subculture media for LT are R2A+$FeCl_3$, R2A+$MnCO_3$, AIA+$FeCl_3$+$MnCO_3$ and for ST is ½ R2A. Lab incubation is 20°C . d-days, y-years, and ≤ less than or equal to.

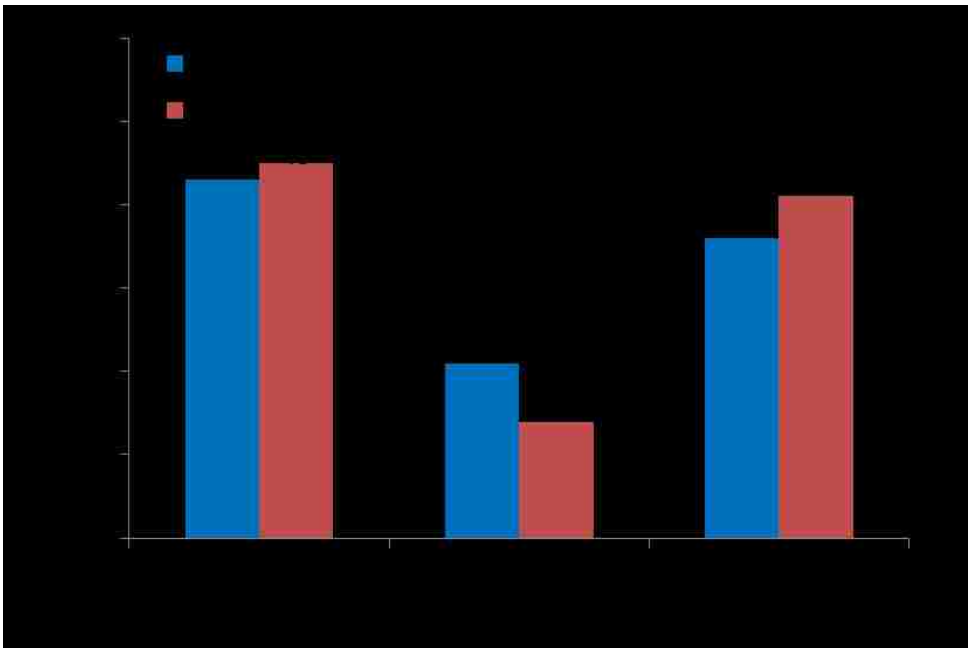

Supplementary Figure S1. Gram stain results of Long-term (LT) and Short-term (ST) bacterial isolates. Both is a category that contains Gram-positive and Gram-negative cells.

References

Afzal I, Iqrar I, Shinwari ZK, Yasmin A. 2017. Plant growth-promoting potential of endophytic bacteria isolated from roots of wild *Dodonaea viscosa* L. Plant Growth Reg 81:399-408.

Altschul SF, Gish W, Miller W, Myers EW. 1990. Basic local alignment search tool (BLAST). J Mol Biol 215:403-410.

Bäckhed F, Ley RE, Sonnenburg JL, Peterson DA, Gordon JI. 2005. Host-bacterial mutualism in the human intestine. Science 307:1915-1920.

Barton HA, Taylor NM, Kreate MP, Spinger AC, Oehrle SA, Bertog JL. 2007. The impact of host rock geochemistry on bacterial community structure in oligotrophic cave environments. Internat J Speleol 36:93-104.

Baskar S, Routh J, Baskar R, Kumar A, Miettinen H, Itävaara M. 2016. Evidences for microbial precipitation of calcite in speleothems from Krem Syndai in Jaintia Hills, Meghalaya, India. Geomicrobiol J 33:906-933.

Bull AT, Asenjo JA. 2013. Microbiology of hyper-arid environments: Recent insights from the Atacama Desert, Chile. Antonie Van Leeuwenhoek 103:1173-1179.

Cacchio P, Ercole C, Contento R, Cappuccio G, Martinez MP, Gallo MD, Lepidi A. 2012. Involvement of bacteria in the origin of a newly described speleothem in the Gypsum Cave of Grave Grubbo (Crotone, Italy). J Cave and Karst Studies 74:7-18.

Chong CW, Pearce DA, Convey P, Yew WC, Tan IKP. 2012. Patterns in the distribution of soil bacterial 16S rRNA gene sequences from different regions of Antarctica. Geoderma 181:45-55.

D'Onofrio A, Crawford JM, Stewart EJ, Witt K, Gavrish E, Epstein S, Clardy J, Lewis K. 2010. Siderophores from neighboring organisms promote the growth of uncultured bacteria. Chem Biol 17:254-264.

Difco M. 1984. Dehydrated Culture Media and Reagents for Microbiology. Michigan:Difco Laboratories.

Dominguez-Monino I, Jurado V, Rogerio-Candelera MA, Hermosin B. 2014. Human impact on show caves: Chewing gum stuck to the walls. The Consertation of Subterranean Cultural Heritage:247-252.

Engel AS, Stern LA, Bennett PC. 2004. Microbial contributions to cave formation: New insights into sulfuric acid speleogenesis. Geol 32:369-372.

Fang BZ, Salam N, Han MX, Jiao JY, Cheng J, Wei DQ, Xiao M, Li WJ. 2017. Insights on the effects of heat pretreatment, pH, and calcium salts on isolation of rare Actinobacteria from karstic caves. Front Microbiol 8:1535.

Fernandez M, Morel B, Ramos JL, Krell T. 2016. Paralogous regulators ArsR1 and ArsR2 of *Pseudomonas putida* KT2440 as a basis for arsenic biosensor development. J Appl Environ Microbiol 82:4133-4144.

Francisco R, Alpoim MC, Morais PV. 2002. Diversity of chromium-resistant and -reducing bacteria in a chromium-contaminated activated sludge. J Appl Microbiol 92:837-843.

Groth I, Schumann P, Laiz L, Sanchez-Moral S, Cañveras JC, Sia-Jimenez C. 2001. Geomicrobiological study of the Grotta dei Cervi, Porto Badisco, Italy. Geomicrobiol J 18:241-258.

Guazzaroni ME, Herbst FA, Lores I, Tamames J, Pelaez AI, Lopez-Cortes N, Alcaide M, Del Pozo MV, Vieites JM, von Bergen M, Gallego JLR, Bargiela R, Lopez-Lopez A, Pieper DH, Rossello-Mora R, Sanchez J, Seifert J, Ferrer M. 2013. Metaproteogenomic insights beyond bacterial response to naphthalene exposure and bio-stimulation. ISME J **7**:122-136.

Gulden B. 2017. USA Longest Caves. The National Speleological Survey (NSS) Geo2 Long & Deep Caves. http://www.caverbob.com/usalong.htm.

Gyaneshwar P, Paliy O, McAuliffe J, Popham DL, Jordan MI, Kustu S. 2005. Sulfur and Nitrogen limitation in *Escherichia coli* K-12: Specific homeostatic responses. J Bacteriol 187:1074-1090.

Hayes PT. 1964. Geology of the Guadalupe Mountains, New Mexico. U.S. Geological Survey 446.

Herrmann G, Jayamani E, Mai G, Buckel W. 2008. Energy conservation via electron-transferring flavoprotein in anaerobic bacteria. J Bacteriol 190:784-791.

Hill CA. 2000. Overview of the geological history of cave development in the Guadalupe Mountains, New Mexico. J Cave and Karst Studies 62:60-71.

Ikner LA, Toomey RS, Nolan G, Neilson JW, Pryor BM, Maier RM. 2007. Culturable microbial diversity and the impact of tourism in Kartchner Caverns, Arizona. Microb Ecol 53:30-42.

Kim MK, Jung HY. 2007. *Chitinophaga terrae* sp. nov., isolated from soil. Int J Syst Evol Microbiol 57:1721-1724.

Lane DJ. 1991. 16S/23S rRNA sequences. In: Stackebrandt E, Goodfellow M, editors. erspectives in Nucleic Acid Techniques in Bacterial Systematics. New York, NY: John Wiley and Sons. P 115-175.

Liang J, Bai Y, Qu J. 2017. Microbial interspecies interactions affect arsenic fate in the presence of Mn^{II}. Microb Ecol 74: 788-794.

Liedy W. 2004. Is There an Answer?. IUBMB Life 56:361-363.

Ludwig RA. 1984. Rhizobium free-living nitrogen fixation occurs in specialized nongrowing cells. PNAS 81:1566-1569.

Miethke M, Marahiel MA. 2007. Siderophore-based iron acquisition and pathogen control. Microbiol Mol Biol Rev 71:413-451.

Minh BQ, Nguyen MAT, von Haeseler A. 2013. Ultrafast approximation for phylogenetic bootstrap. Mol Biol Evol 30:1188-1195.

Monod J. 1949. The growth of bacterial cultures. Annu Rev Microbiol 3:371-394.

Neilands JB. 1994. Iron in Biology. In Manthey JA, Crowley DE, Luster DG, editors. Biochemistry of Metal Micronutrients in the Rhizosphere. Boco Raton, Ann Arbor, London, Tokyo: Lewis Publishers. P 15-28.

Northup DE, Barns SM, Yu LE, Spilde MN, Schelble RT, Dano KE, Crossey LJ, Connolly CA, Boston PJ, Natvig DO, Dahm CN. 2003. Diverse microbial communities inhabiting ferromanganese deposits in Lechuguilla and Spider Caves. Environ Microbiol 5:1071-1086.

Ntougias S, Lapidus A, Han J, Mavromatis K, Pati A, Chen A, Klenk HP, Woyke T, Fasseas C, Kyrpides NC, Zerkvakis GI. 2014. High quality draft genome sequence of

Olivibacter sitiensis type strain (AW-6^T), a diphenol degrader with genes involved in the catechol pathway. Stand Genomic Sci 9:783-793.

O'Sullivan LA, Rinna J, Humphreys G, Weightman AJ, Fry JC. 2005. *Fluviicola taffensis* gen. nov., sp. nov., a novel freshwater bacterium of the family Cryomorphaceae in the phylum Bacteroidetes. Int J Sys Evol Microbiol 55:2189-2194.

Ortiz M, Neilson JW, Nelson WM, Legatzki A, Byrne A, Yu Y, Wing RA, Soderlund CA, Pryor BM, Pierson SL, Maier RM. 2013. Profiling bacterial diversity and taxonomic composition on speleothem surfaces in Kartchner Caverns, AZ. Micro Ecol 65:371-383.

Palmer AN, Palmer MV. 2009. Caves and Karst of the USA. National Speleological Society, Inc., Huntsville, AL. P 272- 285.

Rusznyák A, Akob DM, Nietzsche S, Eusterhues K, Totsche KU, Neu TR, Frosch T, Popp J, Keiner R, Geletneky J, Katzschmann L, Schulze ED, Küsel K. 2012. Calcite biomineralization by bacterial isolates from the recently discovered pristine karstic Herrenberg Cave. Appl Environ Microbiol 78:1157-1167.

Segers P, Vancanneyt M, Pot B, Torck U, Hoste B, Dewettinck D, Falsen E, Kersters K, Vos PD. 1994. Classification of *Pseudomonas diminuta* Leifson and Hugh 1954 and *Pseudomonas vesicularis* Büsing, Döll, and Freytag 1953 in *Brevundimonas* gen. nov. as *Brevundimonas diminuta* comb. nov. and *Brevundimonas vesicularis* comb. nov., respectively. Int J Syst Bacteriol 44:499-510.

Spilde MN, Northup DE, Boston PJ, Schelble RT, Dano KE, Crossey LJ, Dahm CN. 2005. Geomicrobiology of cave ferromanganese deposits: A field and laboratory investigation. Geomicrobiol J 22:99-116.

Thomas F, Hehemann JH, Rebuffet E, Czjzek M, Michel G. 2011. Environmental and gut Bacteroidetes: The food connection. Front Microbiol 2:93.

Tomczyk-Żak K, Zielenkiewicz U. 2016. Microbial diversity in caves. Geomicrobiol J 33:20-38.

Tomova I, Lazarkevich I, Tomova A, Kambourova M, Vasileva-Tonkova E. 2013. Diversity and biosynthetic potential of culturable aerobic heterotrophic bacteria isolated from Magura Cave, Bulgaria. Int J Speleol 41:65-76.

Tóth E, Szuróczki S, Kéki Z, Kosztik J, Makk J, Bóka K, Spröer C, Márialigeti K, Schumann P. 2017. *Brevundimonas balnearis* sp. nov., isolated from the well water of a thermal bath. Int J Sys Evol Microbiol 67:1033-1038.

Velikonja BH, Tkavc R, Pasic L. 2014. Diversity of cultivable bacteria involved in the formation of macroscopic microbial colonies (cave silver) on the walls of a cave in Slovenia. Int J Speleol 43:45-56.

Wasserfallen A, Ragettli S, Jouanneau Y, Leisinger T. 1998. A family of flavoproteins in the domains Archaea and Bacteria. Eur J Biochem 254:325-332.

Zhang WH, Huang Z, He LY, Sheng XF. 2012. Assessment of bacterial communities and characterization of lead-resistant bacteria in the rhizosphere soils of metal-tolerant *Chenopodium ambrosioides* grown on lead–zinc mine tailings. Chemosphere 87:1171-1178.

Siderophore Production by Cave Bacteria from Carlsbad Caverns National Park (CCNP)

Running Title: Cave Bacteria Siderophore Production

Tammi R. Duncan*, Margaret Werner-Washburne, and Diana E. Northup
Department of Biology, University of New Mexico, Albuquerque, New Mexico, 87131

*Address correspondence to Tammi R. Duncan, tammid31@unm.edu
Tammi R. Duncan
1 University of New Mexico
Albuquerque, New Mexico, 87131
Tel: (505) 277-3411
E-mail: tammid31@unm.edu

Abstract

Determining whether siderophores are essential for microbial survival in the subsurface remains an unanswered question for subterranean ecosystems. Despite the oligotrophic conditions of most caves, the microbial diversity is rich in oligotrophic cave environments. This microbial richness may lead to novel siderophores that may have potential use in bioremediation and as new antibiotics. We investigated potential siderophore production in Lechuguilla and Spider caves in Carlsbad Caverns National Park (CCNP). We hypothesize that cave bacteria are using siderophores to acquire ferric-iron that they use for critical cellular processes. We analyzed previous parent cultures inoculated with ferromanganese deposits (FMD) and other secondary minerals from Spider and Lechuguilla Caves and subcultured 80 Long-term (LT) bacteria isolates and 90 Short-term (ST) bacteria isolates. These bacterial isolates were tested for siderophore production and were identified by 16S rRNA gene sequencing. We found that bacterial isolates of the LT group made siderophores more slowly and had a slightly higher number of strong siderophore producers than weak siderophore producers. The ST bacterial isolates had the greatest number of siderophores and made siderophores faster.

Overall, bacterial isolates from both groups had a strong preference for hydroxamate siderophores. Bacterial isolates that tested siderophore positive classified into the Proteobacteria (Alpha, Beta, or Gammaproteobacteria classes), Actinobacteria, Firmicutes, and Bacteroidetes phyla. Our results that the presence of bacterial isolates that produce siderophores supports our hypothesis that cave bacteria are using siderophores to acquire iron. These studies will shed light on the production and use of siderophores in the subsurface and how critical iron may be obtained in oligotrophic environments.

Importance

This study reports on the first collection of siderophore-producing cave bacterial consortia. Using 16S rRNA gene sequencing, we identified potential novel siderophore producers in the subsurface. This study demonstrates the rich microbial diversity of cave bacteria that have the potential to produce siderophores, and this study offers new insights of the essential nature of bacteria that possess siderophore production capabilities in oligotrophic ecosystems.

Introduction

All life needs iron for its cellular processes, but iron is not always easily accessible. Iron is present in the environment in multiple forms of insoluble iron oxides that are not easily accessible by bacteria. Bacteria have developed the strategy of using siderophores, iron-chelating compounds, to scavenge and process insoluble ferric iron from the environment (Ahmed and Holmström 2014). Bacteria, fungi and graminaceous plants are able to produce or use siderophores in response to low intercellular iron levels (Hider and Kong 2010, Ahmed and Holmström 2014). In the environment, this common characteristic allows for competition or cooperation for siderophores among microorganisms and plants (Glick 2003, Chu et al. 2010, Ahmed and Holmström 2014).

Microbial siderophores have been discovered in several environments, leading to their unique characteristics being exploited for ecological and biomedical uses. Ecologically, siderophores can chelate other heavy metals besides iron, so there is potential to aid in bioremediation and in the biocontrol of plants and fish pathogens (Hider and Kong 2010, Ahmed and Holmström 2014, Sorichetti et al. 2014a).

Biomedically, a sideromycin (a siderophore connected to an antibiotic) could be a novel antibiotic to combat antibiotic resistance of human pathogens (Braun et al. 2009). Our knowledge of siderophores in surface environments can be used to determine if siderophores are essential for microbial survival in the subsurface. Discovering siderophore production by oligotrophic microorganisms in caves also may lead to the discovery of novel siderophores or novel siderophore uses.

Siderophores have been identified in several oligotrophic environments, such as the open-ocean, air, oligotrophic lakes, cold deserts, and recently, carbonate caves (Mawji et al. 2008, Sorichetti et al. 2014b, Yadav et al. 2015, Boiteau et al. 2016, Vinatier et al. 2016). Siderophore production was detected in *Pseudochrobactrum kiredjianiae* strain A4 that was isolated from Karaulnaya-2 Cave, Russia (Qin et al. 2017) and by seven isolates collected from Mud Volcano and Lime Cave, Baratang Island, India (Venkadesaperumal et al. 2014). Interestingly, siderophore production was detected from cave bacterial isolates from Lechuguilla Cave, USA that were involved with potential siderophore cross feeding of bacterial members within the same order (O.S. Hersey 2014, unpublished). However, the nature of siderophore type and other roles in an oligotrophic cave remain to be determined.

Lechuguilla and Spider caves, two oligotrophic caves in Carlsbad Caverns National Park, New Mexico, have several cave deposits that represent excellent habitats in which to test for the presence of bacteria that are able to produce siderophores. These habitats include wet carbonate surfaces, moonmilk, and ferromanganese deposits (FMDs) (Northup et al. 2000, Spilde et al. 2005). FMDs have a pH that ranges from 7.1 to 8.3 and have high levels of iron oxides detected in red orange/red brown FMD and high levels of manganese oxides detected in chocolate brown and black FMDs (Northup et al. 2003, Spilde et al. 2005). Combined with nearly 100% cave humidity, FMDs potentially are a moist and slightly alkaline microenvironment that may act as a natural buffer for redox potential for ferric-siderophore complexes (Albrecht-Gary and Crumbliss 1998).

We hypothesized that a variety of cave bacteria synthesize and use siderophores to acquire critical iron needed for cellular processes. We cultured bacterial isolates from cave deposits in Lechuguilla and Spider caves (Figure 1) to determine whether siderophores are produced by cave bacteria, what types of siderophores are preferred, and

the identity of the siderophore producers. Two groups of bacterial isolates, Long-term (LT) and Short-term (ST), were investigated for the production of siderophores along with the phylogenetic diversity of the bacteria that produce siderophores. To our knowledge, this study reports on the first identification of bacterial consortia that use siderophores in a carbonate cave ecosystem.

Methods

Cave site description and sampling

We sampled from two caves, Spider Cave and Lechuguilla Cave, CCNP located in the Guadalupe Mountains in New Mexico (Figure 1A). The Guadalupe Mountains formed on a moderately dissected tilted plateau composed of the Giant reef and back reef strata (above the Guadalupe Escarpment) (Hayes 1964, Palmer and Palmer 2009). Within the same unit of the Giant Reef and back reef strata, Spider Cave formed and has 8.13 km of mapped passageway with 41.5 m of vertical overhead extent (Gulden 2014). Also within a unit of the Giant Reef and back reef strata, Lechuguilla Cave has formed with 222.6 km of mapped passage way and 489 m of vertical overhead extent (Gulden 2014).

Two groups of bacterial isolates termed the LT and ST were collected and named

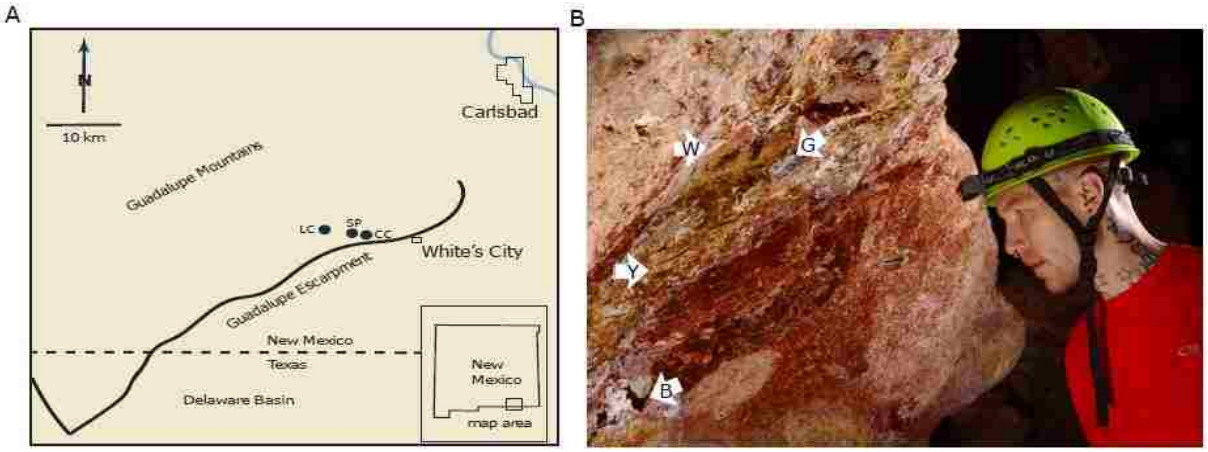

based on the total length of incubation time of the parent culture. This parent culture length of incubation time for LT was 2005—2011 for the Spider Cave parent culture 011505-14, (in-cave incubation), and 2001—2011 for the three Lechuguilla Cave parent cultures, Fe+C^1 011101-72, Mn+$P_0$011101-63, and Mn-$C_0$011101-48, incubated in the lab incubator (Table S1, S3). ST initial incubation of parent cultures was one to three days in the cave (Table S2, S3).

For the LT group, the four cave parent cultures were inoculated with cave deposits listed in Table S1. Representative pictures of the cave deposit, ferromanganese deposits (FMD), are shown in Figure 1B. Using sterile loops, each cave sample was stabbed into test tubes filled with sterile basal medium enriched, or not enriched, with reduced manganese (Mn) or reduced iron (Fe) (Table S1). The test tube agars all consisted of the following basal medium (per liter): 0.5g NaCl, 0.5g $CaCO_3$, 0.5g $MgSO_4 \cdot 7H_2O$, 0.75g K_2HPO_4, 0.25g NaH_2PO_4, 0.1g KNO_3, 4g Bacto agar. For Mn enrichments, 0.02 g/l of $MnCl_2$ was added and for iron enrichments, one sterile reduced iron carpet tack was added to the bottom of the test tube. Each test tube was inoculated with one type of cave sample in the cave (Table S1). The Spider Cave parent culture (011505-14) was inoculated and incubated in the cave for six years and subsequently transferred to a lab incubator and incubated for 5 additional years (20°C and no humidity) (Table S3). The Lechuguilla Cave parent samples (Fe^+ $C^1$011101-72, Mn^+ P^o 011101-63, and Mn- C^o 011101-48) were inoculated and incubated in the cave for 1-3 days and subsequently transferred to a lab incubator (20°C and no humidity) and incubated for 10 years (Table S3). For the ST group, 40 Lechuguilla Cave parent cultures were inoculated within the cave with samples listed in Supplementary Table S2. All swabs used to sample cave deposits were streaked onto sterile ½ Reasoner's 2A medium (R2A, Difco™, Sparks, MD) agar plates in the cave. The ½ R2A agar plates consisted of the following (per liter): 9.1g R2A agar media and 7.5g Bacto agar. The 40 Lechuguilla Cave parent cultures were incubated in the cave for 1-3 days before being transported to the lab and placed in an incubator (20°C and no humidity) where they were incubated for 23 days.

Subculture of bacterial isolates from parent cultures

LT bacteria isolates (n=80) were subcultured by collection of three depths of parent culture using a sterile loop and aseptically streaked onto subculture isolation media, R2A+$FeCl_3$, R2A+$MnCO_3$, and AIA+$FeCl_3$+$MnCO_3$ agar plates (Figure S1). The subculture isolation agar plates were incubated at 20°C and subsequent individual bacterial isolates were collected upon first appearance over a period of four to 25 days (Figure S1, Table S3). The bacterial isolates were then streaked for isolated bacterial colonies onto subculture isolation media and frozen in subculture isolation media and 80% glycerol stocks.

ST bacteria isolates (n=90) were subcultured by collecting a heavy diagonal streak of parent culture growth using a sterile loop and aseptically streaked onto subculture isolation media, ½ R2A agar plates (Figure S2). The subcultures were incubated at 20°C and subsequent individual bacterial isolates were collected upon first appearance at a period of two to seven days from inoculation (Figure S2, Table S3). The individual bacterial isolates were then streaked for isolated colonies on subculture isolation media and individual colonies were frozen in subculture isolation media and 80% glycerol stocks.

Siderophore-inducing iron-limiting growth media conditions

For iron-limiting growth conditions, bacterial isolates were streaked from 20% glycerol freezer stocks onto sterile isolation subculture media and incubated at 20°C for four days (Table S3). Using a sterile loop a heavy streak of the bacterial isolate was subsequently transferred aseptically to ISP4 with added $FeSO_4$-$7H_2O$ agar plates (4 g/l soluble starch, 0.3 g/l casein, 2 g/l KNO_3, 0.5 g/l $MgSO_4 \cdot 7H_2O$, 0.02 g/l $CaCO_3$, 0.01 g/l $FeSO_4 \cdot 7H_2O$ and 25 g/l agar) and grown at 20°C for one week. For Fe-depletion, the bacterial isolates were then transferred to ISP4 no added iron (4 g/l soluble starch, 2 g/l KNO_3, 0.5 g/l $MgSO_4 \cdot 7H_2O$, 0.02 g/l $CaCO_3$, 1 g/l yeast extract, and 25 g/l agar) agar plates or ISP4 no added iron liquid media for subsequent CAS agar plate or Arnow's and $FeCl_3$ assays, respectively. All iron-depletion processes occurred in incubations held at 20°C.

Siderophore assays

Chrome azurol sulfonate (CAS) siderophore indicator plates were prepared as previously described (Schwyn and Neilands 1987). Iron-limiting growth media conditions were used to induce siderophore production and iron-starved bacterial isolates were plated on sterile CAS agar plates using sterile loops. Bacterial isolates were then scored for positive or negative siderophore production base on the color surrounding the bacterial growth. Representative phenotypes of CAS color variations determined as siderophore-strong, -weak, -none, or no growth are shown in Figure 2. Arnow's and $FeCl_3$ assays (Arnow 1937, Neilands 1981) were used to test for production of catecholate- and hydroxamate-type siderophores, respectively, according to protocols detailed in Lee et al. (2012). Catechol (6 μg/ml) and hydroxamate, deferroxamine (1mM), were used as positive controls in Arnow's and $FeCl_3$ assays, respectively. Deionized water (DIH_2O) was used as a negative control.

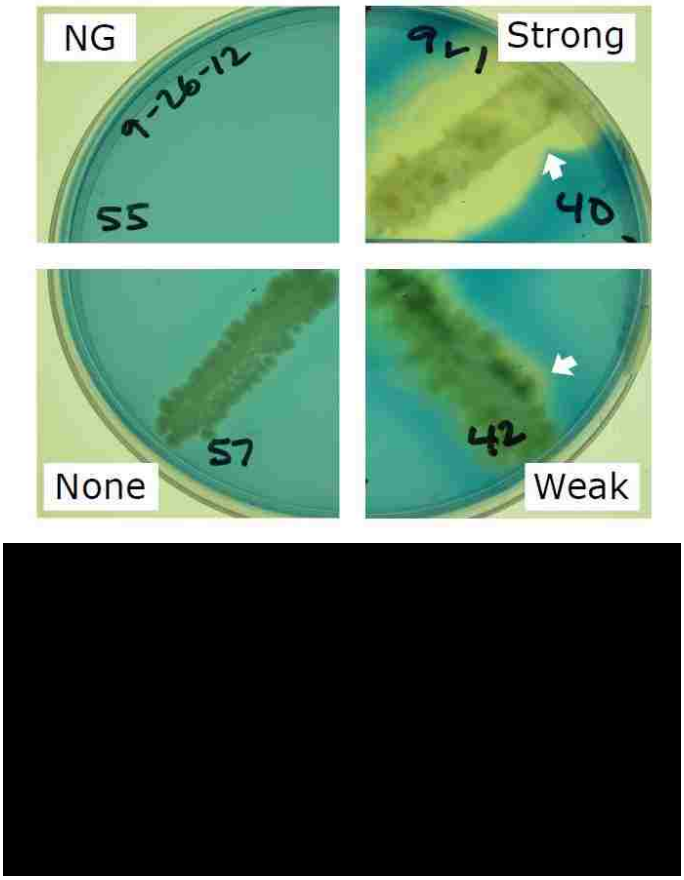

Molecular and microbiological techniques for 16S rRNA gene sequencing

DNA isolation of 27 LT (21 cloned and 6 pure) and 65 (59 clone and six pure) ST siderophore strong bacterial isolates and 12 (nine cloned, three pure) LT and 0 ST siderophore weak bacterial isolates was performed using the MoBio UltraClean Microbial DNA Isolation Kit (MoBio, Carlsbad, CA). The 16S rRNA gene (1362-bp) was amplified with 46F (5'- GCYTAAYACATGCAAGTCG-3') and 1409R (5'-GTGACGGGCRGTGTGTRCAA-3') bacterial primers (Northup et al. 2010). Reactions were carried out in a 25 µl volume with 10X PCR buffer with 15 mM Mg^{2+}, 0.3 µM of each primer, 0.25 mM of each dNTPs, 5 µg of 50 mg/ml BSA (Ambion Austin, TX, USA) and 1U Ampli-Taq LD (Applied Biosystems, Foster City, CA, USA). The PCR reaction was performed with an MJ thermocycler with the program, 94°C for 5 min, 30 cycles at 94°C for 30 s, 55.5°C for 30 s, 72°C for 1.5 min and final extension at 72°C for 7 min. The PCR amplicons were purified using MoBio PCR Clean Up Kit (MoBio, Carlsbad, CA) and cloned into pCR®4-TOPO vector following a modified manufacturer's protocol of the TOPO TA Cloning kit with One Shot TM TOP10 chemically competent *Escherichia coli* cells (Invitrogen). The modifications were made in the ligation and transformation steps. The ligation reaction and transformation steps were modified by using 1/3 the amount of manufacturers protocol. For the ligation reaction 1.33 µl purified PCR product, 0.33 µl 1:4 NaCl, and 0.33 µl vector were used for one reaction. For one transformation reaction, 15 µl *E. coli* competent cells and 83 µl of S.O.C. medium were used and 10 µl, 10 µl, 15 µl, and 20 µl of recovered cells were plated on four Luria Broth (LB) agar plates with 50 µg/ml Amphicillin and 40 µg/ml X-Gal. A total of forty-eight clones were initially collected for each isolate, but twelve clones were randomly selected, and the 16S rRNA genes were sequenced with BigDye 1.1 using the T3 or T7 for the sensed direction of the 16S rRNA gene. Sequencing was performed with the ABI Prism 3130 Automated DNA Sequencer at UNM-Molecular Biology Facility, Albuquerque, NM and an ABI Prism 3730xl Automated DNA Sequencer when sequenced at GENEWIZ Genomics, Danvers, MA.

Phylogenetic analysis of siderophore-high and -weak producers

Using Sequencer 5.1 (Gene Codes Corp., Ann Arbor, MI) ambiguous portions were trimmed and edited. The trimmed sequences started at 46F' were at least 500bp

(one sequence was 483bp) and had greater than 90% sequence quality. Contigs were assembled with 97% sequence similarity with the twelve clones for each bacterial isolate and were separated into siderophore-strong and siderophore-weak. Within each group subsequent contigs were formed with 98% similarity to identify Operational Taxonomic Units (OTU). The longest representative sequence was selected for each OTU and used for taxonomic assignments. Representative taxonomic assignments were determined using BLAST (Altschul et al. 1990). A chimera check of all sequences was completed using QIIME v.1.9.1 program**.** A sequence alignment was performed using default parameters of EMBL-EBI webPRANK (http://www.ebi.ac.uk/goldman-srv/webprank/) and subsequently a similarity matrix was determined using a custom R script. A maximum likelihood tree was constructed by using IQ-TREE web server: fast and accurate phylogenetic trees under maximum likelihood (http://iqtree.cibiv.univie.ac.at/) with 1000 replicates (Minh et al. 2013). The tree files were visualized and annotated with the interactive Tree of Life (iTOL) v.3.5.3 program (http://itol.embl.de/) and vector-drawing program Inkscape v.0.92.1.

Results

A total of 170 bacterial isolates were collected from subcultures of LT and ST parent cultures (Table S1 and Table S2). Eighty bacterial isolates were collected as single colonies from four LT parent cultures. Forty-five percent (n=36) of bacterial isolates were subcultured on R2A+$FeCl_3$, 42.5% (n=34) of bacterial isolates were subcultured on R2A+$MnCO_3$, and 12.5% (n=10) of bacteria isolates were subcultured on AIA+$FeCl_3$+$MnCO_3$ (Table S1). A total of 90 bacterial isolates were collected as single colonies from 40 ST parent cultures. All bacterial isolates were subcultured on ½ R2A, two isolates from each parent culture from Lake Chandelar, Tower Place, and Briny Pool, and three isolates from parent cultures from EA (Table S2).

Long-term and Short-term bacterial isolates produce siderophores

To determine if bacterial isolates use siderophores, we simulated low iron growth conditions and detected siderophores using the CAS assay. A positive result was a color change from blue to orange, beige, or white. The results for LT and ST bacterial isolates

for siderophore detection fell into strong, weak, none, and no growth classes and were distributed across five time periods that represented the time until the color change occurred: less than 10 days, 11-15 days, 16-20 days, 21-25 days and greater than 26 days (Table 1).

Table 1. Siderophore detection in Long-term (n=80) bacteria isolates.

Siderophore Detection Level	Days					Total (%)
	<10	11-15	16-20	21-25	>26	
Strong		7 (9)	1 (1)	2 (3)	18 (23)	28 (36)
Weak		2 (3)			10 (13)	12 (16)
None						13 (16)
NG[a]						27 (32)

a. No growth (NG)- live bacteria isolates that did not grow on CAS media when transferred from Fe-limiting ISP4 media.

For the LT bacterial isolates, a higher proportion of strong siderophore producers were detected in comparison to weak siderophore producers. Thirty-six percent of the total population was strong, 16% were weak, and 16% had no siderophore production. A higher proportion (36%) of siderophores detected occurred in greater than 26 days compared to 16% that were detected in less than 26 days. No siderophores were produced in less than 10 days. Thirty-two percent of LT bacterial isolates did not grow on the CAS assay (Table 1). Overall, the LT bacterial isolates made siderophores more slowly and had a higher proportion of stronger siderophore producers compared to weaker siderophore producers.

For the ST bacterial isolates, a higher proportion of strong siderophore producers were detected overall (Table 2). Seventy-five percent of total population was strong, 1% was weak, and 17% had no siderophore production. A lower proportion (22%) of siderophores detected occurred in greater than 26 days compared to 53% that were detected in less than 26 days. Twelve percent produced siderophores in less than 10 days. Seven percent of ST bacterial isolates did not grow on the CAS assay (Table 2). Overall, ST bacterial isolates made siderophores faster and had a higher proportion of siderophore producers.

Table 2. Siderophore detection in Short-term (n=90) bacteria isolates

Siderophore Detection Level	Days					Total (%)
	<10	11-15	16-20	21-25	>26	
Strong	11 (12)	21 (23)	10 (11)	6 (7)	20 (22)	68 (75)
Weak		1 (1)				1 (1)
None						15 (17)
NG[a]						6 (7)

a. No growth (NG)- live bacteria isolates that did not grow on CAS media when transferred from Fe-limiting ISP4 media.

Long-term and Short-term bacterial isolates produce many hydroxamate and minimal catecholate siderophores

To determine if bacterial isolates produce catecholate or hydroxamate siderophores, the bacterial isolates were grown in low iron conditions and their supernatant tested using Arnow's and $FeCl_3$ assays. For detection of catecholate siderophores, LT had 1% weak and 99% no catecholate production (Figure 3A). ST had 3% weak and 97% no catecholate production (Figure 3A).

For LT hydroxamate detection, 29% were weak, 26% were strong, and 51% had no hydroxamate production (Figure 3B). For ST hydroxamate detection, 37% were weak, 12% were strong, and 51% had no hydroxamate production (Figure 3B). The color phenotypes for the control, none, weak, and strong hydroxamate siderophores are shown in Figure 3C. Overall, the catecholate siderophores were not commonly made by LT or ST bacterial isolates. The $FeCl_3$ assay revealed that the majority of siderophores made were hydroxamates that were either weak or strong.

Ninety-two siderophore-strong and twelve siderophore-weak bacterial isolates were sequenced for a total of 1,095 sequences

Twenty-seven LT and 65 ST siderophore-strong isolates were cloned and sequenced. One LT and three ST siderophore-strong were not cloned. Twenty-one of the LT were cloned and six isolates were pure based on Gram stain for a total of 270 sequences. Fifty-nine ST were cloned and six isolates were pure based on Gram stain for a total of 714 sequences. Together, 984 sequences were completed for the siderophore-strong isolates.

Twelve LT and no ST siderophore-weak isolates were cloned and sequenced. One ST siderophore weak isolate was not cloned. Nine of twelve LT were cloned and three were pure based off of Gram stain for a total of 39 sequences. No ST siderophore-weak isolated were cloned. Together, 111 sequences were completed for the siderophore-weak isolates.

Siderophore-strong bacterial isolates are closely related to members of Proteobacteria (Alpha, Beta, and Gammaproteobacteria), Actinobacteria, Firmicutes, and Bacteroidetes phyla

To determine the closest phylogenetic relationship of siderophore-strong bacterial isolates, 27 LT and 65 ST siderophore-positive bacterial isolates were sequenced. A total of 984 16S rDNA sequences were grouped into 87 operational taxonomic units OTUs. The 87 OTUs classified into Proteobacteria (Alpha, Beta, and Gammaproteobacteria classes), Actinobacteria, Firmicutes, and Bacteroidetes phyla (Figure 4, Table S4).

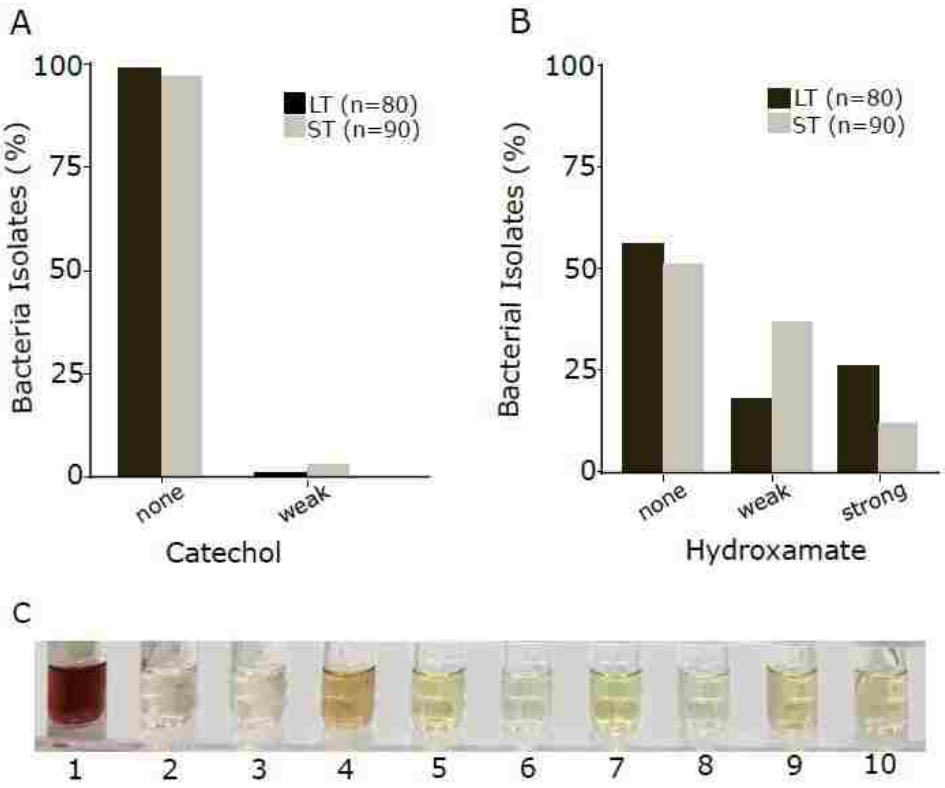
A
100
75
50
25
0
Bacteria Isolates (%)
LT (n=80)
ST (n=90)
none
weak
Catechol
B
100
75
50
25
0
Bacterial Isolates (%)
LT (n=80)
ST (n=90)
none
weak
strong
Hydroxamate
C
1
2
3
4
5
6
7
8
9
10

[redacted]

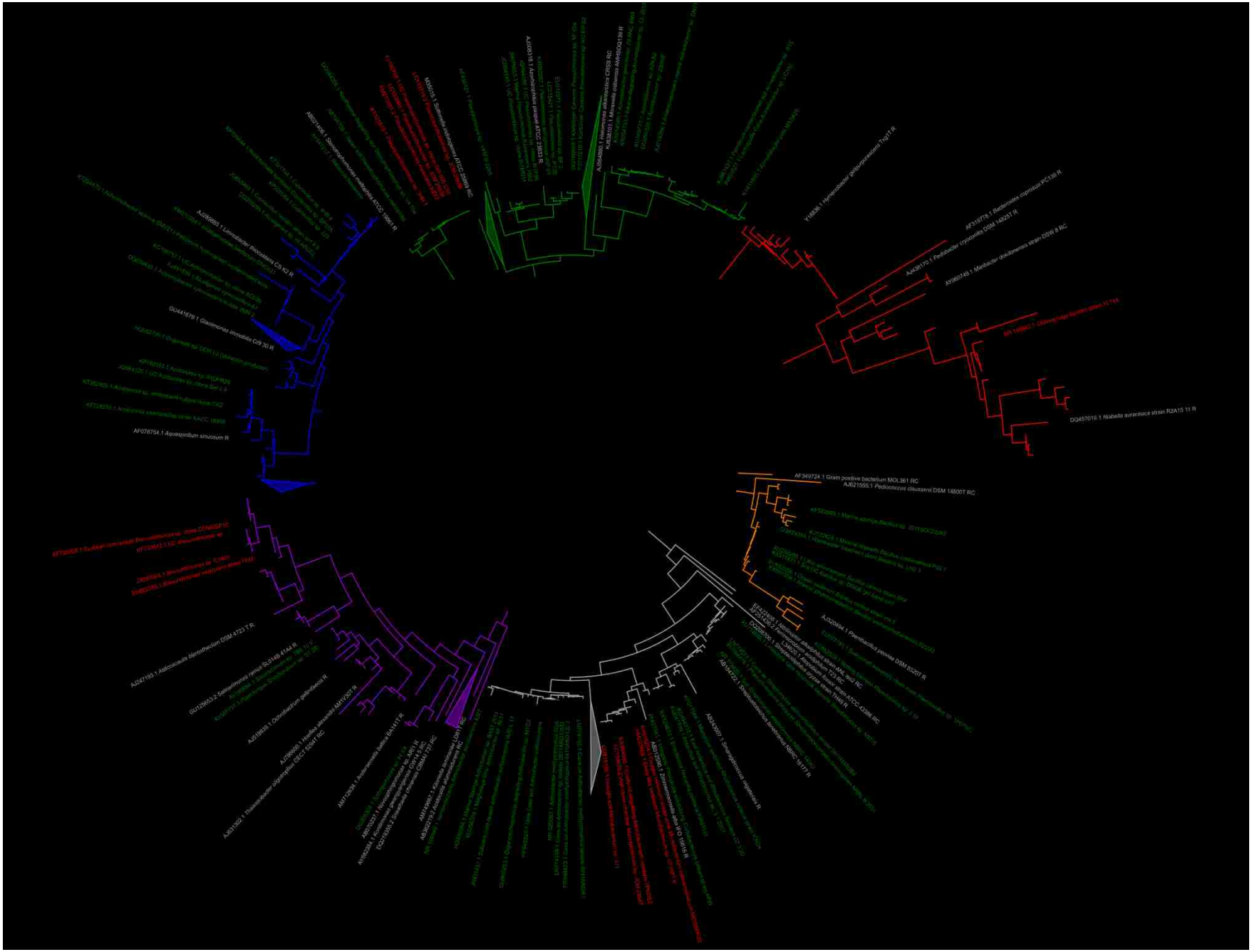
AJ854893.1 Limnobacter thiooxidans CS K2 R
GU441678.1 Glaciimonas immobilis Cr9 30 R
AF078754.1 Aquaspirillum sinuosum R
AJ420199.1 Aldercreutzia filiformis DSM 4723 T R
GU726513.2 Senegalimassilia rainei SL-014B-A1A4 R
AJ519928.1 Olivibacillifirm gelatinilacus R
AJ519929.1 Haloflex alexandrii AM1/V267 R
AJ631582.1 Thalassobacter arenigenus KEC1 ES081 RC
AM710636.1 Aquimarina balfae EBA14 T R
AB271231.1 Novosphingobium sp. KA1 R
AB362749.1 Sphingomonas sp. OH-1 RC
AB362750.1 Sphingomonas sp. OH-2 RC
AB362751.1 Sphingomonas sp. OH-3 RC
AB362752.1 Sphingomonas sp. OH-4 RC
AB362753.1 Sphingomonas sp. OH-5 RC
AB362754.1 Sphingomonas sp. OH-6 RC
AB362755.1 Sphingomonas sp. OH-7 RC
AB362756.1 Sphingomonas sp. OH-8 RC

Figure 4. Phylogenetic tree of siderophore-strong representative OTUs. Ultrabootstrap values are >70% or otherwise stated on 1000 replicates. The scale bar corresponds to 0.1 nucleotide substitutions per site. Long-term representative strains start with 1- and Short-term representative strains start with 2- for OTU representative sequence names. The numbers of clones per representative sequence are in parenthesis. Color code of branches: Grey-Actinobacteria, Orange-Firmicutes, Purple-Alphaproteobacteria, Blue-Betaproteobacteria, Green-Gammaproteobacteria, and Red-Bacteroidetes. Name color code: grey-reference strain, green-a member of the same genus is known as a siderophore producer, red-a member of the same genus is known as a non-siderophore producer, and black-strain is uncultured (UC) or has not been reported as a siderophore producer. Triangles are collapsed reference strain clades.

Proteobacteria was the most abundant phylum with 46 total OTUs (Table S4). The Proteobacteria were represented by 20 genera that classified into Alphaproteobacteria (12 OTUs), Betaproteobacteria (15 OTUs), and Gammaproteobacteria (19 OTUs). There were no Epsilon-, Zeta- or Delta-proteobacteria identified (Figure 4, Table S4). The seven most abundant OTUs for Proteobacteria that had greater than 20 sequences were identified. These seven OTUs were identified as 2-22 (109 sequences), 2-69 C1 (98 sequences), 1-19 A8 (52 sequences), 2-49 B8 (31 sequences), 2-65 (31 sequences), 1-30 (27 sequences), and 1-12 (20 sequences) and were closely related to *Pseudomonas fluorescens* 1582, *Ralstonia basilensis*, *Achromobacter xylosoxidans* isolate 2M-2, *Acinetobacter radioresistens*, *Acinetobacter* sp. GN71, *Sphingopyxis* sp. TP340-3, and *Stenotrophomonas maltophilia*, respectively (Figure 4, Table S4).

Actinobacteria was the second most abundant phylum with 16 OTUs (Figure 4, Table S4). The Actinobacteria were represented by six genera. The six most abundant OTUs had greater than 20 sequences. These six OTUs were identified as 2-56 A3 (37 sequences), 1-31 B5 (35 sequences), 2-15 A5 (33 sequences), 2-42 (32 sequences), 2-30 A11 (23 sequences), and 2-81 B3 (23 sequences) that were closely related to *Arthrobacter methylotrophus*, uncultured Yanshan Mountain clone 3-324, *Microbacterium* sp. 0710P1-6, *Arthrobacter siccitolerans* 4J27, *Curtobacterium luteum*, and *Norcardia coeliaca* INA01131, respectively (Figure 4, Table S4).

Bacteroidetes was the third most abundant phylum with 14 OTUs (Figure 4, Table S4). The Bacteroidetes were represented by four genera. The two most abundant OTUs had greater than 20 sequences. These two OTUs were 1-27 A8 (46 sequences) and 2-1 B8

(20 sequences) that were closely related to an uncultured soil diffusion chamber system CCRA H03 clone and an uncultured urban aerosol clone NDB4, respectively (Table S4).

Firmicutes was the least abundant phylum 11 OTUs (Figure 4, Table S4). The Firmicutes were represented by three genera. There was one OTU that had greater than 20 sequences. This OTU was 2-83 (64 sequences) that was closely related to *Bacillus* sp. LH2-3 (Table S4).

Siderophore-weak bacterial isolates are closely related to members of Proteobacteria (Alpha and Beta), Actinobacteria, Firmicutes, and Bacteroidetes phyla

To determine the closest phylogenetic relationship of siderophore-weak bacterial isolates 12 LT and 0 ST siderophore-weak positive bacterial isolates were sequenced. A total of 111 sequences were grouped into 15 OTUs. The 15 weak siderophore OTUs classified into the Proteobacteria (Alpha, Beta), Actinobacteria, Firmicutes, and Bacteroidetes phyla (Figure 5, Table S5).

Proteobacteria was the most abundant phylum with seven total OTUs (5 Alpha- and 2 Beta-) (Figure 5, Table S5). Proteobacteria were represented by four genera that classified into three Alphaproteobacteria and one Betaproteobacteria. There was no Gamma, Delta, Zeta, or Epsilon-proteobacteria. The most abundant OTU in Proteobacteria was 1-52 B7 (12 sequences) that was identified as closely related to *Erythrobacter* sp. p52 2011 (Figure 5, Table S5).

Three additional phyla were identified. Actinobacteria had three total OTUs (Figure 5, Table S5). Actinobacteria was represented by three genera. The most abundant OTU was 1-31 B5 (24 sequences) that was identified as closely related to *Lentzea violacea* 174493 (Figure 5, Table S5). Firmicutes had three total OTUs representing one genus. The most abundant OTU was 2-35 A5 (13 sequences) that was closely related to *Bacillus simplex* strain IR 523 (Figure 5, Table S5). Bacteroidetes had two total OTUs and was represented by one genus. The most abundant OTU was 1-5 A2 (16 sequences) that was closely related to *Chitinophaga barathri* YLT18 (Figure 5, Table S5).

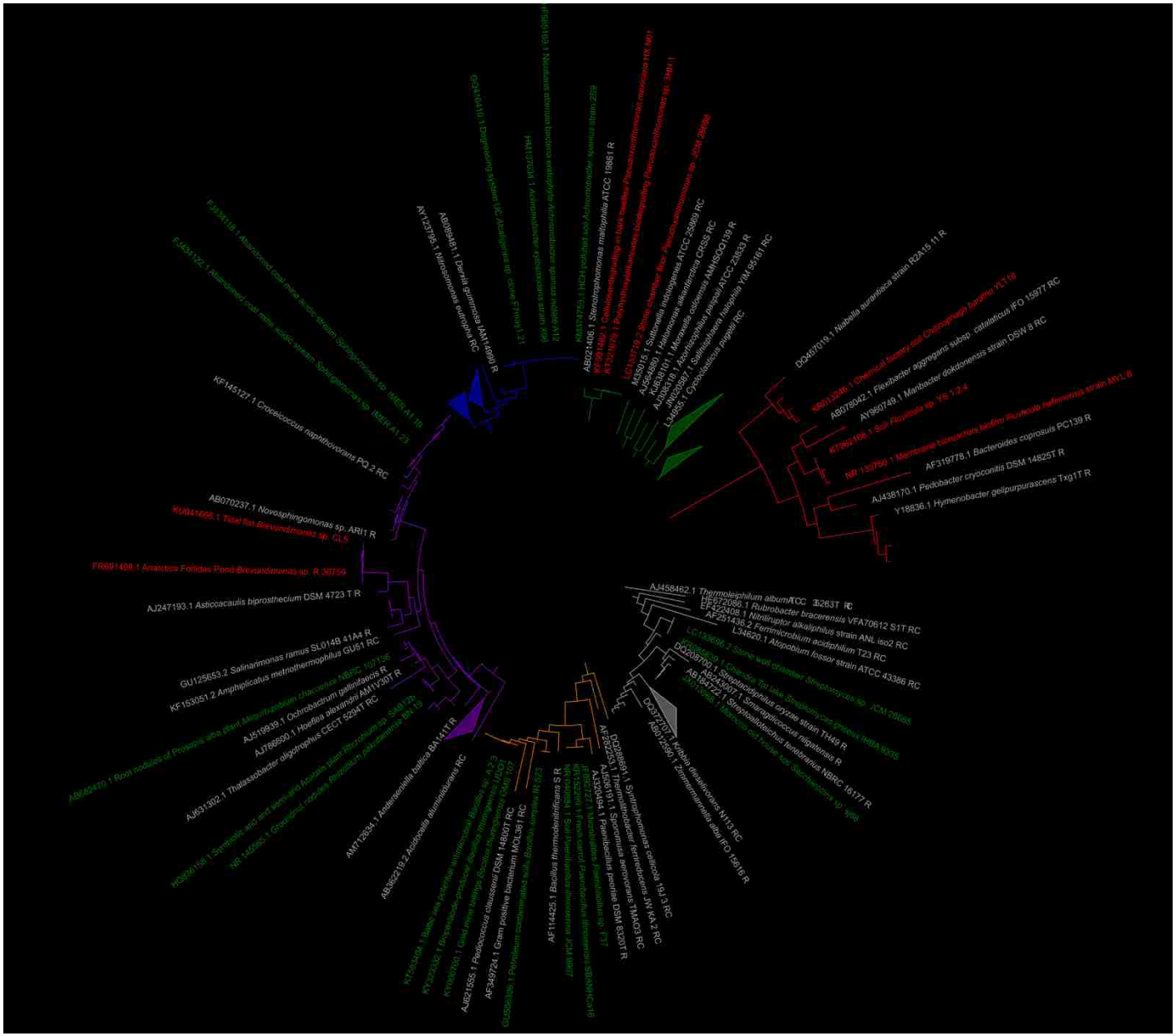
AB070237.1 Novosphingomonas sp. ART1 R
AJ247193.1 Asticcacaulis biprosthecium DSM 4723 T R
KF145127.1 Croceicoccus naphthovorans PQ-2 RC
AB070236.1 Novosphingomonas sp. ART2 R
AB698481.1 Daryeli ginmisoja IAM14899 R
AY123795.1 Mimosmonas europea RC
AB021406.1 Sternotrophomonas maltophilia ATCC 18661 R
M35015.1 Sulfonella radiobacens ATCC 25389 RC
AJ354890.1 Halomonas alimentaria CPSS RC
AJ354191.1 Mevalonate oxidomeis AMRSOO139 R
AJ293187.1 Azotobacillus pregusi ATCC 23583 R
JN009827.1 Sulfolophene halophila YM 95161 RC
L34955.1 Cycloclastica pagalis RC
DQ457019.1 Nubolla aurantiaca strain RRA15 11 R
AB078042.1 Flexibacter aggregans subsp. cattaleticus IFO 15977 RC
AY560749.1 Marlbacter dokdonensis strain DSW-8 RC
AF319778.1 Bacteroides coprosuis PC139 R
AJ438170.1 Pedobacter cryoconitis DSM 14825T R
Y18836.1 Hymenobacter gelipurpurascens Txg1T R
AJ458462.1 Thermoleiphilum album/ATCC 35263T RC
AF251436.2 Fermimicrobium acidiphilus strain ANL iso2 RC
L34620.1 Atopobium fossor strain ATCC 43386 RC
AJ519939.1 Ochrobactrum gallinifaecis R
AJ786600.1 Hoeflea alexandrii AM1V30T R
AJ631302.1 Thalassobacter oligotrophus CECT 5294T RC
AM712634.1 Arctisenella baltica BA141T R
AB362219.2 Acidocella aluminidurans RC
AF114425.1 Bacillus thermodenitrificans S R
AJ821655.1 Pediococcus claussenii DSM 14800T RC
AF249724.1 Gram positive bacterium MOL381 RC
AJ354894.1 Paenibacillus peoriae DSM 8320T R
AJ354191.1 Sporomusa aerovorans TMA03 RC
AF252351.1 Thermolithobacter ferrireducens JW/KA-2 RC
DQ372007.1 Kolpia dikalikorens N113 RC
AB012690.1 Zenmirmimella alba IFO 15616 R
AB078041.1 Flexibacter aggregans subsp. cattaleticus IFO 15977 RC

Figure 5. Phylogenetic tree of siderophore-weak representative OTUs. Ultrabootstrap values are >70% or otherwise stated as 1000 replicates. The scale bar corresponds to 0.1 nucleotide substitutions per site. Long-term representative strains start with 1- and Short-term representative strains start with 2- for OTU representative sequence names. The numbers of clones per representative sequence are in parenthesis. Color code of branches: Grey-Actinobacteria, Orange-Firmicutes, Purple-Alphaproteobacteria, Blue-Betaproteobacteria, Green-Gammaproteobacteria, and Red-Bacteroidetes. Name color code: grey-reference strain, green-a member of the same genera is known as a siderophore producer, red-a member of the same genera is known as a non-siderophore producer, and black-strain is uncultured (UC) or has not been reported as a siderophore producer.

Discussion

Siderophores have been described in several surface and subsurface environments. A large diversity of microorganisms that include human and animal pathogens, terrestrial environmental bacteria, and oligotrophic bacteria has been shown to produce siderophores. While siderophores have been shown in cross feeding by Lechuguilla Cave bacterial isolates (O.S. Hershey 2014, unpublished), how these siderophores are used by bacteria in the cave environment remains to be determined.

We found that LT and ST cave bacterial isolates both produce siderophores. The amount of time that these isolates took to show siderophore production is significantly higher than most bacteria that have been tested in terrestrial soil environments, which showed a positive result within 15 minutes (Lee et al. 2012). In contrast, bacterial isolates took at least 9 days in the ST group and 14 days for bacteria isolates in the LT group to show siderophore production. One explanation may be the slow growth rate of most oligotrophic microorganisms would cause a slower rate of siderophore detection. Some oligotrophic bacteria from Lechuguilla Cave can take up to two years to show colonies (Boston, P.J., June 2017 Personal Communication). A subset of these cave isolates from the LT and ST groups have shown a completion of a traditional growth curve as early as 2 days and as late as 8 days (T.R. Duncan 2017, unpublished).

The slow growth rate of our bacteria isolates may also be related to the mixed nature of our bacterial isolates (T.R. Duncan 2017, unpublished). Lau et al. (2016) proposed that consortia bacteria in oligotrophic environments share the metabolism of nutrients for survival of the whole community. One study (O.S Hershey 2014, unpublished) showed that bacterial isolates from Lechuguilla Cave were able to grow on

iron-free media mixed with purified siderophores from bacteria isolates from the same order. It is possible that one member of the bacterial isolate consortia would be in charge of making the siderophore for the group. If this member grew using the products of the first bacteria, then it would take longer for the second consortia bacteria to recognize the need for siderophores, thus causing a delayed color change in CAS media. In this manner a relationship of siderophore cross feeding encourages a mutualistic relationship. However, more research would have to be completed in order to conclude a mutualistic interaction between our cave bacterial isolates.

The no growth phenotype on CAS occurred in both the LT and ST groups. It may be explained by the presence of the detergent in CAS that has been described to be toxic to Gram positive cell walls (Pérez-Miranda et al. 2007). Because the LT group had a higher percentage of gram positive bacteria, due to the strong selective pressures of a cave and the subsequent selective pressure of living in a test tube for 6 or 10 years, a greater amount of no growth occurred in comparison to the ST group.

Hydroxamate siderophores preferred by cave bacterial isolates

We found that the bacterial isolates had a preference for hydroxamate siderophores, which is possibly due to the larger energy requirement in synthesizing catecholate siderophores by the non-ribosomal peptide synthases (NRPS)-dependent pathway (Crosa and Walsh 2002). The catecholate siderophore, enterobactin, contains three aromatic rings that are added in a repetitive assembly line that would require a lot of energy (Crosa and Walsh 2002). Furthermore enterobactin has a $1Fe^{3+}$:1catecholate stability constant of $K= 10^{52}$ (Ahmed and Holmström 2014), which allows enterobactin to be stable and compete with the host molecules for Fe^{3+} compounds.

In contrast, a hydroxamate siderophore might be preferred for the smaller cost to build (i.e. it doesn't require a multi-enzyme complex, but uses available substrate derivatives in a NRPS-independent pathway (Challis 2005) and the smaller need to compete with host molecules. The hydroxamates, ferrichrome and ferrioxamine B, have a $1Fe^{3+}$:1 hydroxamate stability constant of $K=10^{29}$ and $K=10^{31}$, respectively (Ahmed and Holmström 2014). Not only have hydroxamate siderophores been described to be more water soluble, hydroxamate siderophores are largely resistant to environmental degradation, thus commonly found in soil environments (Winkelmann 2007). Caves have

been described as more soil-like environments (Spilde et al. 2009); therefore, there is a greater chance for hydroxamate siderophores to be found opposed to catecholate siderophores.

We found that LT and ST bacteria use hydroxamate siderophores, but bacteria in the ST group have more hydroxamate weak than hydroxamate strong siderophore producers. In contrast, bacteria in the LT group have equal amounts of strong and weak siderophore producers. To confirm that this weak hydroxamate phenotype was not due to using dH_2O in the ISP4 no iron-added media prior to completing the $FeCl_3$ assay, a subset of LT and ST isolates were tested. We found that an iron remanence in dH_2O does not have a large effect on the hydroxamate phenotype. Therefore, we hypothesize that the weak phenotype may be related to the presence of a mixed-type of siderophore, which would have at least one hydroxamate group on the siderophore.

Bacterial isolates that show a weak hydroxamate phenotype may have at least one hydroxamate functional group, which is consistent with our broad spectrum curve data. All of our weak hydroxamate siderophore producers had an absorbance maximum of 500 nm (data not shown) and hydroxamate siderophores commonly have an absorbance maximum of 425 to 500 nm when bound to iron (Ali and Vidhale 2013). Rhodotorulic Acid (RA), a hydroxamate siderophore, had a positive color change to orange and an absorbance maximum at 480 nm with the $FeCl_3$ assay (Atkin et al. 1970). When our positive control, Desferrioxamine B was tested, it consistently had a positive color change and had an absorbance maximum at 500 nm even with varying concentrations (data not shown). In comparison, when the catecholate positive control was tested with $FeCl_3$ it had a black color change (data not shown). Thus, it is unlikely that any bacterial isolates that showed a color change from darker yellow to orange are catecholate-types. Some bacteria in caves have been described as acquiring energy by breaking down aromatic compounds (Barton and Jurado 2007). Therefore, if any catecholate or catecholate-mix types of siderophores are available, they would more likely be used as a source of energy in addition to ferric-iron acquisition. By having the ability to break down aromatic compounds in an area where there is an abundance of hydrocarbons, the bacteria in Lechuguilla and Spider caves have potentially developed an efficient energy source through this process. The caves of CCNP formed in the Delaware Basin where

there is the presence of crude oil (Hill 2000). Several of our siderophore strong and siderophore weak bacteria are closely related to bacteria that are involved in crude-oil degrading, pyrene-degrading, naphalene-degrading, and nonnylphenol-degrading (all structures containing aromatic rings). In addition, these bacteria have been isolated from oil fields and heavy metal contaminated sites. Future research will test this hypothesis and quantify the presence of hydrocarbons in cave bedrock.

Siderophore producing microbial diversity

The majority of our bacterial isolates that showed siderophore production were members of the Proteobacteria, Firmicutes, Actinobacteria, and Bacteroidetes phyla. Several members of the identified genera for the siderophore strong or weak isolates were similar to bacteria isolated from previous CCNP studies (Northup et al. 2003, Barton et al. 2007). Northup et al. (2003) identified the Proteobacteria (Alpha, Beta, and Gamma), Nitrospira, Firmicutes, and Actinobacteria divisions from FMD in Lechuguilla and Spider caves. We identified *Afipia* sp., *Stenotrophomonas* sp., and *Micrococcus* sp. in this study that had previously been detected in Lechuguilla and Spider caves (Northup et al. 2003). Similarly, Barton et al. (2007) identified members from the Proteobacteria (Alpha, Beta, and Gamma-), Actinobacteria, Bacteroidetes, Chloroflexi, and Aquificales divisions in Carlsbad Cavern. In the Fe_2O_3-rich siltstone in Carlsbad Cavern, sequences that are similar to our sequences were *Brevundimonas nasdae*, *Massilia* sp., *Stenotrophomonas* sp., *Caulobacter* sp., *Acidovorax* sp., *Psuedomonas* sp., *Rhodococcus* sp., and *Curtobacterium* sp. In the Capitan Formation, a plain carbonate formation within Carlsbad Cavern, the sequences that are similar to our sequences were *Pseudonocardia* sp., Bacterium Chibacore 1500, *Actinomyces* sp., *Acinetobacter johnsonii*, *Saccharothrix* sp., and *Actinobacterium* sp. (Barton et al. 2007)

In comparison to other oligotrophic and terrestrial environments, we found that that our cave bacterial isolates were closely related to bacteria that live in Antarctic soil, Atacama Desert soil, and in heavy metal terrestrial environments. Chong et al. (2012) reviewed 13 independent Antarctic soil studies that showed that Acidobacteria, Bacteroidetes, Actinobacteria, Firmicutes, and Proteobacteria (Alpha, Beta, and Gamma) were the common phyla present. In the Atacama Desert (the oldest and driest desert on Earth) habitats, Actinobacteria were described as the dominant taxon with the following

genera found in the soil: *Norcardia*, *Streptomyces*, *Microlunatus*, and *Prauserella* (Bull and Asenjo 2013). In an analysis of microbial mats of an Atacama Desert high altitude wetland, a high number of Proteobacteria and Actinobacteria were present (Bull and Asenjo 2013). An assessment of bacterial communities in the rhizospheres of a metal-tolerant plant also identified Proteobacteria (Alpha, Beta, and Gamma), Actinobacteria, and Bacteroidetes, among others, as phyla in this terrestrial rhizosphere soil (Zhang et al. 2012). The occurrence of similar genera of siderophore producing cave bacteria with CCNP studies and in other oligotrophic environments illustrates the similar nature of microbial diversity in oligotrophic environments.

We identified closest relatives of siderophore positive isolates that have been tested for siderophore production in previous work and shown to not produce siderophores. One explanation would be the consortial nature of our bacteria isolates. Identifying the genera of siderophore producers and non-siderophore users could help define the roles of other bacterial members in the isolate. We can potentially use close relatives in BLAST to predict general functions of the species, the metabolic capabilities, and use the place from which the bacteria were originally isolated, to help determine possible supportive functions of the bacteria in the isolate (Barton et al. 2007). However, close relatives have been shown to have different metabolic capabilities so further research would have to be completed to identify siderophore use by cave bacteria consortial interactions.

The OTUs that were non-siderophore producers in other literature, but were identified as siderophore-strong or -weak producers in our study, were closely related to *Brevundimonas* sp. (Alphaproteobacteria), *Pseudoxanthomonas* sp. (Gammaproteobacteria), *Microbacterium* sp. (Actinobacteria), and *Chitinophaga* sp. (Bacteroidetes). *Brevundimonas* sp. is from the *Caulobacter* family that is composed of oligotrophic bacteria that are able to adapt to oligotrophic environments (Dworkin 2002). Interestingly, our *Brevundimonas* sp. OTU is closely related to a Tiashan glacier and deep ocean Caulobacterales bacterium clones, both of which are oligotrophic environments.

Pseudoxanthomonas sp. is in the family of Xanthomonadales. The Xanthomonadales are known as sulfur-oxidizing bacteria (Tomczyk-Żak and

Zielenkiewicz 2016). Our bacterial isolates are similar to *Pseudoxanthomonas* sp. isolated from a stone chamber floor and *Pseudoxanthomonas mexicana* KZ22 isolated from a cold environment soil (Salwan et al. 2010). *Pseudoxanthomonas* sp. could be involved with sulfur-oxidation with the oxidized product of being gypsum in the caves. However, *P. mexicana* KZ22 was identified as a high alkaline protease-producer in the temperature range of 15-25°C (Salwan et al. 2010). Thus, it is likely that *Pseudoxanthomonas* sp. in the cave environment may have a vital role in the degradation of organic waste rich in proteins.

As a member of the family Microbacteriaceae, *Microbacterium* sp. is described as a chemoorganotroph. A survey of *Microbacterium* sp. metabolism indicates that *Microbacterium* sp. can break down several forms of aromatic ring-containing compounds (Zhou et al. 2007, de los Cobos-Vasconcelos et al. 2012, Jin et al. 2017). Our study indicated that the closest relatives to *Microbacterium* sp. were isolates from deep-sea sediment and drought-impacted soil. Taken together, the *Microbacterium* sp. may likely contribute to an oligotrophic consortium community by deriving energy from metabolizing organic aromatic-containing compounds.

*Chitinophag*a sp. and other members of Bacteroidetes are known as critical degraders of complex organic matter (Thomas et al. 2011). As a chemoheterotroph, *Chitinophaga* sp. is a possible degrader of complex organic compounds including proteins and polysaccharides and could release degrading enzymes to target cellulose, pectin, and xylan (Thomas et al. 2011). Additionally, Bacteroidetes as a phylum has many members that share an interaction with an animal host. This interaction causes the increase of fitness for both parties, indicating a mutualism relationship (Bäckhed et al. 2005). The ability to break down complex organic compounds combined with potential mutualism ability, identifies *Chitinophaga* sp. as a possible recycler of large biomolecules.

Siderophores in consortia isolates

We propose that many of our bacterial isolates are working in a mutualistic relationship. It is hardly surprising that the consortial nature of our bacterial isolates may have effects on the slower growth rate and the presence of known non-siderophore producing bacteria that were identified within our siderophore strong and weak bacteria

isolates. Barton and Jurado (2007) proposed a microbial community energetics diagram of cave ecosystems that suggests some species are better adapted for energy acquisition from the available sources, which subsequently would release secondary metabolic products to support other species. Furthermore, a cooperative and mutualistic association among the microbes allow for all necessary metabolic reactions to support growth to occur. Boston (unpublished results) has shown that many cave bacteria in culture will not grow on their own, further supporting our hypothesis that bacterial consortia represent mutualistic associations.

The limiting availability of nutrients occurring in caves would encourage cooperative and mutualistic relationships (Barton and Jurado 2007). Interestingly, the persistence of consortia is based on nutrient exchange and one form of nutrient exchange could be siderophores. D'Onofrio et al. (2010) showed that siderophores from a culture can promote growth of the uncultured consortia bacteria, which is consistent with the siderophore cross-feeding of cave microbes studied by O.S. Hersey (unpublished studies in 2014). Thus, it is likely that our consortial bacterial isolates are sharing siderophores among the consortial community in a mutualistic and cooperative manner.

Conclusions

We present findings that show microbial siderophore production in caves and suggest that these processes are potentially essential to survival in an oligotrophic environment. Although siderophores are ferric iron gatherers, these compounds may also have the potential to promote nutrient exchange for possible mutualistic relationships. Cave microorganisms have a preference for hydroxamate siderophores, which might be due to the organism's adaptability to make the lower energy cost and most water-soluble compound. Whether siderophore production by cave microorganisms is used primarily as ferric iron gathering or nutrient exchange within a consortial isolate, or both, remains to be determined.

The study of siderophores is significant for potential use in bioremediation and biomedical uses. An ongoing search for new antibiotics is critical and the combination of the rich diversity of cave bacteria, the potential of novel cave bacteria, and new siderophores, makes the exploration of cave bacteria a promising venue for exploring bioremediation possibilities and for searching for compounds with biomedical uses.

Acknowledgements

We thank Cristina Takacs-Vesbach, Cliff Dahm, and Penelope Boston for helpful discussions. We are grateful to Ara Winter, Jenny Hathaway, Nicole Caimi, and Anthony Rigoni for technical assistance. We would also like to thank the staff at the Cave Resource Office at Carlsbad Caverns National Park and Patricia Seiser for their invaluable assistance with sample collection. We thank the UNM Molecular Biology Core Facilities for equipment and DNA sequencing, supported by the National Institute of General Medical Sciences and the National Institutes of Health under award number P30 GM110907. The research reported in this publication is solely the responsibility of the authors and does not represent the official views of the National Institutes of Health.

Funding information

This work would not have been possible without the funding provided by Initiative to Maximize Student Development (IMSD) at UNM Biology and the American Society for Microbiology (ASM) Robert D. Watkins Graduate Research Fellowship.

Supplemental Table S1. Metafile of Long-term parent cultures and subcultured bacteria isolates (n=80).

Parent Cultures	Parent Media	Cave	Parent Sample type	No. of isolates collected from subculture media			Total
				R2A[a]	R2A[b]	AIA[a,b]	
011505-14	Mn-enriched	Spider	Yellow FMD	21	14	5	41
Fe+C[1] 011101-72	Oxidized-Fe enriched	Lechuguilla[c]	Brown and orange FMD	5	8	0	13
Mn+P_o 011101-63	Mn-enriched	Lechuguilla[c]	Punk Rock	6	6	2	14
Mn- C_o 011101-48	No enrichment	Lechuguilla	Brown and orange FMD	4	6	3	13

[a]-$FeCl_3$ added, [b]-$MnCO_3$ added, [c]-EA sample site, Ferromanganese deposit (FMD), P-Punk rock white with brown flecks color, Fe+-with cofactors, Mn^+ -with cofactors, Mn^- -with no cofactors, P_o- Punk rock $2x10^{-1}$, C_1-FMD $2x10^{-2}$, and C_o-FMD $2x10^{-1}$

Supplementary Table S2. Metafile of Short-term parent cultures

Parent Cultures	Parent Sample type
[a]L120303-2	Grey FMD
[a]L120303-3	Grey FMD
[a]L120303-5	Grey FMD
[a]L120303-6	Brown FMD
[a]L120303-10	Brown FMD
[a]L120303-12	Plain Carbonate
[a]L120303-14	Plain Carbonate
[a]L120303-17	Yellow FMD
[a]L120303-18	Yellow FMD
[a]L120303-20	Yellow FMD
[b]L120303-21	Wet Carbonate
[b]L120303-22	Wet Carbonate
[b]L120303-28	Calcite on Wet Carbonate
[b]L120303-30	Calcite on Wet Carbonate
[b]L120303-32	Wet Carbonate
[b]L120303-35	Wet Carbonate
[b]L120303-36	Soil and Plain Carbonate
[b]L120303-37	Soil and Plain Carbonate
[b]L120303-38	Soil and Plain Carbonate
[b]L120303-40	Soil and Plain Carbonate
[c]L120304-41	Wet Carbonate
[c]L120304-43	Wet Carbonate
[c]L120304-47	Wet Carbonate
[c]L120304-48	Wet Carbonate
[c]L120304-49	Wet Carbonate
[c]L120304-52	Red FMD
[c]L120304-53	Red FMD
[c]L120304-55	Red FMD
[c]L120304-57	Wet Carbonate
[c]L120304-58	Wet Carbonate
[d]L120305-81	Wet Carbonate
[d]L120305-82	Wet Carbonate
[d]L120305-84	Wet Carbonate
[d]L120305-85	Plain Carbonate
[d]L120305-87	Plain Carbonate
[d]L120305-88	Plain Carbonate
[d]L120305-89	Plain Carbonate
[d]L120305-91	Plain Carbonate
[d]L120305-94	Plain Carbonate
[d]L120305-95	Plain Carbonate

[a]EA, [b]Lake Chandalar, [c]Tower Place, [d]Briny-locations inside of Lechuguilla Cave. All were incubated in the cave for 1-3 days.

Supplementary Table S3. Overall incubation times for Long-term (LT) and Short term (ST) bacteria isolate collections

	Parent Culture	Parent Cave incubation	Parent Lab incubation	Total Parent incubation	Subculture Isolation media[a]	ISP4+Fe[b]	ISP4-Fe[b]	CAS
LT	011505-14	6y	5y	11y	≤ 25d	7d	7d	n
	Fe^{+} C^{1}011101-72	1-3d	10y	≤10y 3d	≤ 25d	7d	7d	n
	Mn^{+} P^{o} 011101-63	1-3d	10y	≤10y 3d	≤ 25d	7d	7d	n
	Mn- C^{o} 011101-48	1-3d	10y	≤10y 3d	≤ 25d	7d	7d	n
ST	All parent cultures	1-3d	23d	≤26d	≤7d	7d	7d	n

a. Isolation subculture media for LT are R2A+$FeCl_3$, R2A+$MnCO_3$, AIA+$FeCl_3$+$MnCO_3$ and for ST is ½ R2A. b. Siderophore-inducing iron-limiting growth media. Lab incubation is 20°C , n-days to show CAS color change, d-days, y-years, and ≤- less than or equal to.

Supplemental Table S4. Phylogenetic similarities of 16S rRNA gene sequences identified for strong siderophore producing bacteria isolates

Phylogenetic group	Representative sequence (n=87 OTU)	No. of Clones in group	Closest identified relative (BLAST Accession no.)	Query, Identity (%)
Alphaproteo-bacteria (n=12)	1-30 (1023bp)	27/79	*Sphingopyxis* sp. TP340 3 (DQ376583.1)	100, 99
	1-26 A1 (529bp)	1/79	*Devosia* sp. R41 (KC464823.1)	98, 99
	1-42 B7 (870bp)	7/79	Bacterium enrichment clone heteroA15 4W (GU731266.1)	99, 97
	2-90 A7 (623bp)	3/79	*Aminobacter aminovorans* LZ1304 3 1 (KT597534.1)	100, 99
	1-15 A8 (570bp)	1/79	*Sinorhizobium* sp. S1 2B (AY505137.1)	99, 94
	2-87 A11 (673bp)	4/79	*Sinorhizobium* sp. S1 2B (AY505137.1)	100, 99
	2-90 B7 (877bp)	2/79	*Afipia massiliensis* 34633 (NR_025646.1)	94, 97
	2-76 B4 (720bp)	3/79	*Phenylobacterium haematophilum* (NR_041991.1)	100, 99
	2-75 C12 (797bp)	1/79	*Phenylobacterium haematophilum* (NR_041991.1)	99, 97
	2-74 C6 (815bp)	2/79	*Phenylobacter* sp. V7 (KU041677.1)	97, 98
	2-82 B1 (799bp)	17/79	*Mycoplana* sp. LC360 (JQ014333.1)	98, 99
	1-33 (641bp)	11/79	UC *Brevundimonas* sp. (KF733612.1)	99, 99
Betaproteo-bacteria (n=15)	1-19 A8 (915bp)	52/221	*Achromobacter xylosoxidans* isolate 2M-2 (DQ659433.1)	99, 99
	1-21 C3 (828bp)	1/221	Alcaligenaceae bacterium GMCo21 (KM370354.1)	75, 96
	2-77 A10 (800bp)	1/221	*Cupriavidus* sp. 4HB 6 (KT321704.1)	97, 94
	2-23 B7 (640bp)	15/221	*Cupriavidus* sp. 4HB 6 (KT321704.1)	98, 96
	2-74 A10 (743bp)	10/221	UC Beta proteobacterium clone DBS1v58 (GQ984332.1)	100, 95
	2-73 A4 (760bp)	5/221	*Cupriavidus necator* strain ss1 6 6 (JQ655461.1)	100, 99

Supplemental Table S4. (contd.)

Phylogenetic group	Representative sequence (n=87 OTU)	No. of Clones in group	Closest identified relative (BLAST Accession no.)	Query, Identity (%)
	2-87 A3 (680bp)	2/221	UC Beta proteobacterium clone DBS1v58 (GQ984332.1)	72, 88
	2-72 B6 (647bp)	5/221	*Ralstonia basilensis* (AY047217.1)	99, 98
	2-69 C1 (858bp)	98/221	*Ralstonia basilensis* (AY047217.1)	100, 98
	2-3 A10 (804bp)	2/221	*Telluria mixta* DSM 29330T clone 2 (LN794201.1)	100, 97
	2-41 B12 (528bp)	1/221	*Duganella* sp. DDR b3 (HQ882705.1)	96, 97
	2-41 B10 (883bp)	3/221	*Duganella* sp. DDR b3 (HQ882705.1)	99, 97
	2-76 A2 (720bp)	13/221	UC beta proteobacterium clone 22b (JN178902.1)	100, 97
	2-41 D9 (633bp)	1/221	*Acidovorax* sp. clone CR2 (KT262955.1)	99,97
	2-39 A11 (825bp)	12/221	UC *Acidovorax* sp. clone Set 2 9 (JQ684120.1)	100, 99
Gamma-proteobacteria (n=19)	2-89 B5 (650bp)	1/240	*Pseudomonas* sp. MI 45a (DQ180955.1)	100, 99
	2-89 A7 (738bp)	3/240	*Pseudomonas* sp. VKM B 2265 (AF430121.1)	99, 92
	2-22 (900bp)	109/240	*Pseudomonas fluorescens* strain 1582 (JN679853.1)	100, 99
	2-16 B3 (518bp)	1/240	*Pseudomonas fluorescens* strain 1582 (JN679853.1)	95, 98
	2-36 B7 (738bp)	3/240	*Pseudomonas fluorescens* strain 1582 (JN679853.1)	99, 99
	2-32 C4 (748bp)	2/240	*Pseudomonas fluorescens* strain 1582 (JN679853.1)	99, 99
	2-32 B1 (640bp)	1/240	UC Bacterium clone EDW07B006 (HM066708.1)	100, 93
	2-32 B10 (616bp)	1/240	*Acinetobacter* sp. ST5 (KJ867437.1)	99, 99
	2-49 B8 (636bp)	31/240	*Acinetobacter radioresistens* (AM495259.1)	100, 99
	2-49 A6 (654bp)	6/240	*Acinetobacter radioresistens* (AM495259.1)	99, 98
	2-58 C1 (784bp)	1/240	UC Bacterium clone B18 45 B03 (JQ088448.1)	99, 99

Supplemental Table S4. (contd.)

Phylogenetic group	Representative sequence (n=87 OTU)	No. of Clones in group	Closest identified relative (BLAST Accession no.)	Query, Identity (%)
	2-8 A7 (802bp)	1/240	*Acinetobacter* sp. LG BR 12343 (JQ247325.1)	100, 99
	2-3 A5 (483bp)	12/240	*Acinetobacter* sp. LG BR 12343 (JQ247325.1)	99, 98
	2-65 (959bp)	31/240	*Acinetobacter* sp.GN71 (KJ719386.1)	100, 100
	2-58 D4 (641bp)	2/240	*Acinetobacter* sp. 2009I8 (GU290325.1)	100, 99
	2-58 B9 (702bp)	1/240	*Acinetobacter* sp. 2009I8 (GU290325.1)	99, 99
	1-12 (1022bp)	20/240	*Stenotrophomonas maltophilia* (AB194708.1)	100, 99
	1-2 B3 (825bp)	2/240	*Pseudoxanthomonas* sp. JCM 28688 (LC133719.2)	100, 100
	1-26 C3 (680bp)	10/240	*Pseudoxanthomonas mexicana* KZ22 (FM213381.2)	100, 99
Firmicutes (n=11)	2-82 A8 (932bp)	1/98	*Paenibacillus* sp. J16 (KC862503.1)	100, 99
	2-35 A5 (776bp)	7/98	*Bacillus* sp. 2011SOCCUA3 (KF582893.1)	98, 99
	2-35 A4 (850bp)	5/98	*Bacillus* sp. 2011SOCCUA3 (KF582893.1)	99, 99
	1-3 B1 (849bp)	1/98	UC urban aerosol clone AKIW1001 (DQ129445.1)	79, 99
	2-63 B2 (800bp)	11/98	*Geobacillus stearothermophilus* YX5 (KP742996.1)	99, 99
	2-53 C6 (764bp)	2/98	*Bacillus* SP. LH2-3 (GQ423394.1)	99, 99
	2-68 B8 (760bp)	1/98	*Bacillus cereus* strain ME5 (EU652058.1)	100, 99
	2-83 (1053bp)	64/98	*Bacillus* SP. LH2-3 (GQ423394.1)	100, 99
	2-84 B1 (760bp)	4/98	*Bacillus* SP. LH2-3 (GQ423394.1)	98, 99
	2-86 C5 (731bp)	1/98	*Bacillus weihenstephanensis* R22U3(KX881508.1)	97, 95
	2-7 B6 (849bp)	1/98	*Bacillus weihenstephanensis* R22U3(KX881508.1)	97, 99

Supplemental Table S4. (contd.)

Phylogenetic group	Representative sequence (n=87 OTU)	No. of Clones in group	Closest identified relative (BLAST Accession no.)	Query, Identity (%)
Actinobacteria (n=16)	2-90 B3 (675bp)	17/252	*Streptomyces wedmorensis* NBRC 14062 (NR_112429.1)	100, 99
	1-56 A9 (800bp)	12/252	*Streptomyces spiroverticillatus* isolate 0911MAR2B4 (LN774577.1)	100, 99
	1-31 B5 (880bp)	35/252	UC Yanshan Mountain clone 3-324 (KC554158.1)	100, 99
	2-10 B6 (656p)	13/252	*Rhodococcus opacus* strain ICN24 (KF017568.1)	100, 99
	2-12 A12 (585bp)	11/252	*Rhodococcus fascians* (KC494315.1)	100, 99
	2-81 B3 (832bp)	23/252	*Norcardia coeliaca* INA01131 (KX129823.1)	97, 99
	2-30 A11 (588bp)	23/252	*Curtobacterium luteum* (JX437941.1)	97, 98
	2-15 A5 (890bp)	33/252	*Microbacterium* sp. 0710P1 6 (HM222669.1)	100, 99
	2-33 (920bp)	1/252	Crude oil-degrading strain TPKD2 (KX984040.1)	100, 99
	2-26 A8 (837bp)	1/252	*Microbacterium* sp. 3J1(GU815136.1)	99, 99
	2-82 B10 (587bp)	1/252	*Arthrobacter methylotrophus* (FR848423.1)	96, 99
	2-56 A3 (579bp)	37/252	*Arthrobacter methylotrophus* (LN774193.1)	98, 99
	2-34 D1 (780bp)	11/252	*Arthrobacter siccitolerans* 4J27 (NR_108849.1)	99, 98
	2-42 (888bp)	32/252	*Arthrobacter siccitolerans* 4J27 (NR_108849.1)	100, 99
	2-25 B8 (531bp)	1/252	*Arthrobacter sulfonivorans* strain IARI L 17 (JN411437.1)	93, 99
	2-31 C1 (607bp)	1/252	*Arthrobacter* sp. M1D3 (GU902283.1)	99, 96
Bacteroidetes (n=14)	2-1 C4 (920bp)	1/94	*Hymenobacter* sp. HMF3095 (KT273903.1)	100, 97
	2-3 A1 (887bp)	1/94	*Hymenobacter* sp. HMF3095 (KT273903.1)	100, 97
	2-1 A9 (847bp)	1/94	UC clone NDB4 (HM366526.1)	100, 97

Supplemental Table S4. (contd.)

Phylogenetic group	Representative sequence (n=87 OTU)	No. of Clones in group	Closest identified relative (BLAST Accession no.)	Query, Identity (%)
	2-3 A11 (790bp)	1/94	*Hymenobacter* sp. HMF3095 (KT273903.1)	100, 96
	2-4 A3 (770bp)	1/94	*Hymenobacter* sp. HMF3095	99, 96
	2-1 A10 (742bp)	1/94	UC clone NDB4 (HM366526.1)	100, 97
	2-1 B8 (877bp)	20/94	UC clone NDB4 (HM366526.1)	100, 97
	1-16 A8 (781bp)	6/94	*Olivibacter* sp. JCM 28679 (LC133710.2)	100, 99
	1-19 B2 (921bp)	10/94	UC Bacterium clone JEG.b12 (DQ228391.1)	100, 93
	1-17 B11 (842bp)	1/94	UC Bacterium clone CCRA C08 (JF489512.1)	94, 91
	1-19 A10 (841bp)	1/94	UC Bacterium clone Llauset 1 C9 (HE857428.1)	90, 90
	1-27 A8 (800bp)	46/94	UC Bacterium clone CCRA H03 (JF489563.1)	99, 100
	1-21 A2 (800bp)	3/94	*Flavihumibacter cheonanensis* KACC 17467 (NR_134031.1)	100, 99
	1-15 B2 (760bp)	1/94	UC Sphingobacteriales bacterium clone 45d B8 (GU929375.1)	100, 98

Supplemental Table S5. Phylogenetic affinities of 16S rRNA gene sequences identified for weak siderophore producing bacteria isolates.

Phylogenetic group	Representative sequence (n=15 OTU)	No. of Clones in group	Closest identified relative	Query, Identity (%)
Alphaproteo-bacteria (n=5)	1-5 B4 (870bp)	3/25	Arsenic-contaminated soil clone (GU731266.1)	99, 97
	1-23 (680bp)	1/25	UC Nonylphenol-degrading clone C6 48 (KF155622.1)	100, 100
	1-52 B7 (640bp)	12/25	*Erythrobacter* sp. p52 2011 (HQ652571.1)	100, 99
	1-5 A4 (640bp)	1/25	*Sphingomonas* sp. IMER A1 19 (FJ434118.1)	100, 99
	1-5 C4 (880bp)	8/25	*Sphingopyxis alaskensis* RB2256 (NR_114627.1)	100, 99
Betaproteo-bacteria (n=2)	1-8 B2 (796bp)	7/9	*Achromobacter xylosoxidans* X96 (HM137034.1)	99, 99
	1-6 C4 (680bp)	2/9	*Achromobacter xylosoxidans* X96 (HM137034.1)	100, 99
Actinobacteria (n=3)	1-80 A8 (829bp)	10/47	*Streptomyces* sp. JCM 28665 (LC133696.2)	100, 100
	1-31 B5 (880bp)	24/47	*Lentzea violacea* 174493 (EU593719.1)	99, 99
	1-47 (740bp)	13/47	*Knoellia locipacati* isolate 0511TES14N1 (LN774289.1)	100, 98
Firmicutes (n=3)	2-35 A5 (776bp)	13/25	*Bacillus simplex* strain IR 523 (GU586306.1)	100, 99
	1-80 A12 (560bp)	5/25	*Bacillus* sp. A2 3 (KT583404.1)	100, 99
	1-80 B8 (684bp)	7/25	*Bacillus* sp. A 2 3 (KT583404.1)	100, 99
Bacteriodetes (n=2)	1-8 B1 (791bp)	1/17	UC Mineral photocatalysis clone NDB4 (HM366526.1)	96, 96
	1-5 A2 (560bp)	16/17	*Chitinophaga barathri* YLT18 (KR013246.1)	100, 97

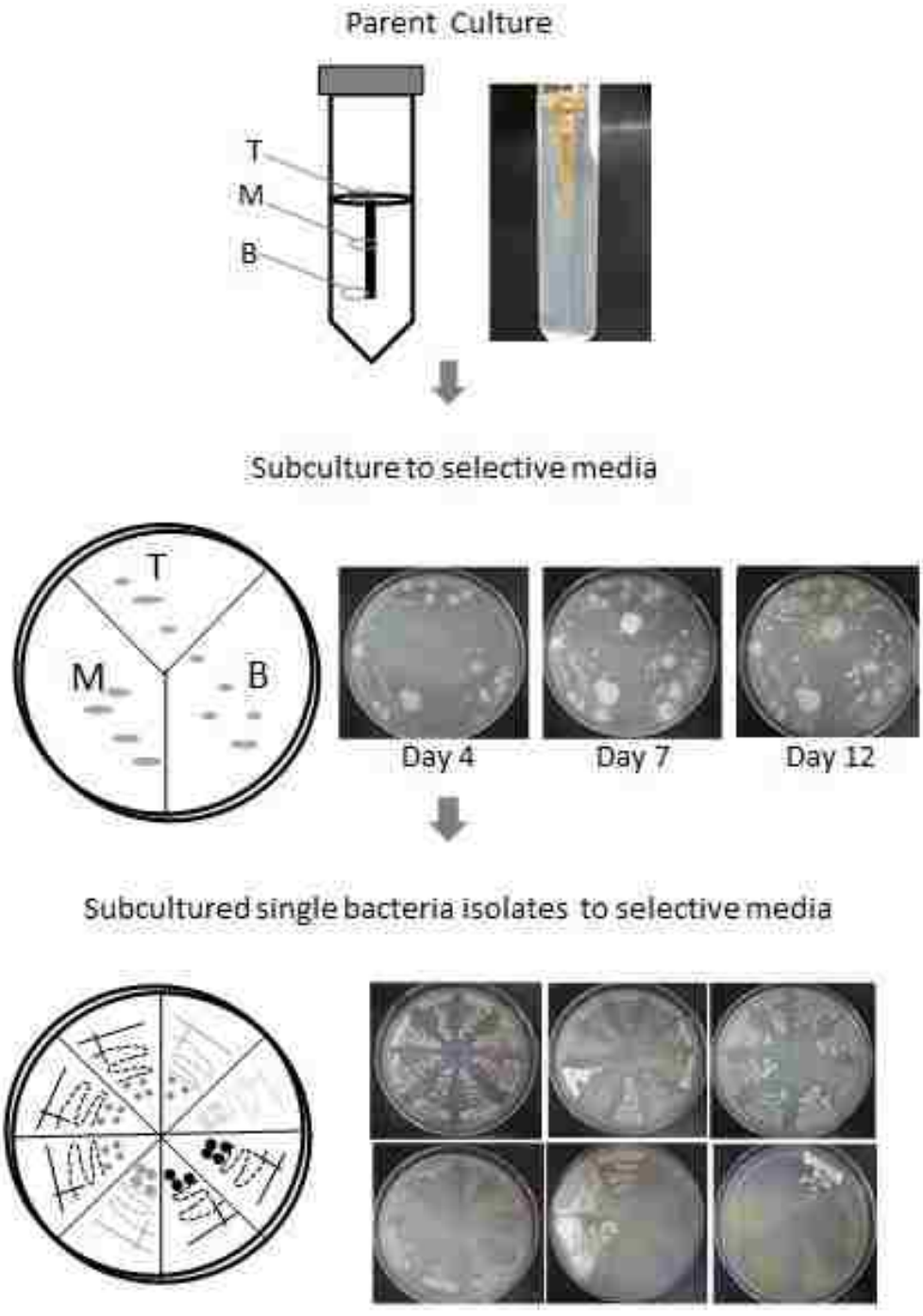

Supplemental Figure S1. The Subculture process for Long-term group from Parent cultures to bacteria isolates (n=80). A sterile loop was used to collect bacteria from T-Top, M- middle, B-Bottom areas of Parent culture. The collected bacteria were streaked heavily on selective media (R2A +$FeCl_3$, R2A+$MnCO_3$, and AIA+$FeCl_3$ +$MnCO_3$) and incubated in the lab at 20°C. Isolated colonies were picked over a series of days and a total of 80 bacteria isolates were collected and stored in 20% glycerol stocks.

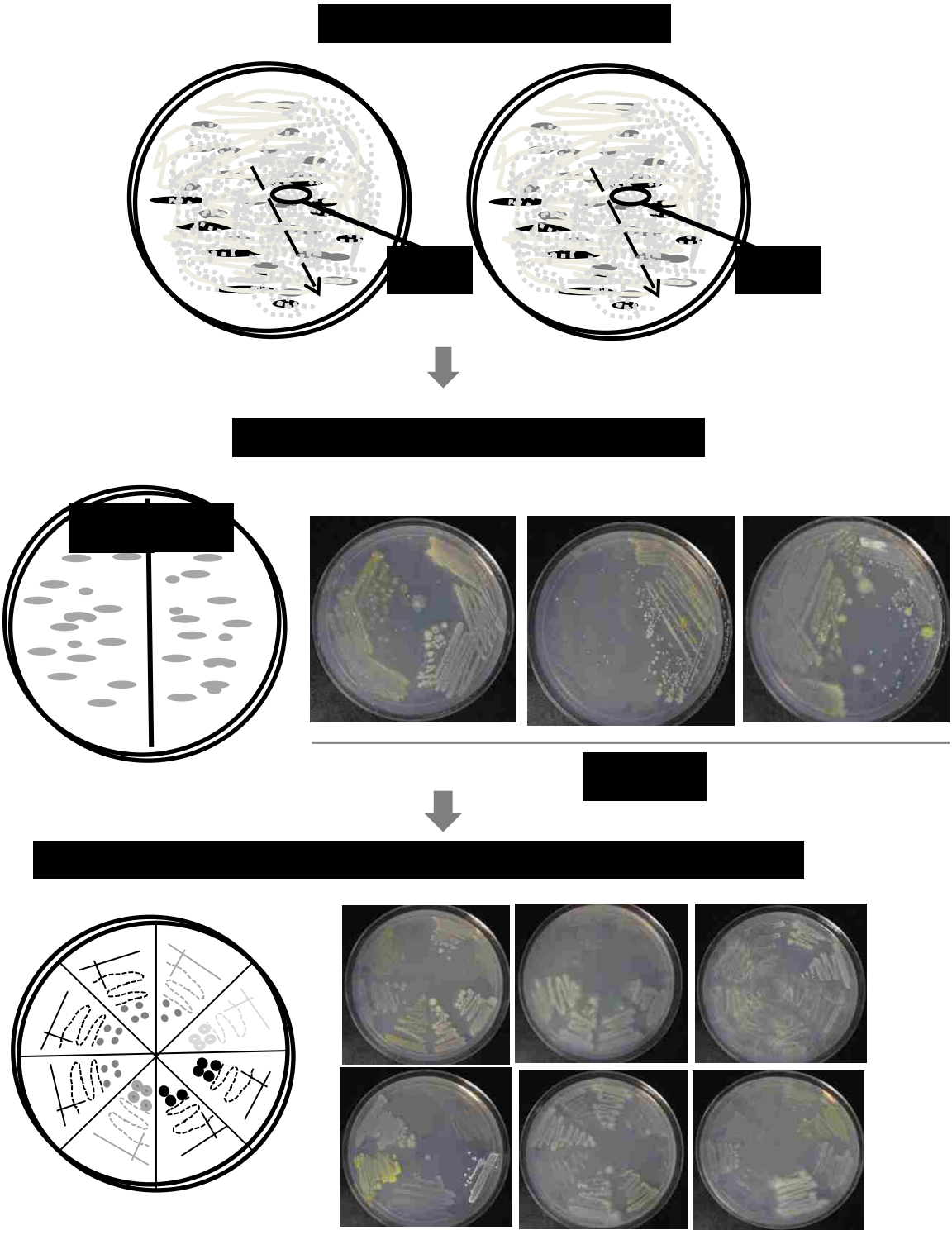

Supplemental Figure S2. The Subculture process for Short-term group from Parent cultures to bacteria isolates (n=90). A sterile loop was used to collect bacteria from heavy growth areas of Parent (P) cultures (40 total parent cultures plates). The collected bacteria were streaked for isolated colonies on selective media ½ R2A (20 total subcultured plates) and incubated in the lab at 20°C. Isolated colonies were picked at Day 7 of incubation and a total of 90 bacteria isolates were collected and stored in 20% glycerol stocks.

References

Ahmed E, Holmström SJM. 2014. Siderophores in environmental research: roles and applications. Microbial Biotech 7:196-208.

Albrecht-Gary AM, Crumbliss AL. 1998. Coordination chemistry of siderophores: thermodynamic and kinetics of iron chelation and release. In Sigel A, Sigel H, editors. Metal ions in biological systems-iron transport and storage in microorganisms, plants, and animals., New York, NY: Marcel Dekker, Inc. P 240-316.

Ali SS, Vidhale NN. 2013. Bacterial siderophore and their application: A review. Int J Curr Microbiol Appl Sci 2:303-312.

Altschul SF, Gish W, Miller W, Myers EW. 1990. Basic local alignment search tool (BLAST). J Mol Biol 215:403-410.

Arnow LE.1937. Colorimetric determination of the components of 3,4-dihydroxphenylalaninetyrosine mixtures. J Biol Chem 118:531-537.

Atkin CL, Neilands JB, Phaff HJ. 1970. Rhodotorulic acid from species of Leucosporidium, Rhodosporidium, Rhodotorula, Sporidiobolus, and Sporobolomyces, and a new Alanine-containing ferrichrome from *Cryptococcus melibiosum*. J Bact 103:722-733.

Bäckhed F, Ley RE, Sonnenburg JL, Peterson DA, Gordon JI. 2005. Host-bacterial mutualism in the human intestine. Science 307:1915-1920.

Barton HA, Jurado V. 2007. What's up down there? Microbial Diversity in Caves. Microbe. 2:132-138.

Barton HA, Taylor NM, Kreate MP, Spinger AC, Oehrle SA, Bertog JL. 2007. The impact of host rock geochemistry on bacterial community structure in oligotrophic cave environments. Int J Speleol 36:93-104.

Boiteau RM, Mende DR, Hawco NJ, McIlvin MR, Fitzsimmons JN, Saito MA, Sedwick PN, DeLong EF, Repeta DJ. 2016. Siderophore-based microbial adaptations to iron scarcity across the eastern Pacific Ocean. PNAS 113:14237-14242.

Braun V, Pramanik A, Gwinner T, Köberle M, Bohn E. 2009. Sideromycins: tools and antibiotics. Biometals 22:3-13.

Bull AT, Asenjo JA. 2013. Microbiology of hyper-arid environments: Recent insights from the Atacama Desert, Chile. Antonie Van Leeuwenhoek 103:1173-1179.

Challis GL. 2005. A widely distributed bacterial pathway for siderophore biosynthesis independent of nonribosomal peptide synthetases. ChemBioChem 6:601-611.

Chong CW, Pearce DA, Convey P, Yew WC, Tan IKP. 2012. Patterns in the distribution of soil bacterial 16S rRNA gene sequences from different regions of Antarctica. Geoderma 181:45-55.

Chu B, Garcia-Herrero A, Johanson T, Krewulak K Lau C, R. Peacock RS, Slavinskaya Z, Vogel H. 2010. Siderophore uptake in bacteria and the battle for iron with the host; a bird's eye view. Biometals 23:601-611.

Crosa JH, Walsh CT. 2002. Genetics and assembly line enzymology of siderophore biosynthesis in bacteria. Micro Mol Bio Rev 66:223-249.

D'Onofrio A, Crawford JM, Stewart EJ, Witt K, Gavrish E, Epstein S, Clardy J, Lewis K. 2010. Siderophores from neighboring organisms promote the growth of uncultured bacteria. Chem Biol 17:254-264.

de los Cobos-Vasconcelos D, Ruiz-Ordaz N, Galíndez-Mayer J, Poggi-Varaldo H, Juàrez-Ramírez C, Aarón LM. 2012. Aerobic biodegradation of a mixture of sulfonated azo dyes by a bacterial consortium immobilized in a two-stage sparged packed-bed biofilm reactor. Eng Life Sci 12:39-48.

Dworkin M. 2002. The Prokaryotes: An evolving electronic resource for the microbiological community. In Springer-Verlag, New York, NY.

Glick BR. 2003. Phytoremediation: synergistic use of plants and bacteria to clean up the environment. Biotechnol Adv 21:383-393.

Gulden B. 2017. USA Longest Caves. The National Speleological Survey (NSS) Geo2 Long & Deep Caves. http://www.caverbob.com/usalong.htm.

Hayes PT. 1964. Geology of the Guadalupe Mountains, New Mexico. U.S. Geological Survey 446

Hershey OS, Akel Z, Barton HA. 2014. Siderophore crossfeeding in cave microbes. General Meeting of the American Society for Microbiology: 2218.

Hider RC, Kong X. 2010. Chemistry and biology of siderophores. Nat Prod Rep 27:637-657.

Hill CA. 2000. Overview of the geological history of cave development in the Guadalupe Mountains, New Mexico. J Cave and Karst Studies 62:60-71.

Jin J, Yao J, Liu W, Zhang Q, Liu J. 2017. Fluoranthene degradation and binding mechanism study based on the active-site structure of ring-hydroxylating dioxygenase in *Microbacterium paraoxydans* JPM1. Environ Sci Pol Res 24:363-371.

Lau MCY, Kieft TL, Kuloyo O, Linage-Alvarez B, van Heerden E, Lindsay MR, Magnabosco C, Wang W, Wiggins JB, Guo L, Perlman DH, Kyin S, Shwe HH, Harris RL, Oh Y, Yi MJ, Purtschert R, Slater GF, Ono S, Wei S, Li L, Sherwood Lollar B, Onstott TC. 2016. An oligotrophic deep-subsurface community dependent on syntrophy is dominated by sulfur-driven autotrophic denitrifiers. PNAS 113:7927-7936.

Lee J, Postmaster A, Soon HP, Keast D, Carson KC. 2012. Siderophore production by actinomycetes isolates from two soil sites in Western Australia. Biometals 25:285-296.

Mawji E, Gledhill M, Milton JA, Tarran GA, Ussher S, Thompson A, Wolff GA, Worsfold PJ, Achterberg EP. 2008. Hydroxamate siderophores: Occurrence and importance in the Atlantic Ocean. Environ Sci Tech 42:8675-8680.

Minh BQ, Nguyen MAT, von Haeseler A. 2013. Ultrafast approximation for phylogenetic bootstrap. Mol Biol Evol 30:1188-1195.

Neilands JB. 1981. Iron absorption and transport in microorganisms. Ann Rev Nutr:27-46.

Northup DE, Barns SM, Yu LE, Spilde MN, Schelble RT, Dano KE, Crossey LJ, Connolly CA, Boston PJ, Natvig DO, Dahm CN. 2003. Diverse microbial communities inhabiting ferromanganese deposits in Lechuguilla and Spider Caves. Environ Microbiol 5:1071-1086.

Northup DE, Dahm CN, Melim LA, Spilde MN, Crossey LJ, Lavoie KH, Mallory LM, Boston PJ, Cunningham KI, Barns SM. 2000. Evidence for geomicrobiological interactions in Guadalupe Caves. J Cave and Karst Studies 62:80-90.

Northup DE, Snider JR, Spilde MN, Porter ML, van de Kamp JL, Boston PJ, Nyberg AM, Bargar JR. 2010. Diversity of rock varnish bacterial communities from Black Canyon, New Mexico. J Geophys Res Biogeosci 115:1-19.

Palmer AN, Palmer MV. 2009. Caves and Karst of the USA. National Speleological Society, Inc., Huntsville, AL.

Pérez-Miranda S, Cabirol N, George-Téllez R, Zamudio-Rivera LS, Fernández FJ. 2007. O-CAS, a fast and universal method for siderophore detection. J Microbiol Methods 70:127-131.

Qin Y, Fu Y, Kang W, Li H, Gao H, Vitalievitch KS, Liu H. 2017. Isolation and identification of a cold-adapted bacterium and its characterization for biocontrol and plant growth-promoting activity. Ecol Eng 105:362-369.

Salwan R, Gulati A, Kasana RC. 2010. Phylogenetic diversity of alkaline protease-producing psychrotophic bacteria from glacier and cold environments of Lahaul and Spiti, India. J Basic Microbiol 50:150-159.

Schwyn B, Neilands JB. 1987. Universal chemical assay for the detection and determination of siderophores. Anal Biochem 160:47-56.

Sorichetti RJ, Creed IF, Trick CG. 2014a. Evidence for iron-regulated cyanobacterial predominance in oligotrophic lakes. Freshwater Biol 59:679-691.

Sorichetti RJ, Creed IF, Trick CG. 2014b. The influence of iron, siderophores and refractory DOM on cyanobacterial biomass in oligotrophic lakes. Freshwater Biol 59:1423-1436.

Spilde MN, Kooser A, Boston PJ, Northup DE. 2009. Speleosol: A subterranean soil. In Proceedings of the 15th International of Speleogy. Kerrville, Texas, pp 338-344.

Spilde MN, Northup DE, Boston PJ, Schelble RT, Dano KE, Crossey LJ, Dahm CN. 2005. Geomicrobiology of cave ferromanganese deposits: A field and laboratory investigation. Geomicrobiol J 22:99-116.

Thomas F, Hehemann JH, Rebuffet E, Czjzek M, Michel G. 2011. Environmental and gut Bacteroidetes: The food connection. Front Microbiol 2:93.

Tomczyk-Żak K, Zielenkiewicz U. 2016. Microbial diversity in caves. Geomicrobiol J 33:20-38.

Venkadesaperumal G, Amaresan N, Kumar K. 2014. Plant growth promoting capability and genetic diversity of bacteria isolated from mud volcano and lime cave of Andaman and Nicobar Islands. Brazilian J Microbiol 45:1271-1281.

Vinatier V, Wirgot N, Joly M, Sancelme M, Abrantes M, Deguillaume L, Delort AM. 2016. Siderophores in cloud waters and potential impact on atmospheric chemistry: Production by microorganisms isolated at the Puy de Dôme Station. Environ Sci Tech 50:9315-9323.

Winkelmann, G. 2007. Ecology of siderophores with special reference to the fungi. Biometals 20:379-392.

Yadav AN, Sachan SG, Verma P, Saxena AK. 2015. Prospecting cold deserts of north western Himalayas for microbial diversity and plant growth promoting attributes. JBiosci Bioeng 119:683-693.

Zhang WH, Huang Z, He LY, Sheng XF. 2012. Assessment of bacterial communities and characterization of lead-resistant bacteria in the rhizosphere soils of metal-tolerant *Chenopodium ambrosioides* grown on lead–zinc mine tailings. Chemosphere 87:1171-1178.

Zhou J, Gu Y, Zou C, Mo M. 2007. Phylogenetic diversity of bacteria in an earth-cave in Guizhou Province, Southwest of China. J Microbiol 45:105-112.

Siderophore Production of Bacterial Isolates Collected from Cave Deposits in Spider Cave, Carlsbad Caverns National Park (CCNP)

Duncan, T.R., Werner-Washburne, M., Northup D.E.
University of New Mexico, Department of Biology, Albuquerque, NM
Corresponding Author Email: tammid31@unm.edu

Abstract

Determining siderophore-rich areas in oligotrophic caves may lead to the discovery of novel microbial diversity that produces novel siderophores or other important biological compounds. These novel siderophores may have potential use in bioremediation and antimicrobial therapies. We investigated siderophore production of cave bacteria isolated from tyuyamunite, white bedrock/punk rock, moonmilk, orange ferromanganese deposits (FMD), dark red FMD, and purple-stained secondary mineral crusts from Spider Cave in Carlsbad Caverns National Park (CCNP). We hypothesized that bacterial isolates collected from cave deposits with low iron and manganese concentrations would have a higher production of siderophores. Using geochemical analytical methods, we measured the elemental content, total organic carbon (TOC), and total organic nitrogen (TON) of the substrates. We found that orange and dark red FMD had the highest iron concentration. We isolated 187 bacterial isolates from the cave deposits and found that the majority of the bacterial isolates produced siderophores. Our results show a potential relationship of increasing iron and manganese concentrations causing a decrease in siderophores produced within 141 days. These studies shed light on the characteristics of siderophore usage by cave bacteria in the subsurface.

Introduction

Iron is essential for life on Earth (Hider and Kong 2010, Saha et al. 2013). However, iron is not always readily available in the surface environment for use in microbial physiological processes (Saha et al. 2013). Iron is usually present in various forms of insoluble iron oxides that are not easily accessible to bacteria (Drechsel and Winkelmann 1997). In order to find and process insoluble iron oxides from the environment, bacteria have developed the strategy of synthesizing and using

siderophores, which are iron-chelating compounds of ferric iron (Drechsel and Winkelmann 1997). Determining whether subsurface bacteria also use siderophores to chelate ferric iron remains an unanswered question for subsurface oligotrophic environments.

Microorganisms from several oligotrophic environments, such as the open-ocean, air, oligotrophic lakes, and cold deserts have been shown to produce siderophores (Mawji et al. 2008, Sorichetti et al. 2014, Yadav et al. 2015, Boiteau et al. 2016, Vinatier et al. 2016). However, surveys of siderophore detection in carbonate cave deposits, which are often oligotrophic, are lacking. A limited number of studies have isolated bacteria from limestone and mud volcano cave walls and soil and tested for siderophore production (Venkadesaperumal et al. 2014, O.S Hersey 2014, unpublished, Qin et al. 2017). The surveys range from testing one bacterium isolated from cave soil from Karaulnaya-2 Cave, Eastern Sayan Mountain area, Russia (Qin et al. 2017) to 24 bacterial isolates from a mud volcano and limestone cave from the Island of Baratang (Venkadesaperumal et al. 2014), to 92 bacterial isolates from a cave wall in Lechuguilla Cave, Carlsbad Caverns National Park, New Mexico (O.S. Hersey 2014, unpublished).

The outcomes of the combined studies showed that there was siderophore production by a subset of the bacterial isolates tested. Though cave walls and soils present evidence for siderophore production, other cave deposits may house a larger percentage of bacteria that produce siderophores. A more comprehensive study of the siderophores present in caves will increase the chance of identifying novel siderophores and also will increase the probability of identifying other important biological compounds. Siderophores are one type of secondary metabolite that may lead to other secondary metabolic compounds such as antimicrobial compounds. Understanding why siderophore production occurs in these oligotrophic carbonate caves also may lead to identifying new roles for microbial siderophore usage in oligotrophic environments.

Investigations of siderophore production by microorganisms collected from different oligotrophic cave deposits have not located siderophore-rich areas in the caves. There are occurrences where bacteria isolated from the cave wall and soil were found to make siderophores, but downstream applications of determining whether these isolates also make important biological secondary metabolic compounds have not be completed.

For example, some deposits, like moonmilk, have been shown to have a higher percentage of Actinobacteria, which are known to promote antimicrobial activity (Roth 1995). Other deposits, such as ferromanganese deposits (FMDs) have yet to be verified to have bacteria that promote antimicrobial activity or other secondary metabolic compounds. A comprehensive survey that includes nutrient analyses and isolation of bacteria may lead to identification of novel antimicrobial and other important biological compounds by cave bacteria.

We hypothesize that cave deposits with iron concentration equal to or lower than the iron concentration in the bedrock will have bacteria that have a higher percentage of strong siderophore producers. We surveyed bacterial isolates subcultured from several cave deposits from Spider Cave, Carlsbad Cavern National Park, New Mexico. We determined the elemental composition of the deposits and determined whether siderophores are produced by cave bacteria subcultured from the same deposit. To our knowledge, this is the first study to report on the correlation of siderophore production with different types of cave deposits.

Methods

Cave site description and sampling

We sampled from Spider Cave in Carlsbad Caverns National Park (CCNP) located in the Guadalupe Mountains. The Guadalupe Mountains formed on a moderately dissected tilted plateau composed of the Giant Reef and back reef strata (above the Guadalupe Escarpment) (Hayes 1964, Palmer and Palmer 2009). Within a unit of the Giant Reef and back reef strata, Spider Cave formed and has 5.7 km of mapped passageway with 41 m of vertical overhead extent (Gulden 2014).

Using sterile loops, six parent cultures were inoculated with six cave deposit samples (Figure 1) that were stabbed into sterile test tubes filled with ½ Reasoner's 2B medium (R2B, Difco^{TM}, Sparks, MD) or 1/10 R2B with 0.6% or 1.5% Bacto agar and left to incubate in the cave in an isolated alcove until visual microbial growth appeared (approximately 7 months).

The differences in the four groups of cave deposits are; FMDs occur in light and dark colors. The light colors are white/pink, yellow/ocher, and orange. The dark colors are red orange, red brown, chocolate brown/black, and jet black. The deposits are light

and fluffy when collected from the cave wall (Northup et al. 2003, Spilde et al. 2005); Punk rock is white or light pink with porous bedrock (Northup et al. 2003, Spilde et al. 2005); secondary minerals-tyuyamunite and purple-stain mineral crusts, are yellow (Polyak and Provencio 2001) and purple color, respectively; and moonmilk is microcrystalline carbonate (Perrone 2005, Perrone-Vogt and Giles 2006, Cacchio et al. 2014, Maciejewska et al. 2017). From within an approximate five-inch radius of the cave deposit sampled for parent inoculations, approximately 15 cc of each cave deposit were collected for geochemistry analyses.

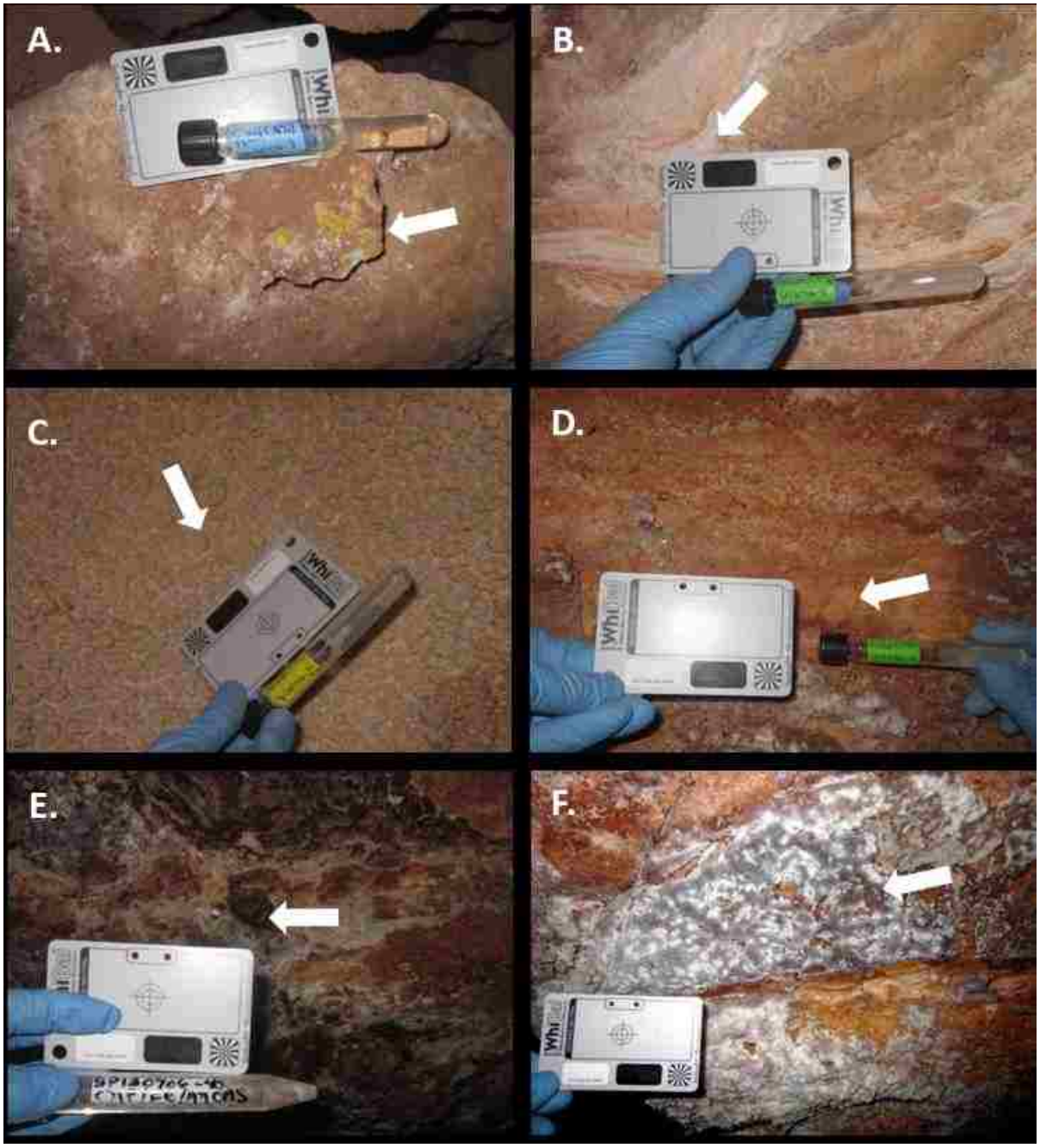

To subculture parent cultures, three depths starting from the top of the agar to the final depth of sample in agar were sampled using a sterile loop and streaked onto ½ R2A or 1/10 R2A agar plates and incubated at 20°C for two days. Using a loopful of the heavy lawn that appeared, serial dilutions (10^{-1} to 10^{-5}) were completed for each set, using a

sterile loop to collect the starting bacterial cells, which were added to 1 ml of sterile 1/10 R2B liquid medium. Serial dilutions were completed and 200µl of the 10^{-5} or 10^{-4} dilutions were plated on four types of agar plates, ½ R2A or 1/10 R2A, R2A+$FeCl_3$ (0.005g/L), R2A+$MnCO_3$ (0.05g/L), and Actinomycetes Isolation Agar (AIA, Difco™)+$FeCl_3$+$MnCO_3$ and incubated at 20°C. Plates were monitored and individual bacterial isolates were collected at two days and eight days incubation time. Each isolate was stored at -80°C in 20% glycerol and media stock.

Geochemistry analysis

To measure total organic carbon (C) and organic nitrogen (N), samples were dried at 60°C for 12 hours and crushed to a fine powder with a pestle and mortar. Approximately 20 mg of ground sample was measured and added to silver capsules in triplicate. A method described by Walther et al. (2010) was used for samples with a pH greater than 6.0, which removes carbonates by adding HCl and exposing the samples to a series of HCl vapors of different concentrations. Briefly, 50 µl of 1% HCl was added slowly to each capsule and placed into a desiccator. The capsules were then exposed to vapor from varying HCl concentrations in the following series: i) 37% HCl for 8 h, ii) 32% HCl for 24 h with the addition of 50 µl of deionized water to each capsule, and iii) 37% HCl or 8 h. Upon completion of the HCl vapor series, the samples were exposed to a vacuum for 24 h to clear residual HCl vapor and placed in a vacuum oven at 200-300 hPa at 35-40°C for 3-7 d. The C and N content of the samples were then analyzed using high temperature combustion (NC2100 Elemental Analyzer, ThermoQuest Italia S.p.A., Rodano, Italy).

To measure cations and anions, cave samples were crushed with pestle and mortar and then pulverized using a SPEX shatter box, if needed, and sieved through a 200 micron mesh sieve. One to two hundred mg of prepared sample was transferred into a 30 ml Teflon digestion tube. Samples were pre-digested for four hours with 3 ml of nitric acid, 2 ml of hydrofluoric acid, and 5 ml of hydrochloric acid using a programmable digestion block. Temperatures were slowly ramped up to a maximum of 95°C. Upon completion of digestion, the acids were evaporated to almost dryness and cooled to room temperature. Samples were then diluted using 2% nitric acid to 50 ml final volume into a 50 ml volumetric flask. The samples were then vortexed and filtered using 0.45 micron

filters and analyzed for major and minor elements using a PerkinElmer Optima 5300DV inductively coupled plasma atomic emission spectroscopy (ICP-AES) following a method comparable to the US EPA 200.7. The elemental peaks were examined, peaks and background points were set, and data were reprocessed for final reporting.

Chrome azurol s (CAS) assay

The assessment of siderophore production by CAS agar plate assay was carried out according to the method of Lee et al. (2012). Bacterial isolates were streaked from -80°C freezer stocks using a sterile loop onto secondary media, which was ½ R2A or 1/10 R2A, R2A+$FeCl_3$, R2A+$MnCO_3$, and AIA+$FeCl_3$+$MnCO_3$ and incubated at 20°C for three days. Each cave isolate was transferred to modified ISP4 agar plates with iron (per litre): soluble starch (4 g), casein (0.3 g), KNO_3 (2g), $MgSO_4 \cdot 7H_2O$ (0.5 g), $CaCO_3$ (0.02 g), $FeSO_4 \cdot 7H_2O$ (0.01 g) and agar (25 g) and incubated at 20°C. After three days, the isolates were iron-starved by plating onto ISP4 agar plates without added iron (4 g/l soluble starch, 2 g/l KNO_3, 0.5 g/l $MgSO_4 \cdot 7H2O$, 0.02 g/l $CaCO_3$, 1 g/l yeast extract, and 25 g/l agar). After one week of iron starvation, cave bacterial isolates were diagonally streaked onto one quadrant of a CAS agar plate and incubated at 20°C. The CAS assay contains chrome azurol S/iron (III)/hexadecyltrimethylammonium bromide (HDTMA) that, upon removal of the iron (III), causes a color change of the liquid from blue to orange (Schwyn and Neilands 1987). CAS plates with streaked cultures were monitored for strength of color change over time. A color change to orange or yellow surrounding the cultured was scored as a positive result for presence of siderophores.

Statistical analysis

The relationships between elemental concentrations of cave deposits and siderophore production were analyzed using Spearman's rank correlation coefficient (Davis 2002). Briefly, the rank correlation coefficient (r´) value was calculated and cross referenced to the n value of the Spearman's critical value table and against our pre-determined alpha value ($\alpha = 0.10$). An $\alpha = 0.10$ was used for n=4 in a two-tailed (directional) Spearman's test. Data were considered significant at r´=0.8 to 1.0, but data were considered indicative of trend up to a r´=1.1 result. An r´ value over 1.1 was not considered because it indicated a more approximate correlation than exact correlation. A

positive correlation means as X increases, Y increases. A negative correlation means as X increases, Y decreases or vice versa.

Results

Geochemistry of cave deposits

To determine the elemental composition, six cave deposit samples (SP130706-7, SP130706-12, SP130706-34, SP130706-19, SP130706-40, and SP130706-26) were analyzed with ICP-AES and specific elemental results are listed in Table 1. In addition, the elemental composition calculated from XRD analysis of SP17-WR (collected and analyzed by M. Spilde unpublished 1998), a Spider Cave wall bedrock sample collected outside of the cave is also listed in Table 1.

Orange and dark red FMD had Fe and Mn content above the detection limits. Dark red FMD had more Fe and Mn content than the Fe and Mn content in orange FMD. All other deposits had below or very close to the detection limit for Fe and Mn. For all samples, there was less Mn content compared to Fe as they had a low Mn/Fe ratio of <0.2 to 0.2 (Table 1).

The amount of organic carbon and organic nitrogen was low in all cave deposits (Table 1). The amount of organic carbon was below the detection level (<0.1 weight percent) for secondary deposits (tyuyamunite and purple-stained secondary mineral crust) and FMDs (orange and dark red). For moonmilk and punk rock, the organic carbon content was at least four times more, 0.4 and 0.56 weight percent, respectively, to the detection limit. The range of total organic nitrogen in samples was 0.03 to 0.09 weight percent (Table 1).

Table 1. Results of chemical analyses for selected elements, TOC and TON, total isolates collected, and strong to weak siderophore production ratio.

Sample	SP17 WR[a]	SP 130706-7	SP 130706-12	SP 130706-34	SP 130706-19	SP 130706-40	SP 130706-26
Sample Type	Bedrock	Tyuyamunite	White Bedrock/ Punk rock	Moonmilk	Orange FMD	Dark red FMD	Purple-stained Secondary Mineral Crust
Analyte Wt%							
Al	0.13	<0.3	<0.3	<0.3	0.36	<0.3	<0.3
Fe	0.05	<0.06	<0.06	<0.06	0.80	2.49	0.09
Mn	<0.01	<0.01	<0.01	<0.01	0.03	0.50	<0.01
Mg	11.7	0.59	8.58	0.07	6.13	7.36	2.78
Ca	28.2	26.5	16.0	6.0	11.8	13.3	25.7
Na	0.05	0.24	0.32	0.25	0.30	0.30	0.29
Mn/Fe	<0.2	<0.2	<0.2	<0.2	0.04	0.2	<0.2
TOC%	NA	<0.1	0.56	0.41[b]	<0.1	<0.1[c]	<0.1
TON%	NA	0.04	0.09	0.05[b]	0.04	0.03[c]	0.05
No. Isolates	NA	51	NA	52	38	NA	46
Siderophore Strong:Weak	NA	9.75:1	NA	1.7:1	9.5:1	NA	1.7:1

a. Analyte Wt% calculated from XRD analysis from unpublished study, M. Spilde 1998. Two samples from same cave deposit collected, b. SP 161127-2 (Moonmilk) and c. SP 161127-3 (Dark red FMD). NA- Not analyzed. Analyte Wt% measured with ICP-AES.

Siderophore detection from cave bacterial isolates.

To determine if bacterial isolates subcultured from cave deposits produced siderophores, we simulated low iron growth conditions and detected siderophores using the CAS assay. A positive color change was blue to orange, beige, or white. The results for siderophore detection fell into strong, weak, none, and no growth (NG) classes and were distributed across two time periods (1 to 140 days and 141 to 282 days), which represented the day bacterial isolates were streaked onto CAS plate until the color change (Table 2).

Bacterial isolates from tyuyamunite, orange FMD, purple-stain secondary mineral crust, and moonmilk produced 86%, 84%, 76%, and 90% total (strong and weak) siderophores, respectively (Table 2). The bacterial isolates subcultured from tyuyamunite and orange FMD had an approximate 9.5:1 strong:weak siderophore detection compared to the bacterial isolates from the purple-stain secondary mineral crusts and moonmilk, which had an approximate 1.7:1 strong:weak siderophore detection (Table 1). Tyuyamunite had 0% of bacterial isolates that produced no siderophores, whereas, bacterial isolates from orange FMD, purple-stain secondary mineral crusts precipitate, and moonmilk had 11, 9, and 6%, respectively, that produced no siderophores. The majority of bacterial isolates from tyuyamunite (51%), purple-stain secondary precipitate (74%), and moonmilk (85%) produced siderophores in less than 140 days compared to bacterial isolates from orange FMD that had 100% that produced siderophores later than 141 days. The range of bacterial isolates for all deposits that did not grow on CAS was 4 to 15% (Table 2).

Table 2. Percent of siderophore detection by bacterial isolates for each cave deposit.

Deposit Type	Siderophore Detection	Time (days) 1-140	141-282	Total (%)
Orange FMD n=38	Strong	0	76	76
	Weak	0	8	8
	None	0	11	11
	NG	0	5	5
	Total	0	100	100
Purple-stain[a] n=46	Strong	39	9	48
	Weak	28	0	28
	None	7	2	9
	NG	0	15	15
	Total	74	26	100
Tyuyamunite n=51	Strong	45	33	78
	Weak	6	2	8
	None	0	0	0
	NG	0	14	14
	Total	51	49	100
Moonmilk n=52	Strong	46	11	57
	Weak	33	0	33
	None	6	0	6
	NG	0	4	4
	Total	85	15	100

a. Purple-stained secondary mineral crust. FMD- Ferromanganese deposit; No growth (NG) are bacterial isolates that grew on all media until plated on CAS assay and did not grow.

Correlation of cave deposit chemical analyses with siderophore production.

To determine if there are relationships between elemental compositions of cave deposits with siderophore production, we applied Spearman's rank correlation co-efficient (Davis 2002). A significant correlation was determined to be a value of 0.8 to 1.1. The significant correlations occurred within three groups, the Fast and Slow siderophore production times and the total of siderophore detection phenotypes (Table 3).

There were two significant correlations with Fe and one significant correlation with Mn (Table 3). There was a positive correlation (.95) between Fe concentration and

with Total/None siderophore production. This correlation means that as the Fe concentration increases, the total percentage of bacterial isolates that don't produce siderophores also increases. There was a negative correlation (-.85) between Fe concentration and Fast/Strong siderophore production (Table 3). This correlation means that as Fe concentration increases, Fast/Strong siderophore production decreases. As for Mn, there was a negative correlation (-.95) with Total/Fast siderophore production. This correlation means that as Mn increases, the Total/Fast siderophore production decreases. The ratio of Mn/Fe also had a significant negative correlation to Slow/Strong and Slow/Weak siderophore production, with the latter having the stronger correlation. This means that as the ratio of Mn to Fe concentration increases, the Slow/Strong and Slow/Weak siderophore production decreases (Table 3).

Table 3. Spearman's correlation of element, Mn/Fe, Total Organic Carbon (TOC), or Total Organic Nitrogen (TON) with siderophore detection phenotype.

Time (days) and Total	Detection phenotype	Al	Fe	Mn	Mg	Ca	Na	Mn/Fe	TOC	TON
Fast	Strong	**-.85**	**-.85**	.75	**-.85**	-.65	**-.85**	.35	-.35	**.95**
(0-140)	Weak	-.55	-.55	.25	-.55	-.15	-.55	.65	-.05	.65
Slow	Strong	.35	.35	.35	.35	-.25	.35	**-.85**	.25	-.25
(141-282)	Weak	.35	.35	-.05	.35	-.25	.35	**-1.05**	.25	-.65
Total	Production	-.25	-.65	-.25	-.45	-.25	-.25	.55	.65	.25
	Strong	-.15	-.15	.65	-.15	-.55	-.15	-.55	-.05	.25
	Weak	-.55	-.55	-.15	-.55	-.15	-.55	.45	-.05	.25
	Fast	**-.95**	-.55	**-.95**	-.55	-.35	-.15	.65	.55	**.95**
	Slow	.75	.35	.75	.55	-.05	.35	-.05	-.75	-.75
	None	.55	**.95**	.55	.75	-.65	**.95**	-.25	**-.95**	-.15
	No growth	-.55	.25	-.55	.45	.65	.05	.25	-1.45	-.05

Significant correlation is .8 to 1.1 and bolded. Positive correlation means as X increases, Y increases. Negative correlation means as X increases, Y decreases or vice versa. X is element, Mn/Fe, TOC, or TON. Y is siderophore detection phenotype.

Discussion

Siderophores have been identified in several oligotrophic environments (Mawji et al. 2008, Yadav et al. 2015, Vinatier et al. 2016), including oligotrophic caves (O.S. Hershey 2014, unpublished, Venkadesaperumal et al. 2014, Qin et al. 2017). However, the relationship between Fe and Mn concentration in cave deposits to siderophore production by cave bacteria has yet to be described. We hypothesized that as Fe and Mn concentrations decrease in cave deposits the percentage of cave bacterial isolates that are capable of siderophore production would increase.

We found that the six cave deposits we collected fell into four different groups based on observations of the deposits (Figure 1). The four groups are FMDs, moonmilk, secondary mineral deposits, and bedrock/punk rock. We found that orange and dark red FMDs contained a higher amount of Fe and Mn when compared to other cave deposits. Though our analysis did not measure whether the Fe or Mn was in an oxidized or reduced form, we expect that the FMDs would have higher amounts of Fe- and Mn-oxides than moonmilk. These predictions could be verified with x-ray diffraction (XRD) analysis. Moreover, when our elemental results were calculated into projected XRD oxide concentrations, they were comparable to previous FMD and moonmilk mineral oxide studies (Spilde et al. 2005). Our orange and dark red FMDs had similar Fe/Mn ratios to previous FMD studies in CCNP (Northup et al. 2003, Spilde et al. 2005) and in Carter Saltpeter Cave, Tennessee, USA (Carmichael et al. 2013). Our moonmilk has a similar Fe/Mn ratio to previous moonmilk samples from CCNP (M. Spilde 1999, unpublished) and in Grotto Nera Cave, Abruzzi, Central Italy (Cacchio et al. 2014).

For the secondary mineral deposit, tyuyamunite, it has been described as a secondary speleogenetic byproduct from H_2SO_4 speleogenesis in CCNP (Polyak and Provencio 2001). Based on observations, the deposit is yellow and appears as small patches on carbonate rock. Tyuyamunite ($Ca(UO_2)_2V_2O_8$•5-$8H_2O$), has been found in two other CCNP caves, and has been found in association with quartz and opal coatings on dolomite and gypsum crusts and floor clays (Polyak and Mosch 1995, Polyak 1998). To confirm our deposit is tyuyamunite, an XRD analysis of the mineral should reveal a high amount of Vanadium and Uranium (M. Spilde 2017, personal communication).

For the Purple-stained secondary mineral crust, it seems to be closely associated with the calcite crusts based on additional observations. The mineral was similar in hardness to other calcite crystals. Based on the elemental analysis, Fe is slightly higher in the purple-stained secondary crust (0.09 wt%) than Tyuyamunite (<0.06 wt%). This slightly higher Fe content may explain the purple-stained color. A XRD analysis would define its mineral content. There are no previous reports describing purple-stained secondary mineral crusts in CCNP.

Siderophore production is detected from bacterial isolates subcultured from cave deposits.

We found that the majority of bacterial isolates collected from tyuyamunite, white bedrock/punk rock, moonmilk, and orange FMD produced siderophores and didn't have any significant correlations with overall siderophore production. We hypothesized that lower Fe concentrations in cave deposits would cause higher siderophore production by the bacterial isolates collected from the same cave deposits. Because Spider Cave is an oligotrophic environment with many habitats likely to be Fe- and Mn-limited, bacterial isolates may almost always use siderophores. Thus, siderophores will be widely used by bacterial isolates in Spider Cave.

Interestingly, we found that the length of time (at least four days) that the cave bacterial isolates took to produce siderophores was significantly longer than human pathogenic bacteria and terrestrial soil bacteria (Lee et al. 2012). Similarly, we showed in separate study of bacterial isolates collected from deposits or structures in Lechuguilla and Spider caves that siderophore production took at least nine days for siderophore detection (T.R. Duncan 2017, unpublished). The slow growth rate of oligotrophic bacteria compared to non-oligotrophic bacteria may be the reason for a slower rate of siderophore production. A previous study of bacterial isolates collected from Lechuguilla Cave showed that bacterial isolates can take up to two years to show bacterial colonies (P.J. Boston, June 2017 personal communication).

A potential trend between Fe and Mn concentrations with siderophore production.

A trend between the concentrations of Fe and Mn of different cave deposits to the production of siderophores by bacterial isolates subcultured from the same deposits was identified. This trend supported our hypothesis that as Fe concentration increased in cave deposits the amount of siderophore production by cave bacterial isolates would decrease. Although this relationship did not occur in overall bacterial siderophore production, it occurred when comparing the relationship of how fast the siderophores are produced to the concentration of Fe. Thus, with a lower concentration of Fe, the bacterial isolates would produce siderophores faster.

A similar trend occurred when comparing Mn concentration and siderophore production. Specifically, as Mn increased the total fast siderophore production decreased. Although there are several significant correlations with Fe and Mn concentrations, future studies that include a larger sample size would be needed to determine if these trends are significant within a wider variety of cave environments.

Predictions of siderophore production in white bedrock/punk rock and dark red FMD.

Bacterial isolates from two cave deposits, white bedrock/punk rock and dark red FMD, were not tested for siderophore production. We predict that both deposits would also have a majority of their bacterial isolates test positive for total siderophore production. The percent positive for white bedrock/punk rock is hypothesized to be similar to the purple-stained secondary mineral crust because their chemical concentrations were very similar. Because the dark red FMD had the highest concentration of Fe, we expect that this substrate would have the lowest amount to siderophore production in the fast siderophore production test and would be similar to the orange FMD results, even if lower overall due to the higher Fe concentration in the dark red FMD.

Are other metals important in siderophore production in cave deposits?

We found that Al and Mg had a similar significant effect on siderophore production in cave deposits. As Al or Mg increased in concentration, there was a decrease in total fast siderophore production for Al and a decrease in fast and strong siderophore

production for both Al and Mg. These results may be due to the ability of siderophores to chelate other metals in soil and natural water environments (Hider and Kong 2010, Ahmed and Holmström 2014). Siderophores generally have a preference for Fe^{3+}, but can also chelate several divalent and trivalent cations that include Mn^{2+}, Mg^{2+} and Al^{3+} respectively, among others (Juwarkar et al. 2007, Hider and Kong 2010, Ahmed and Holmström 2014). Although a significant relationship was shown for Al and Mg to siderophore production, future studies would have to be completed to understand whether these concentrations would have a direct effect on the ability of siderophores to form complexes with Fe.

Conclusions

Chemical analysis of cave deposits in Spider Cave revealed the areas of low Fe and Mn, as well as other key elemental concentrations that are needed for the survival of oligotrophic bacteria. This study also revealed the elemental concentrations of tyuyamunite and purple-stained secondary mineral deposits, both of which we know very little about. Exploring new mineral deposits that are different from other common cave minerals adds to our knowledge and understanding of the relationship of abiotic and/or biotic processes in cave mineral formation.

The extent to which Fe and Mn concentrations in cave deposits control bacterial siderophore production remains to be determined. Our study provided a survey of this relationship within cave deposits and indicated a trend that as Fe or Mn concentrations increase, the total amount of siderophore production decreases. The small sample size and the lack of replicates for nutrient analysis limit this study to providing potential correlations for predicting future study results and the type of environments in which siderophores can be produced.

The discovery of a potential relationship between cave deposits and siderophore production provides support for conservation of sites of high siderophore production in cave environments. Oligotrophic caves, such as Spider Cave, are excellent sites for the investigation of novel microbial diversity that might lead to discovery of novel siderophores. Such siderophores could be used in environmental or biomedical applications as siderophores can chelate other metals that could be used in bioremediation or as sideromycins where siderophores are connected to an antibiotic.

Acknowledgements

We thank Cristina Takacs-Vesbach, Cliff Dahm, Penelope Boston, and Mike Spilde for helpful discussions. We are grateful to Jenny Hathaway, Joe Medley, Gabi Albert, and Dave Vanhorn for technical assistance. We thank the UNM Analytical Geochemistry Laboratory and Abdul-Mehdi Ali for technical assistance. We would also like to thank the staff at the Cave Resources Office at Carlsbad Caverns National Park for assistance with sample collection and granting our collection permit. Patricia Seiser, Matthew Medina, Krystal Charley, and Monica Moya helped with fieldwork. This research would not have been possible without the funding provided by Initiative to Maximize Student Development (IMSD) at UNM Biology and the American Society for Microbiology (ASM) Robert D. Watkins Graduate Research Fellowship.

References

Ahmed E, Holmström SJM. 2014. Siderophores in environmental research: roles and applications. Microb Biotech **7**:196-208.

Boiteau RM, Mende DR, Hawco NJ, McIlvin MR, Fitzsimmons JN, Saito MA, Sedwick PN, DeLong EF, Repeta DJ. 2016. Siderophore-based microbial adaptations to iron scarcity across the eastern Pacific Ocean. PNAS 113:14237-14242.

Cacchio P, Ferrini G, Ercole C, Gallo MD, Lepidi A. 2014. Biogenicity and characterization of moonmilk in the Grotta Nera (Majella National Park, Abruzzi, Central Italy). J Cave and Karst Studies 76:88-103.

Carmichael MJ, Carmichael SK, Santelli CM, Strom A, Bräuer SL. 2013. Mn(II)-oxidizing bacteria are abundant and environmentally relevant members of ferromanganese deposits in caves of the Upper Tennessee River Basin. Geomicrobiol J 30:779-800.

Davis JC. 2002. Statistics and Data Analysis in Geology. New York: John Wiley & Sons, Inc. 106-107 p.

Drechsel H, Winkelmann G. 1997. Iron chelation and siderophores. In: Harwood academic publishers, editors. Erspectives in Transition Metal in Microbial Metabolism. Netherlands: Overseas Publishers Association. P 1-50.

Gulden B. 2017. USA Longest Caves. The National Speleological Survey (NSS) Geo2 Long & Deep Caves. http://www.caverbob.com/usalong.htm.

Hayes PT. 1964. Geology of the Guadalupe Mountains, New Mexico. U.S. Geological Survey 446.

Hider RC, Kong X. 2010. Chemistry and biology of siderophores. Nat Prod Rep 27:637-657.

Juwarkar AA, Kumar GP, Nair A. 2007. Biomolecules in Environmental Applications. In Mishra CSK, editor. Environmental Biotechnology. New Delhi: APH Publishing Corporation. P 23.

Lee J, Postmaster A, Soon HP, Keast D, Carson KC. 2012. Siderophore production by actinomycetes isolates from two soil sites in Western Australia. Biometals 25:285-296.

Maciejewska M, Adam D, Naômé A, Martinet L, Tenconi E, Całusińska M, Delfosse P, Hanikenne M, Baurain D, Compère P, Carnol M, Barton HA, Rigali S. 2017. Assessment of the potential role of Streptomyces in cave moonmilk formation. Front Microbiol 8. 1181.

Mawji E, Gledhill M, Milton JA, Tarran GA, Ussher S, Thompson A, Wolff GA, Worsfold PJ, Achterberg EP. 2008. Hydroxamate siderophores: Occurrence and importance in the Atlantic Ocean. Environ Sci Tech 42:8675-8680.

Northup DE, Barns SM, Yu LE, Spilde MN, Schelble RT, Dano KE, Crossey LJ, Connolly CA, Boston PJ, Natvig DO, Dahm CN. 2003. Diverse microbial communities inhabiting ferromanganese deposits in Lechuguilla and Spider Caves. Environ Microbiol 5:1071-1086.

Palmer AN, Palmer MV. 2009. Caves and Karst of the USA. National Speleological Society, Inc., Huntsville, AL.

Perrone-Vogt M, Giles K. 2006. Got moonmilk? The characterization of moonmilk in Spider Cave, Carlsbad Caverns National Park, New Mexico. New Mexico Geological Society Guidebook 57:175-184.

Perrone, M. 2005. MS thesis. Experimental determination of the biogenecity of moonmilk, and the characterization of moonmilk and its depositional environment in Spider Cave, Carlsbad Caverns National Park, New Mexico. New Mexico State University, Las Cruces, NM.

Polyak VJ. 1998. PhD thesis. Clays and associated minerals in caves of the Guadalupe Mountains, New Mexico. Texas Tech University, Lubbock, TX.

Polyak VJ, Mosch CJ. 1995. Metatyuyamunite from Spider Cave, Carlsbad Caverns National Park. National Speleological Society Bulletin 57:85-90.

Polyak VJ, Provencio P. 2001. By-product of materials related to H2S-H2SO4 influenced speleogenesis of Carlsbad, Lechuguilla, and other caves of the Guadalupe Mountains, New Mexico. J Cave and Karst Studies 63:23-32.

Qin Y, Fu Y, Kang W, Li H, Gao H,Vitalievitch KS, Liu H. 2017. Isolation and identification of a cold-adapted bacterium and its characterization for biocontrol and plant growth-promoting activity. Ecol Eng 105:362-369.

Roth J. 1995. Moonmilk and Cave-dwelling Microbes. In Park CLN, editor. Nature Notes. P 67.

Saha R, Saha N, Donofrio RS, Bestervelt LL. 2013. Microbial siderophores: A mini review. J. Basic Microbiol 53:303-317.

Schwyn B, Neilands JB. 1987. Universal chemical assay for the detection and determination of siderophores. Anal Biochem 160:47-56.

Sorichetti RJ, Creed IF, Trick CG. 2014. Evidence for iron-regulated cyanobacterial predominance in oligotrophic lakes. Freshwater Biol 59:679-691.

Spilde MN, Northup DE, Boston PJ, Schelble RT, Dano KE, Crossey LJ, Dahm CN. 2005. Geomicrobiology of cave ferromanganese deposits: A field and laboratory investigation. Geomicrobiol J 22:99-116.

Venkadesaperumal G, Amaresan N, Kumar K. 2014. Plant growth promoting capability and genetic diversity of bacteria isolated from mud volcano and lime cave of Andaman and Nicobar Islands. Brazilian J Microbiol 45:1271-1281.

Vinatier V, Wirgot N, Joly M, Sancelme M, Abrantes M, Deguillaume L, Delort AM. 2016. Siderophores in cloud waters and potential impact on atmospheric chemistry: Production by microorganisms isolated at the Puy de Dôme Station. Env Sci Tech 50:9315-9323.

Yadav AN, Sachan SG, Verma P, Saxena AK. 2015. Prospecting cold deserts of north western Himalayas for microbial diversity and plant growth promoting attributes. J Biosci Bioeng 119:683-693.

Conclusions and Future Studies from These Cave Bacterial Siderophore Production Studies

Conclusions

My studies have addressed the question of whether cave bacteria cultured from Lechuguilla and Spider caves, CCNP, have the ability to produce siderophores to acquire essential iron. This required a mixture of classical and molecular microbiological and geochemical techniques. Classical microbiological characterizations showed that cave bacteria from an approximately decade long parent incubation have similar traditional and diphasic growth curve patterns to *Escherichia coli* (Monod 1949). The classical physiological assays revealed Gram-positive phenotypes predominate over Gram-negative phenotypes. The catalase and oxidase assays revealed that the parent incubation from the approximately decade long incubation of cave bacterial isolates lacked both enzymes and the cave bacterial isolates from shorter-term parent incubations contained both enzymes. Taken together, these patterns indicated that the most cave-adapted bacteria have thicker cell walls that can help protect or possibly prolong the survival of cave bacteria in a cycle of extremely low nutrients. The diphasic growth pattern of the cave-adapted bacteria may also help in adjusting to different carbon sources, thus promoting survival in a cycle of extremely low nutrients. Lastly, a greater number of bacterial isolates in the approximately decade long parent incubations lack both catalase and oxidase enzymes. These bacterial isolates may have deturb the need for iron by selecting to use enzymes that don't require iron as a key structure component.

Siderophore characterizations of mixed bacterial isolates present in carbonate speleothems, bedrock/punk rock, ferromanganese deposits (FMDs), secondary mineral deposits, and moonmilk showed the capability of these isolates to produce siderophores with an overall preference for hydroxamate siderophores. This preference may be related to the NRPS-independent biosynthesis method, (most common for hydroxamates and reuses available substrate derivatives to build the siderophore), which potentially leads to a requirement of less energy. Moreover, the lack of catecholate siderophores might be due to the efficient breakdown of aromatic compounds for energy that bacteria in the CCNP caves may have acquired by flourishing in an oligotrophic environment. The identities of these bacteria were revealed by molecular phylogenetic characterizations of

the unique OTUs from bacterial isolates that produce a strong or weak color change in the CAS-siderophore assay. Together, the siderophore-producing OTUs classified, from most abundant to least, into the Proteobacteria, Actinobacteria, Bacteroidetes, and Firmicutes phyla. Lastly, a potential relationship was revealed between iron and manganese concentrations in cave deposits with the fast siderophore production bacterial isolates. These findings support a possible essential need for siderophores in oligotrophic cave environments. Confirmation of whether cave bacteria actually employ their ability to produce siderophores to acquire iron remains to be answered.

Future studies

While the study of siderophores in biomedical and surface microbiology is a developed field, the study of siderophores in oligotrophic caves is new (first cave siderophore published study was Venkadesaperumal et al. 2014). My studies explored the capability of cave bacterial isolates to produce siderophores. Testing for siderophore production in the cave, perhaps by the development of a field siderophore assay, could establish in situ siderophore production and map hot spots for siderophore synthesis. It would also be valuable to determine the bacterial member of the mixed cave bacterial isolates that makes the siderophore. This could lead to the discovery of novel siderophore producers, which might then lead to the discovery of novel siderophore compounds. Testing whether there is a relationship between siderophore producers to antimicrobial compound production also would be an interesting topic to study. By establishing such a relationship, it could help guide future investigations for exploring new and understudied environments for potential novel antimicrobial compounds.

References

Monod J. 1949. The growth of bacterial cultures. Annu Rev Microbiol 3:371-394.

Venkadesaperumal G, Amaresan N, Kumar K. 2014. Plant growth promoting capability and genetic diversity of bacteria isolated from mud volcano and lime cave of Andaman and Nicobar Islands. Brazilian J Microbiol 45:1271-1281.